

**Scope of emission tomography for assessment of
myocardial viability in patients with coronary artery
disease**

by

Norma Vasconcelos Saldanha Marinho

August 1994

Thesis submitted for the PhD Degree to the University of London (Faculty of Medicine,
University College of London and Medical School)

ProQuest Number: 10105724

All rights reserved

INFORMATION TO ALL USERS

The quality of this reproduction is dependent upon the quality of the copy submitted.

In the unlikely event that the author did not send a complete manuscript and there are missing pages, these will be noted. Also, if material had to be removed, a note will indicate the deletion.



ProQuest 10105724

Published by ProQuest LLC(2016). Copyright of the Dissertation is held by the Author.

All rights reserved.

This work is protected against unauthorized copying under Title 17, United States Code.
Microform Edition © ProQuest LLC.

ProQuest LLC
789 East Eisenhower Parkway
P.O. Box 1346
Ann Arbor, MI 48106-1346

This work is dedicated to the persons that are not only the reason of my life, but all my life: my husband Fernando, my daughter Juliana and the baby who is coming in a short time.

ABSTRACT

This thesis deals with the clinical and difficult problem of identifying viable myocardium in patients with coronary artery disease and chronic wall motion abnormalities that may improve after coronary revascularization. Assuming that viable myocardium is chronically hypoperfused, "hibernating myocardium", and with reduced wall motion properties, we attempted to investigate the predictive power of pre-revascularization status of flow and glucose metabolism using positron emission tomography techniques in myocardium at risk that would be able to improve after restoration of the coronary circulation.

This thesis aims to further assess the pathophysiology of hibernating myocardium using emission tomography. For this purpose, absolute measurements of regional myocardial blood flow in ml/min/g and metabolic rate of glucose utilization in $\mu\text{mol}/\text{min}/\text{g}$ during hyperinsulinaemic euglycaemic clamp, using positron emission tomography was performed. One hundred patients with hibernating myocardium were studied. All patients underwent radionuclide ventriculography before surgery and thirty before and after surgery. These thirty patients with follow-up scans will be the object of the present study. Control values for myocardial blood flow and metabolic rate of glucose utilization were obtained respectively in twenty five and nine age matched normal volunteers.

This thesis is composed of eight chapters. The first four chapters review the available literature dealing with similar problem, myocardial viability definition, regulatory mechanism of coronary blood flow and methodology available to study hibernating myocardium, particularly positron emission tomography. In chapter five the materials, subjects and methodology, as well as protocols employed in this thesis are described. Chapter six describes all the results pointing to the predictive ^{accuracy} of positron emission tomography measurements of flow and metabolism in determining viable myocardium pre-myocardium. Chapter seven discusses these results in the light of available literature and state the main conclusions. Finally, some thoughts for further research in the subject are exposed.

Acknowledgments

I am very grateful to Brazilian agency CAPES for the financial support without which this thesis would not have been possible.

I am very grateful to Dr. Durval Campos Costa for all his support, accessibility, guidance, suggestions, corrections and friendship during all the research period.

I am also grateful to Prof Peter J. Ell who gave me the opportunity to carrying out this work.

I am specially thankful to Prof. Paolo G. Camici. His enthusiasm and guidance must be acknowledged.

Special thanks go to Ms Heather Boyd for her friendship and expertise in positron emission tomography data analysis.

I would like to express my gratitude to the Radiochemistry Department of the Medical Research Centre Cyclotron Unit for the preparation of radiotracers; to Mr Andrew Blythe and Ms Andreanna Williams for their help in the acquisition of the positron emission tomography data.

I also would like to thank the staff of the Institute of Nuclear Medicine for their cooperation during the acquisition of the studies.

Special thanks go to my parents and Anita Saldanha whose support at all time helped to make this thesis possible. I am also very grateful to my mother and father-in-law for their support, assistance and advices.

I also would like to give thanks to Eliana, Eliseu, Cynesia, Leonardo and Claudio Meneguetti for their friendship during this period of my "life" in London.

List of Figures

Chapter 2 Coronary Blood Flow	Page
<i>Figure 2.1 Schematic representation of the control of coronary blood flow</i>	10
<i>Figure 2.2 Effect of mild decrease in coronary perfusion pressure</i>	12
<i>Figure 2.3 Effect of severe decrease in coronary perfusion pressure</i>	12
<i>Figure 2.4 Effect of an increase in myocardial oxygen consumption</i>	14
Chapter 3 Myocardial Ischaemia	
<i>Figure 3.1 Outcome of myocardial ischaemia</i>	23
<i>Figure 3.2 Cardiac metabolism</i>	41
<i>Figure 3.3 Schematic representation of major metabolic fate of free fatty acids (FFA) and iodinated analogs in myocardium</i>	45
<i>Figure 3.4 Simplified schematic representation of myocardial utilization of glucose and physiologic analog, 2-deoxyglucose labelled with F-18 (¹⁸F-FDG)</i>	46
<i>Figure 3.5 Changes in intracellular substrate metabolism during ischaemia</i>	52
<i>Figure 3.6 Flow metabolism "match" in a patient assessed for myocardial viability before coronary artery by-pass surgery</i>	54
<i>Figure 3.7 Diagrammatic representation of the calculation of perfusable tissue index</i>	57
Chapter 4 Positron Emission Tomography and the Assessment of Myocardial Function	
<i>Figure 4.1 Emission of a positron from the nucleus of a molecule of 15-oxygen</i>	63
<i>Figure 4.2 Region of interest for arterial input function</i>	71
<i>Figure 4.3 Sources of true, accidental and scatter coincidences</i>	75
<i>Figure 4.4 Extravascular volume image</i>	80

Chapter 5 Materials and Methods

<i>Figure 5.1 Generation of myocardial blood flow image</i>	93
<i>Figure 5.2 Regions of interest drawn to be projected onto the dynamic ^{18}F-FDG and H_2^{15}O data set</i>	96

Chapter 6 Results

<i>Figure 6.1 Myocardial blood flow in dysfunctional segments</i>	104
<i>Figure 6.2 Metabolic rate of glucose in normal segments in patients and in controls</i>	106
<i>Figure 6.3 Metabolic rate of glucose in patients</i>	107

Chapter 7 Discussion

<i>Figure 7.1 Predictive accuracy of metabolic rate of glucose and percentage of segments corrected identified</i>	114
--	-----

List of Tables

Chapter 2 Coronary Blood Flow **Page**

Table 2.1 - Major sites of coronary resistance to blood flow 9

Chapter 3 Myocardial Ischaemia

Table 3.1 Survival of patients with ejection fraction less than 35% 28

Table 3.2 Operative mortality according to ejection fraction 29

Table 3.3 Methods to assess viability by measuring systolic function 30

Table 3.4 Thallium-201 studies with follow-up after revascularization 34

Table 3.5 Studies using late thallium-201 redistribution image 35

Table 3.6 Studies using stress-redistribution and reinjection 37

Table 3.7 Comparison between ²⁰¹Tl and ¹⁸F-Fluorodeoxyglucose uptake in fixed defects 38

Table 3.8 Rest-redistribution studies 39

Table 3.9 Studies using ¹⁸F-FDG and positron emission tomography 48

Table 3.10 Accuracy of ¹⁸F-FDG metabolic criteria for detecting viable myocardium 55

Chapter 4 Positron Emission Tomography and the Assessment of Myocardial Function

Table 4.1 Positron-emitting tracers for myocardial blood flow measurements 82

Chapter 6 Results

Table 6.1 Results of ventricular function and metabolic profile 100

Table 6.2 Patients characteristics 102

Table 6.3. Results of myocardial blood flow and metabolic rate of glucose 105

Contents

	Page
Abstract	ii
Acknowledgment	iv
Contents	v
List of Figures	ix
List of Tables	xi
Chapter 1 Introduction	1-5
1.1 General considerations	1
1.2 Aims	3
1.3 Organization of the thesis	4
Chapter 2 Coronary Blood Flow	6-21
2.1 Introduction	6
2.2 Coronary resistive vessels	8
2.3 The control of coronary perfusion	9
2.4 Methods for Studying of the Human Coronary Microcirculation In Vivo	15
2.4.1 Doppler catheterisation	16
2.4.2 Coronary Angiography	16
2.4.3 Coronary Sinus Thermodilution	16
2.4.4 Gas Clearance Methods	17
2.4.5 Radionuclide Imaging Techniques	18
2.5 Interplay Between Myocardial metabolism and Coronary Blood Flow	19
Chapter 3 Myocardial Ischaemia	22-59
3.1 Definition of myocardial ischaemia	22

4.3 The Block Detector Positron Emission Tomography	65
4.4 Quantification	67
4.4.1. Calibration	67
4.4.2 Image Reconstruction	68
4.4.3 Attenuation correction	68
4.4.4 Tracer Kinetic modelling	70
4.5 Limitations of PET scanning	72
4.5.1 Resolution	72
4.5.2. Accidental and scatter coincidences	74
4.5.3 Dead-time Losses	76
4.6 Myocardial PET scanning	76
4.6.1 Partial volume effect	78
4.6.2 Spillover	81
4.6.3 Arterial Activity	81
4.7 Measurement of Myocardial Blood Flow Using PET	82
4.7.1 ¹³ N-ammonia	83
4.7.2 Rubidium-82	84
4.7.3 ¹⁵ O-water	85
Chapter 5 Materials and Methods	87-98
5.1 Introduction	87
5.2 Methods	87
5.2.1 Study Population	87
5.2.1.1 Patients	88
5.2.1.2 Normal controls	88
5.3 Study Protocol	88
5.3.1 Coronary Arteriography	89
5.3.2 Radionuclide Ventriculography	89
5.3.3 Hyperinsulinaemic euglycaemic glucose clamp	90
5.3.4 Positron Emission Tomography	90
5.3.4.1 Positron Emission Tomography Data Analysis	94
5.4 Statistical Analysis	97

Chapter 6 Results	99-107
6.1 Introduction	99
6.2 Ventricular Function and Metabolic Profile	99
6.2.1 Before Surgery	99
6.2.2 After Surgery	100
6.3 Myocardial Blood Flow	103
6.4 Metabolic Rate of Glucose	105
Chapter 7 Discussion	108-115
7.1 Introduction	108
7.2 Discussion	110
7.3 Conclusions	115
Chapter 8 Recommendations for future research	116
8.1 Future Research	116
References	117

Chapter 1

Introduction

1.1 General considerations

The idea of developing this thesis^{is} based upon the inherent uncertainties when answering questions about the outcome of patients with coronary artery disease and left ventricular dysfunction referred to coronary artery by-pass surgery. Coronary revascularization procedures have been, in the past, carried out mainly to relieve angina, rarely with the primary purpose of improving depressed left ventricular function. This has been traditionally justified assuming that persistent left ventricular dysfunction in patients with coronary artery disease resulted from myocardial infarction and irreversibly damaged myocardium. However, the observations by Rahimtoola in 1985 challenged this assumption, and introduced the idea that myocardial dissynergy was not always irreversible, but a transient condition, in which the depressed function matched the reduced blood flow. He called "hibernating myocardium" to the tissue with matched reduced blood flow and inotropic function. Thus, the importance of distinguishing clinically viable myocardium from irreversibly damaged tissue was born. It was therefore hypothesized that wall motion abnormalities due to hibernation would improve following restoration of flow, while those due to myocardial infarction would not. In cases of hibernating myocardium, coronary revascularization might be beneficial. First, by preventing stunning, which might follow periods of ischaemia when, even a temporary loss of a small amount of function could have significant clinical

consequences. Second by inducing functional recovery in zones of dysfunctional myocardium due to hibernation. The conventional diagnostic tools for detecting reversible myocardial dysfunction are based on the evidence of persistent metabolic activity (measured by glucose uptake), membrane integrity (assessed by thallium-201) and wall motion evaluation after inotropic stimulation. The accuracy of these techniques have been tested against glucose uptake using [^{18}F]2-fluoro-2-deoxy-D-glucose (^{18}F -FDG) and positron emission tomography. Although comparison with ^{18}F -FDG provides important information on the myocardial metabolism and accuracy of the other methods, there are several aspects on the clinical protocols using ^{18}F -FDG that must be criticised

The ^{18}F -FDG-blood flow mismatch, which is accepted as the gold standard for assessment of myocardial viability, is apparently affected by false-positive (Schwaiger 1986) and false negative results (Tillisch 1986 and Tamaki 1989), despite the high accuracy in the prediction of reversible myocardial dysfunction (Tillisch 1986 and Tamaki 1989). This might be due to the fact that several metabolic variables, such as insulin loading, exercise and dietary conditions might affect the myocardial ^{18}F -FDG uptake. In addition, quantification must always be performed in order to enable the definition of circulatory levels of ^{18}F -FDG and consequent influence in its differential uptake in the myocardium. Qualitative image analysis is not enough and gives poor reliability (Parodi 1992). The knowledge of the physiological variability of myocardial ^{18}F -FDG utilisation together with the appropriate protocol for evaluation of viability should allow a better understanding of the different patterns of

myocardial tracer uptake in chronically hypoperfused dysfunctional myocardium.

1.2 Aims

The main objective of this thesis is to give new insights on the pathophysiological knowledge of myocardial metabolism in patients with coronary artery disease and left ventricular dysfunction. It is recognized that in order to better understand the mechanisms involved in the recovery of dysfunctional myocardium it is necessary to build on a physiological background, basically from utilising adequate protocols in this subset of patients. This knowledge is believed to be essential for the understanding of the processes involved in this transitory and reversible myocardial dysfunction.

The detailed objectives of this research are listed below.

1. To present a comprehensive literature review on coronary blood flow in order to understand its control.
2. To investigate the relationship of coronary blood flow and myocardial metabolism.
3. To analyse the relationships between myocardial ischaemia and inotropic dysfunction.
4. To investigate the effect of standardisation of dietary state using hyperinsulinaemic euglycaemic clamp on the metabolic rate of myocardial glucose utilization in patients with coronary artery disease and in normal controls.
5. To improve the use of the positron emission tomography by producing quantitative results of myocardial blood flow and glucose utilisation in patients and in normal controls.

6. To establish values of myocardial glucose utilisation rates to predict the functional outcome of surgical revascularization in this subset of patients with "hibernating myocardium".

1.3. Organization of the thesis

This thesis presents a prospective study of 100 patients selected from the waiting list for coronary artery by-pass graft surgery from the Royal Post-Graduate Medical School and Hammersmith Hospital. Positron emission tomography was used to measure myocardial blood flow and glucose utilisation. Radionuclide ventriculography was employed to assess regional wall motion before and after surgery. All patients selected had regional wall motion abnormalities and coronary artery stenoses confirmed on coronary angiography. From the initial selected group, eight subjects died before surgery, forty five had coronary artery by-pass grafting done by the same surgeon in the same institution (Royal Post-Graduate Medical School and Hammersmith Hospital), and forty seven did not undergo surgical revascularization. Thirty out of the forty five, who underwent coronary by-pass surgery had follow-up studies performed four to six months after revascularization. The remaining fifteen did not reach the minimum time period for follow-up studies by the time this thesis was written.

In chapter 1 the clinical problem has been introduced, and the aims described.

In chapter 2 a comprehensive review of coronary blood flow and its regulatory mechanisms is presented. The basic aspects of the control of coronary

perfusion are discussed and a brief description of the available methods for studying the human coronary microcirculation in vivo is presented.

Chapter 3 contains a literature review of myocardial ischaemia. The aim of this chapter is to present information on outcome of patients with myocardial ischaemia. The concept of hibernating myocardium, and the proposed mechanisms for hibernation are described. The importance and the methods used to assess myocardial viability are reviewed. Recent new developments for measuring myocardial viability are highlighted.

Chapter 4 deals with the theory of positron emission tomography, highlighting the physical principles involved and the quantitative aspect of the method (with its limitations), particularly for myocardial studies. Techniques available to measure myocardial blood flow using positron emission tomography are described.

Chapter five contains a description of the patient population, the techniques and procedures used in this thesis. The employed protocols are described with detail.

In Chapter six the results are presented in detail. This is followed by the necessary discussion in chapter seven which includes the conclusions directly assembled from the results.

Chapter 8 contains recommendations for future research on assessment of myocardial viability.

Chapter 2

Coronary Blood Flow

2.1 Introduction

The link between ischaemic heart disease and pathology of coronary circulation is established beyond doubt. For the purpose of this thesis I consider ischaemic heart disease and coronary artery disease synonyms of a singular pathology. Coronary artery disease has been diagnosed through coronary angiography for a long time. Coronary angiography has clearly demonstrated a definite relationship between severity of coronary artery disease and survival (Mock 1982 and Kawaguchi 1993). Animal studies have shown that reduction of epicardial vessel calibre alters myocardial metabolism and regional wall motion secondary to decrement in blood flow (Vatner 1980, Neely 1981 and Lee 1986). Clinical studies have confirmed these findings (Lewis 1991). Therefore, reduction in the lumen of epicardial coronary arteries due to atherosclerotic lesions increasing resistance to blood flow is supposed to be the major cause of myocardial ischaemia in patients (Gould 1974 and Lipscomb 1975) with coronary artery disease.

However, in some patients there is often no direct correlation between clinical manifestations of ischaemia and the severity and extent of epicardial coronary stenoses (Patterson 1991). These observations have led to the concept of dynamic stenoses (Gould 1980) and suggested that additional factors may contribute to the physical obstruction to blood flow posed by stenosis of an epicardial artery and, hence to myocardial ischaemia (Selwyn 1992 and Maseri

1992). Clinical and experimental studies have implicated autonomic and serotonergic stimulation of the coronary vessels (Newman 1990, McFadden 1991 and Tousoulis 1993) as well as endothelial dysfunction (Nabel 1988) as important modulators of epicardial coronary stenosis behaviour.

However, recent clinical studies (Maseri 1991a, Pupita 1990 and Maseri 1992) have suggested that vasoconstriction of small coronary vessels may also play a role in the genesis of myocardial ischaemia in patients with coronary artery disease. Vasoconstriction of small intramyocardial vessels can be induced by:

1. drop in perfusion pressure distal to the epicardial stenosis, because of energy losses incurred when blood crosses through the narrowing (Epstein 1986). Thus, in order to restore the perfusion pressure pathologically reduced to an acceptable physiological level, it will occur vasoconstriction of the small vessels.
2. endothelial cells dysfunction in microvessels that do not exhibit gross lesions and are nevertheless exposed to abnormally high levels of circulating lipids and cholesterol, which may be sufficient pathological stimulus to produce changes in microvascular reactivity, reducing its capacity to dilate, thus enhancing excessive local vasoconstriction (Zeiber 1991 and Kuo 1992); and
3. endothelial release of neurohumoral factors that cause vasoconstriction [e.g. endothelin (Larkin 1989), neuropeptide Y (Clarke 1987), serotonin (McFadden 1991 and Tousoulis 1993), and Sympathetic stimulation (Nabel 1988, Zeiber 1989 and Vita 1992)].

However, there are some patients in whom symptoms and signs of myocardial ischaemia may be present even with no identifiable abnormality in coronary angiography (Chambers 1990). Thus, it is conceivable that abnormalities of the

coronary microcirculation may play a role in the reduction of blood flow in such patients (Maseri 1991). Coronary microcirculation is responsible for the resistance to blood flow, whereas epicardial vessels act as conduits of blood in the coronary circulation.

2.2 Coronary Resistive vessels

In the microcirculation small coronary vessels or resistive vessels regulate myocardial blood flow by continuously adapting coronary blood flow to the myocardial metabolic requirements. Under normal circumstances, these small coronary arterioles below 100 μm in diameter are believed to be the major determinant of coronary vascular resistance (Chilian 1988 and Marcus 1990) . However, this concept of coronary resistance is not limited to the compartment of arterioles smaller than 100 μm in diameter; as it has been demonstrated resistance coexists in the different arteriolar compartments (table 2.1). In animal preparations 50-60% of coronary resistance is in smaller vessels (<100 μm in diameter), and about 20% of coronary resistance is in larger vessels (> 140 μm in diameter) under basal conditions (Tillmanns 1981, Nellis 1981 and Chilian 1986). It is important to realise that the resistance relationship between the different compartments may change depending on the perfusion pressure and local metabolite environment. However, this relationship between blood flow and tissue metabolism may be disturbed in patients with coronary artery disease.

	Large % (diameter)	Medium % (diameter)	Small % (diameter)
Tillmanns 1981	4%(150-300 μ m)	-	33% (25-100 μ m)
Nellis 1981	-	17%(>140 μ m)	43% (<140 μ m)
Chillian 1986	7% (220-240 μ m)	23% (210-160 μ m)	44% (70-130 μ m)

Table 2.1 - Major sites of coronary resistance to blood flow. Percentage of pressure drop in relation to aortic pressure. The greatest pressure drop occurs in the small arterioles less than 100 μ m in diameter

2.3 The Control of myocardial perfusion

Myocardial perfusion is controlled by the modulation of coronary blood flow - autoregulation - and tissue metabolism at the level of the resistive vessels. However, the response of the resistive vessels to different physiological stimuli is heterogeneous. In order to provide a useful framework for studying the behaviour of the small coronary vessels one could, on theoretical grounds, separate them in two groups on the basis of their function and diameter (Epstein 1986), although this demarcation in vivo is rather blurred (Maseri 1992). The first group : the distal arteriolar vessels (<100 μ m) are predominantly responsive to local tissue metabolism. Its main function is to maintain the intracellular environment within optimal biochemical limits for myocardial contractile function and it is modulated primarily by tissue oxygen and carbon dioxide tension (Duling 1972, Duling 1973 and Gellai 1973). The flow in this distal arteriolar vessels is dependent on their inherent tone and the perfusion pressure at origin. This perfusion pressure is determined by the second group - the proximal "pre-arteriolar" vessels (100-350 μ m) - influenced only by

coronary perfusion pressure (Maseri 1991). So that, when there is an increase in myocardial oxygen demand with arteriolar vasodilatation, a pressure drop

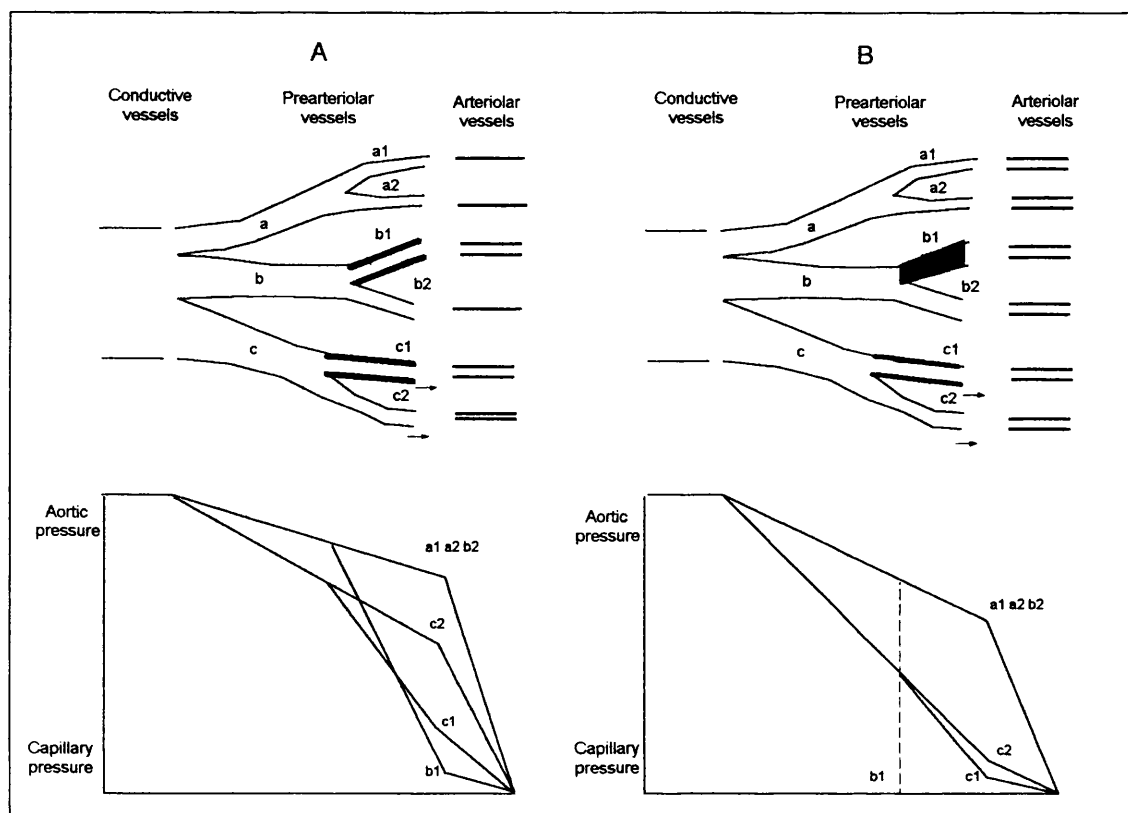


Figure 2.1 - Schematic representation of a conduit coronary artery and prearteriolar and arteriolar vessels with patchily distributed prearteriolar constriction in control conditions (A, upper panel) and during arteriolar vasodilatation (B, upper panel). In this functional classification, conduit coronary arteries do not have appreciable flow resistance, arteriolar vessels are responsible for the metabolic autoregulation of coronary blood flow and prearteriolar vessels with appreciable coronary flow resistance that are responsible for maintaining perfusion pressure at the origin of arterioles within optimal levels. The vasodilatory reserve of arterioles distal to constricted prearteriolar vessels is reduced because they are already dilated to preserve rest flow. In conduit coronary arteries, the pressure remains similar to aortic pressure, but decrease progressively across prearteriolar vessels in proportion to their degree of constriction (A, lower panel). During metabolic or pharmacological arteriolar vasodilatation, the pressure drop increases only slightly distal to some prearteriolar vessels (a1,a2,b2) because vasodilatation related to flow-mediated release of endothelium derived relaxing factor compensates nearly completely for the increased flow. The pressure drop increases markedly across more constricted prearteriolar vessels (b1,c1,c2) (B, lower panel). Steal can develop when an increase in flow through c2 causes a pressure decrease at the branching point distal to the constricted segment c, so that the driving pressure becomes insufficient to perfuse adequately the most constricted branch c1 and blood flow (as indicated by arrows) can become lower than during rest conditions. The possibility of flow steal is greatly enhanced if branch c2 perfuses subepicardial layers of the ventricular wall with a greater flow reserve and if branch c1 perfuses the subendocardial layers with a smaller flow reserve. At the end of the prearteriolar vessels with the most marked increase in tone (b1), intravascular pressure may become insufficient to maintain patency, resulting in vessel collapse.

would potentially occur across the pre-arteriolar vessels with increasing flow (figure 2.1). The vasodilatation mediated by flow at this level is sufficient to meet tissue needs. In the case of an increase in aortic pressure, arteriolar pressure may be maintained by pre-arteriolar constriction through an increase in myogenic tone (figure 2.1). In the opposite situation, a marked decrease in aortic pressure leads to dilatation of all resistive vessels. In pathological conditions, a failure of pre-arteriolar vessels to dilate or to constrict would lead to a reduction in flow in arteriolar bed despite the maximal dilatation in response to tissue metabolism. The hypothesis of the regulation of the myocardial perfusion at the level of the small vessels may be explained by the two theories described above.

Changes in the resistance at the level of small arterioles will occur if:

1. *Aortic pressure changes* - The regulation of myocardial blood flow when aortic pressure changes is modulated by changes in the coronary perfusion pressure that adapts itself for maintaining nutritive flow in the face of a reduction in the perfusion pressure caused by systemic hypotension or a proximal flow obstruction. This phenomenon is termed autoregulation. This process of autoregulation allows very little change in myocardial blood flow over a wide range of perfusion pressures. With mild decrease in coronary perfusion pressure (to 60 mmHg) as shown in figure 2.2, arterioles with less than 100 μm in diameter always dilate whereas large arterioles do not respond. However, with further decrease in coronary perfusion pressure (to 40 mmHg), small arterioles $<100\mu\text{m}$, again, dilate towards their physiological maximum, whilst vessels larger than $>100\mu\text{m}$ in diameter

reduce calibre (figure 2.3) in order to compensate for the drop in the aortic pressure.

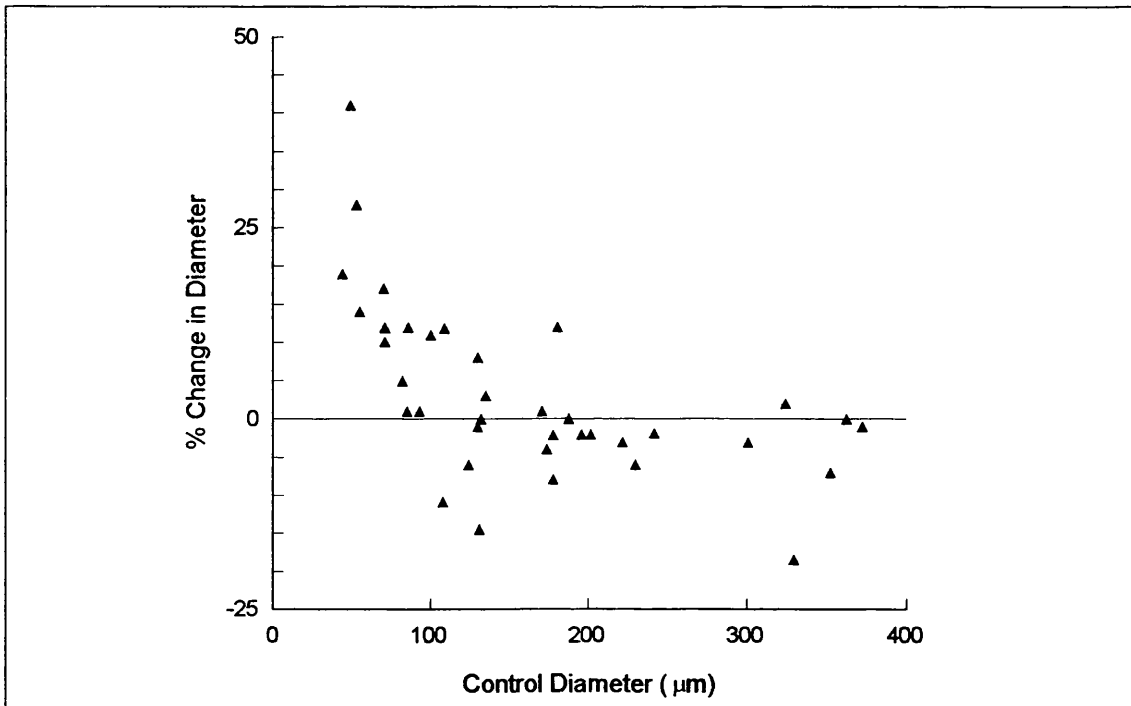


Figure 2.2- Effect of mild decrease in coronary perfusion pressure (to 60 mm Hg) of the left anterior descending artery on diameter of coronary arteries and arterioles in the epicardium of the left ventricle in chloralose anaesthetised dogs. (Adapted from Kanatsuka et al., 1989).

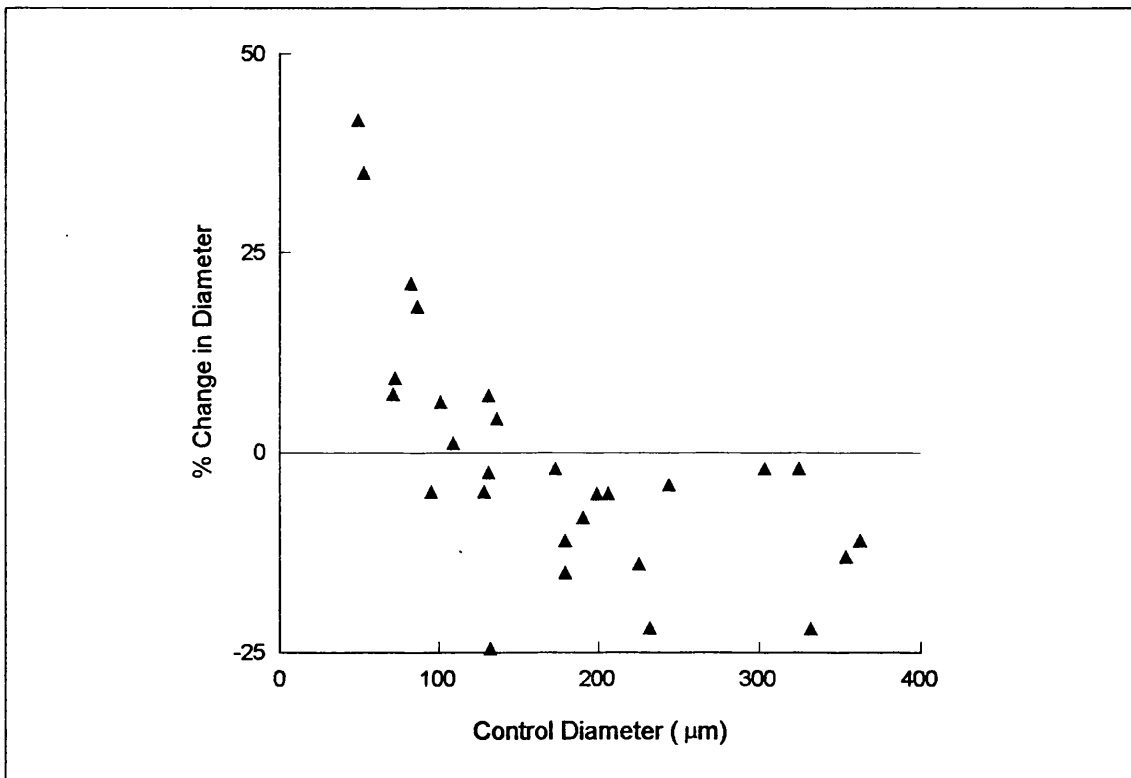


Figure 2.3 - Effect of severe decrease in coronary perfusion pressure (to 40mm Hg) of the left anterior descending artery on diameter of coronary arteries and arterioles in the epicardium of the left ventricle in chloralose anaesthetised dogs. (Adapted from Kanatsuka et al. 1989).

2. *Myocardial oxygen consumption changes* - Vasodilatory metabolites such as ADP, adenosine, H^+ and lactate vary in concentration in the intracellular and hence extravascular compartments in relation to myocardial metabolic activity (Berne 1979). Increased production of these metabolites occurs with increased myocardial oxygen consumption, and, thereby arteriolar vasodilatation is produced and an increase in coronary blood flow occurs with maintained perfusion pressure. Pre-arteriolar vessels vasodilate in response to increased flow velocity in order to maintain optimal pressure across the arteriolar bed (figure 2.4). The mechanisms whereby these vessels dilate are uncertain although flow-mediated release of EDRF (endothelium relaxing factor) has been postulated. An inability to vasodilate in response to changes in blood flow would diminish this metabolic-mediated vasodilatation, particularly in the subendocardium which is more susceptible to a reduction in coronary flow. Thus, the ability of the arteriolar vessels to match flow through resetting of the extravascular fluid composition requires a relatively constant flow at the level of pre-arteriolar vessels .

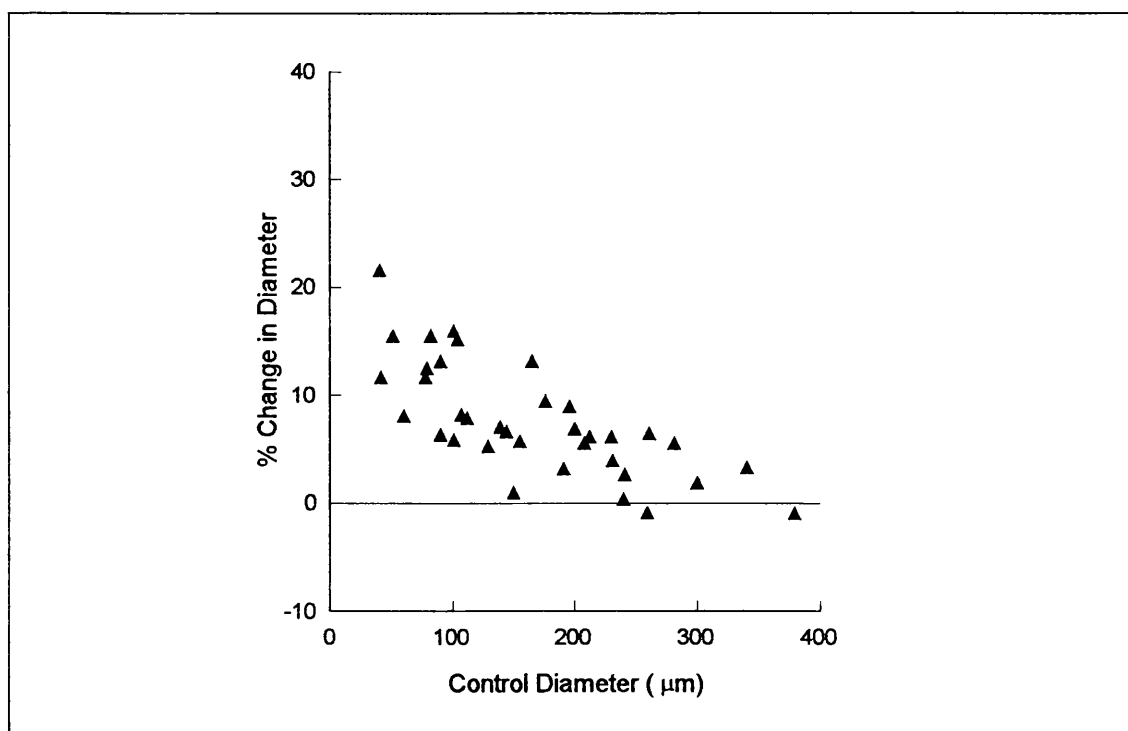


Figure 2.4 - Effect of an increase in myocardial oxygen consumption by rapid pacing on microvascular diameters in the epicardium of the left ventricle in chloralose anaesthetised dogs. (Adapted from Kanatsuka et al., 1989).

Both mechanisms: pressure and metabolic autoregulation may be affected by other stimuli, i.e. autonomic nervous system that has a direct effect on coronary arteries through the release of adrenaline and noradrenaline. However other factors also influence the coronary blood flow. Extravascular forces, particularly due to intramyocardial compression which is generated during the contractile cycle (Hoffmann 1987) influence the status of coronary blood flow. Intramyocardial pressure is maximal in systole and is particularly felt in the subendocardial layers where it exceeds aortic pressure (Hamlin 1982). Based on these facts, there are three major sites for changes in myocardial blood flow:

1. Constriction of arterioles greater than 100 µm in diameter (pre-arterioles),
2. dysfunction of the autoregulatory vessels less than 100 µm in calibre (arterioles),

3. abnormally high intramyocardial pressure.

In order to evaluate the modulatory mechanisms, several attempts have been made to study human microcirculation in order to have a better understanding of the coronary blood flow under pathophysiological conditions.

2.4 Methods to Study Human Coronary Microcirculation In Vivo

Microvascular flow has been studied extensively in animals using experimental techniques with high inherent temporal and spatial resolution. By comparison, many methods developed to study the human coronary circulation are relatively crude and more sophisticated techniques are not widely available in clinical practice. However in some circumstances, human microcirculation may be easily visualised *in vivo* such as the retinal vessels of the optic fundus and the cutaneous microcirculation. Otherwise direct visualisation of microcirculation in other organs is very difficult or almost impossible. For instance, microvessels of the coronary circulation are not visible on angiography. Therefore, study of the human coronary microcirculation is indirect and relies on assessing parameters, which reflect its functional status, such as coronary blood flow. There are a number of techniques available to measure coronary blood flow in man (Marcus 1987), the majority of which involve cardiac catheterization procedures. These measurements are usually performed using Doppler catheter (Hartley 1974 and Cole 1977), quantitative coronary angiography (Goldstein 1987), thermodilution (Ganz 1971), clearance of a radioactive inert gas or by using radionuclide imaging tracers.

2.4.1 Doppler catheterisation

The doppler catheter consists of a 20 MHz piezo-crystal mounted at the top of a steerable 3F gauge catheter which may be inserted into a coronary artery over an angioplasty guide wire. Although multiple regional measurements can theoretically be made in the different coronary arteries with real time Doppler catheter, it measures only epicardial flow velocity as opposed to tissue perfusion. The mass of myocardium supplied by the artery under study cannot be defined. Doppler measurements in the different regions of the heart cannot be made simultaneously. In addition, because of the invasive nature of the procedure, there is a small risk of injury to the coronary artery under study, a risk which is compounded by the relatively unstable free-floating tip which can as well, lead to a variable quality of the recordings. In the presence of epicardial coronary artery disease, the catheter tip may be inserted distal to the stenosis to achieve reliable measurements. This in itself can lead to increased obstruction at the site of the stenosis, with further disturbance of laminar flow.

2.4.2 Coronary Angiography

Quantitative coronary angiography measurements of blood flow are made from epicardial vessel calibre and thus of little value in studying the microcirculation.

2.4.3 Coronary Sinus Thermodilution

Thermodilution techniques are based on the change in temperature of the indicator (saline) usually infused at a lower temperature than the blood. The

indicator is infused into the coronary sinus or great cardiac vein and collected downstream. The change in temperature is proportional to blood flow (White 1988). Thermodilution techniques are limited in that:

1. the measured blood flow cannot be related to the mass of myocardial tissue drained by the sampling vein;
2. anatomical variations in the coronary venous vasculature may severely affect the accuracy of the blood flow measurement;
3. the technique is not sensitive at high flow rates; and
4. the accuracy of blood flow measurement by this method in patients with coronary disease is questionable (Marcus 1987).

In general, global cardiac blood flow measurements are made from coronary sinus blood samples. Regional measurements are restricted to the antero-septal regions of the heart which are drained via the great cardiac vein (Marcus 1987).

2.4.4 Gas Clearance Methods

Clearance techniques enable assessment of myocardial perfusion rather than coronary blood flow. The most commonly used tracer is the inert radioactive gas Xenon-133 (^{133}Xe), administered by intra-arterial injection (Bradley 1986 and L'Abbate 1980). Regional measurements can be achieved by intracoronary injections into the different coronary arteries and the subsequent measurements of the myocardial ^{133}Xe radioactive signal using a multicrystal gamma camera (Bradley 1986). The clearance of ^{133}Xe can be described by a single exponential function. Regional myocardial perfusion can be calculated

from the clearance rate constant and the tissue to blood partition coefficient of ^{133}Xe (L'Abbate 1980). In practice, quantification of regional myocardial perfusion using this technique is hindered by the determination of the partition coefficient, due to the high lipophilicity of ^{133}Xe (Marcus 1987). An alternative technique uses nonradioactive inert gases such as, argon, helium, hydrogen and nitrous oxide that may be given by inhalation. Myocardial perfusion may be calculated from the uptake and washout of the gas with the measurement of coronary arterial and venous samples (Marcus 1987). Similar limitations to the thermodilution method exist such as the inability to measure rapid changes in flow and the problems of variable venous drainage.

2.4.5 Radionuclide Imaging Techniques

More recently a number of radionuclide imaging techniques have emerged for the non-invasive assessment of regional myocardial blood flow. In the past, quantitative measurements of regional blood flow using these techniques have eluded investigators primarily due to technical limitations. These are mainly attenuation correction problems and availability of tracers to study myocardial perfusion. Nowadays, radionuclide imaging techniques are of two main types, dependent upon the radiotracer used. Single photon emission tomography (SPET) uses the properties of single photon emitter radionuclides (mainly $^{99\text{m}}\text{Tc}$, ^{123}I , ^{201}Tl). Positron emission tomography uses the properties of positron emitter radionuclides (mainly ^{15}O , ^{11}C , ^{13}N , ^{68}Ga). Positron emission tomography (PET) together with the use of more appropriate radiotracers, now enables non-invasive quantitative measurement of myocardial blood flow simultaneously in the whole heart (Phelps 1986). The resolution of the current

generation of PET scanners is such that myocardial blood flow can be quantified in small regions of heart muscle and thus, rather than being confined to studying the function of the entire microcirculation derived from a single major epicardial coronary artery as a whole, as in a catheterisation study, more detailed investigation of regional microcirculatory function can be achieved.

2.5 Interplay Between Myocardial metabolism and Coronary Blood Flow

Coronary blood flow is among others, a major determinant of myocardial metabolism under a variety of situations. In normal conditions the heart is able to derive energy from different fuel sources such as fatty acids, glucose, lactate, and ketone bodies (Opie 1991) through the aerobic metabolism. However, there are several factors which affect the utilisation of an individual substrate. These include the plasma concentration of substrate and alternative substrates, myocardial blood flow and oxygen supply, hormone levels and regulatory effects of metabolites arising from the degradation of substrates. The myocardial energy metabolism has been extensively studied in animals during experimental conditions and several comprehensive reviews have been published (Neely and Morgan 1974, Camici 1989 and Opie 1991). However, not all the metabolic changes demonstrated in animals are seen in patients with the various forms of ischaemic heart disease. Possibly, these might be due to differences in the techniques used in experimental models, where individual metabolic changes can be isolated from other factors.

Nevertheless some aspects of the human heart have been studied, among others the effects of dietary state on normal myocardial metabolism at rest that

has been studied invasively in humans by Heiss and co-workers (1977). In the fasting state the free fatty acids are the main source of energy and accounting for 45% of oxygen extraction whilst glucose and lactate account for 17% and 8% respectively. After standardised breakfast the respective values were 41%, 40% and 14%. Thus, although myocardial utilisation of glucose is enhanced during carbohydrate-fed state, free fatty acids still remain an important source of energy.

However, myocardial utilization of different substrates may be affected not only by the dietary state but by work load as it was demonstrated by Camici (1989b) that glucose metabolism is increased during stress induced by atrial pacing and during the recovery period.

In pathological conditions such as in patients with coronary artery disease in which coronary blood flow is reduced, and consequently oxygen delivery is reduced, the metabolism of free fatty acids is inhibited and anaerobic glycolysis increases (Opie 1976 and Camici 1991). During mild ischaemia lactate and other products are washed out from the cell and anaerobic glycolysis can be maintained. However, during severe ischaemia, lactate and protons will accumulate in the myocardium and glycolysis is inhibited, which may contribute to lethal injury (Rovetto 1973). It was observed that lactate was the end product of anaerobic glucose breakdown in both conditions (mild and severe ischaemia) thus, its release has been considered as a metabolic fingerprint of ischaemia (Camici 1989a). Guth and co-workers (1990) confirmed this finding. Their work showed that ischaemia associated with regional dysfunction is

accompanied by increases in lactate release derived both from exogenous glucose and glycogen.

In contrast to normal persons, in whom carbohydrate oxidation is increased during stress, in patients with coronary artery disease oxidation of glucose does not increase in the ischaemic regions (Camici 1991). And although myocardial perfusion returns to baseline values within a few minutes after exercise, higher myocardial glucose utilisation may persist in the nonischaemic muscle, but after stress the increase in myocardial metabolism is more apparent in the ischaemic tissue (Camici 1986). This persistently high glucose utilisation in the post-ischaemic myocardium could indicate a greater flux through glycolysis and/or increased rate of glycogen synthesis, in order to replenish the stores depleted during stress. Based on these observations, it has been proposed that glycolysis has an intimate relationship to the severity of ischaemia, and that it might determine cell viability (Opie 1988). The end product of glycolysis is ATP production. Thus, it was postulated that ATP produced by glycolysis might have a special function in the maintenance of the cell membrane ions gradients and calcium level (Weiss 1987). These concepts support the hypothesis that glycolysis actively contributes to cell viability (Opie 1988). Based on the observation that the uptake of glucose by the myocardium is increased during hypoxia and mild ischaemia and decreased in the presence of severe ischaemia, it has been proposed that monitoring noninvasively the process of glucose transport into the cell would be able to detect viable myocardium in patients suffering from coronary artery disease. This will be the approach used in the present thesis.

Chapter 3

Myocardial ischaemia

3.1 Definition of Myocardial Ischaemia

Under normal circumstances, any increase in cardiac work load is paralleled by a rise in coronary blood flow. This is the *conditio sine qua non* for a physiological cardiac performance. However, if there is a reduction in oxygen delivery either by a primary reduction in coronary blood flow (primary ischaemia, e.g. coronary spasm) or due to an imbalance between oxygen supply and demand (secondary ischaemia, e.g. downstream a coronary stenosis), myocardial ischaemia ensues. In the initial seconds after the initiation of ischaemia, the energy demand of the myocardium most certainly exceeds the reduced energy supply, activating mechanisms that result in a loss of regional contractility in proportion to the loss of blood flow (Gallagher 1980 and Vatner 1980). The potential outcome of myocardial ischaemia is variable (figure 3.1).

In the clinical setting, myocardial ischaemia can be either transient and reversible (angina pectoris) or prolonged, for more than twenty minutes, and irreversible (myocardial infarction) (Reimer 1977). In between these two extremes (angina and infarction) many clinical situations can be recognised in which a variable mixture of viable and necrotic tissue coexist (Camici 1989). In the past it was believed that in these patients, with myocardial ischaemia due to coronary artery disease, regions with left ventricular dysfunction were usually

the consequence of myocardial infarction. Viable myocytes were assumed to be contractile, whereas infarcted myocytes were not. However, with the advent of coronary revascularization and thrombolysis, it has become apparent that the restoration of blood flow to dysfunctional myocardial segments resulted in improved regional and global ventricular function. Thus these viable myocytes with relatively prolonged reversible abnormalities in contractile function have been termed stunned and hibernating myocardium.

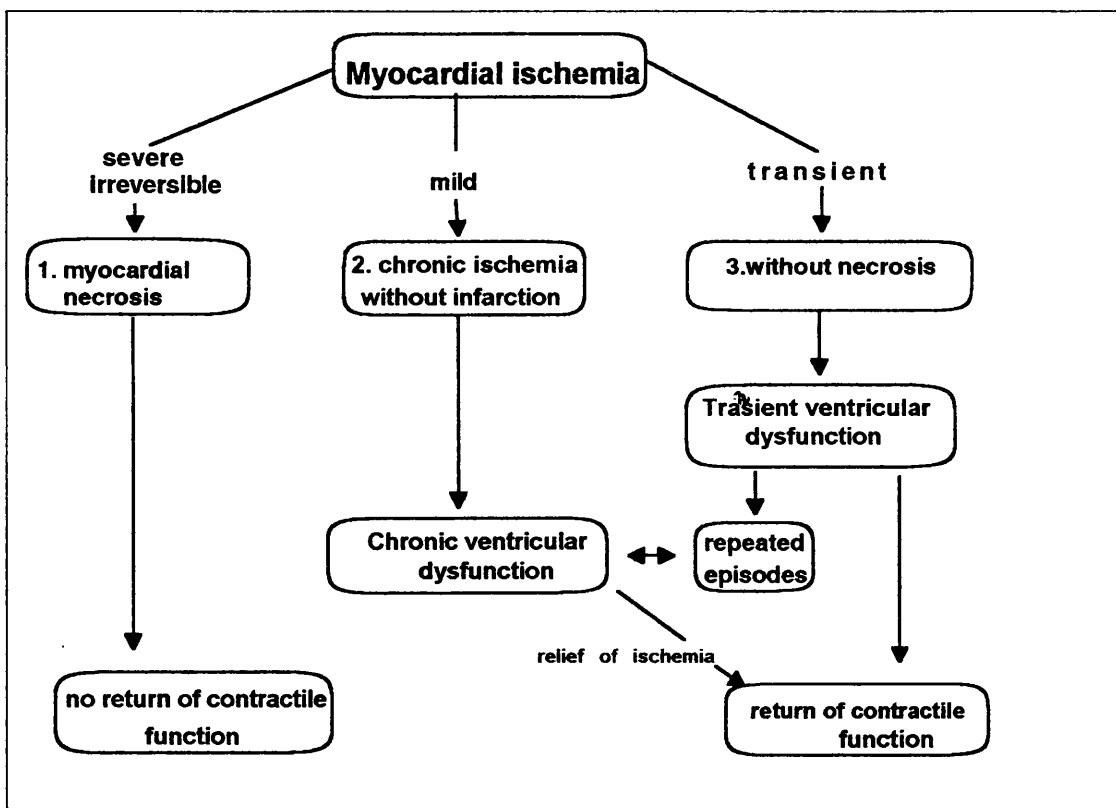


Figure 3.1 - Outcome of myocardial ischaemia.

It is unclear whether or not the mechanisms underlying the contractile dysfunction in hibernating and stunned myocardium are really different (Marban 1991). This thesis will focus in patients with ischaemic heart disease and ventricular wall motion abnormalities who could potentially improve following revascularization (hibernating myocardium).

3.2 Definition of hibernating myocardium

The term "hibernating myocardium" was originally defined as a state of resting hypocontractility thought to be secondary to reduced blood flow, which could be reversed or improved after successful revascularization (Rahimtoola 1985). This definition was based on clinical observations by Rahimtoola 1985, in patients with chronic stable angina who had coronary artery by-pass grafting. From these studies it has become apparent that contractile dysfunction in patients with coronary artery disease does not necessarily correlate with the relative amount of necrotic myocardium.

3.3 Mechanisms of Hibernation

3.3.1 Metabolic down-regulation in response to chronic hypoperfusion

It was originally thought (Ross 1991) that hibernation resulted from a gradual down-regulation of myocardial metabolism, and hence contraction, in response to the reduction in blood flow accompanying the progression of epicardial coronary artery stenosis. This resulted in an equilibrium state in which myocardial perfusion and contraction were matched. Based on this fact it was thought that the contractile dysfunction would be explicable in terms of insufficient energy, in the form of adenosine triphosphate (ATP), to support the energy needs of the contractile apparatus (Hearse 1979). However, this explanation is not acceptable. Although it is well accepted that adenosine triphosphate (ATP) is the ultimate source of energy for the contractile process, the onset of hypocontractility occurs prior to significant changes in the content of myocardial ATP (Guth 1987). Instead, the alternative proposed mechanism

underlying the contractile dysfunction seems to be the relative failure of the excitation-contraction coupling process, a failure that results from a reduced availability of Ca^{+2} for excitation-contraction coupling on a beat-to-beat basis (Marban 1991 and Gasser 1992). To corroborate this hypothesis, coronary flow has been shown to modulate calcium levels, which in turn regulate contractile function (Bristow 1991).

Unfortunately, the development of animal models of chronic, low-flow ischaemia is difficult. However, Matsuzaki in 1983 successfully carried out a 5-hour partial circumflex coronary occlusion in dogs, producing a fall in subendocardial blood flow with a concomitant reduction in wall motion which reversed upon reperfusion. Arai and co-workers in 1991 studied pigs subjected to 70% reduction in transmural blood flow for 60 minutes. Within 5-10 minutes of ischaemia, subendocardial phosphocreatine (PCr) and ATP were depleted to 47% and 63% of control; and net arteriovenous lactate production occurred. Despite continued ischaemia and no significant changes in the external determinants of myocardial oxygen consumption, by 60 minutes subendocardial phosphocreatine and lactate contents returned to control levels and there was net arteriovenous lactate consumption. This study is interesting, in that it shows that there is a time-dependent adjustment in cardiac metabolism that develops fairly rapidly after partial stenosis, with resolution of some metabolic sequelae of ischaemia. This regulation is an active process that is aimed at redressing the oxygen supply-demand imbalance that occurs at the onset of ischaemia, in order to achieve a state of equilibrium in which blood flow, metabolism and contraction are all matched, but at a reduced level

(Bristow 1991). Consequently, these regions subtended by stenotic arteries, by definition are not ischaemic.

Although this is an attractive hypothesis, it is based almost exclusively upon findings from experimental animal studies in which just some features of ischaemia can be mimicked at a time. There is little direct evidence to support it in humans. However, circumstantial supporting evidence has come from several studies (Tillisch 1986 and De Silva 1992) using perfusion imaging in patients with coronary artery disease, which have shown that regions with reversible left ventricular dysfunction may be hypoperfused at rest.

3.3.2 Repeated episodes of myocardial stunning

An alternative hypothesis for the pathogenesis of persistent left ventricular dysfunction has been proposed based on studies in patients with coronary artery disease using positron emission tomography (PET) (Vanoverschelde 1993). Patients with complete occlusion of a proximal coronary artery, filled retrogradely by collateral vessels, both with and without resting left ventricular dysfunction were studied. Patients without left ventricular dysfunction formed the control group. Myocardial blood flow, regional myocardial glucose uptake and oxidative metabolism were measured pre-operatively using PET and were correlated with the histological analysis of tissue biopsies taken at the time of the coronary by-pass graft surgery.

It was shown that myocardial blood flow and oxidative metabolism in asynergic collateralized territories were lower than in the normally contracting remote

regions supplied by angiographically normal coronary arteries. The difference in flow and metabolism between the remote and asynergic region may reflect the greater compensatory workload imposed on the remote regions. It was further demonstrated that myocardial blood flow, regional myocardial uptake and oxidative metabolism were similar in both normally contracting and asynergic collateralised regions.

On histological analysis, myocytes in the dysfunctional collateralized regions showed a number of morphological changes, in particular, reduced number of contractile filaments, glycogen accumulation, reduction of sarcoplasmic reticulum and the appearance of numerous small mitochondria. The ultrastructural features of these organelles were normal.

Therefore, in these patients, the reduction in contractile function in the collateralized regions appeared not to be accompanied by reduced blood flow and metabolism, which argues against the first hypothesis outlined above. Rather, these investigators suggested that left ventricular dysfunction, in this particular group of patients, may have been mediated by serial acute reductions in blood flow owing to repeated episodes of myocardial stunning (Bolli 1992). The mechanisms by which this may occur are not fully understood and have been recently reviewed by Bolli 1992.

The mechanism of myocardial hibernation is still unclear and is the subject of much investigation. Persistent left ventricular dysfunction occurs in a number of clinical situations, in addition to those described by Vanoverschelde 1993 (e.g. unstable angina, chronic stable angina and after myocardial infarction). This

represents a very heterogeneous group of patients and different mechanisms may operate on each group to produce myocardial hibernation.

3.4 The importance of detecting viable (hibernating) myocardium

Viability is a question of concern particularly in patients with myocardial dysfunction either regional or global, because ventricular function does not only reflect ischaemic segments of the myocardium that are jeopardised and might trigger future cardiac events but it also has important prognostic value. This is particularly important in patients with severe left ventricular dysfunction (very low ejection fraction) who may be candidates for coronary artery by-pass surgery as an alternative to cardiac transplantation. In these patients, even small increases in heart function can result in significant improvement in symptoms and survival (Califf 1988), table 3.1.

Reference	EF (%)	Medical treatment			Surgical treatment		
		1year	3 years	5years	1year	3years	5 years
Pigott 1985	< 25	-	-	21	-	-	68
Idem	26-35	-	-	64	-	-	82
Bounous 1988	< 30	86	71	50	88	83	69
Califf 1988	< 35	83	63	53	85	83	82
Elefteriades 1993	< 30	-	-	-	87	87	80

EF = ejection fraction

Table 3.1 - Survival of patients with ejection fraction less than 35%.

However, the operative mortality in this group of patients with very low ejection fraction is higher than usual, varying from 5 to 10% in different series, (table

3.2), and the functional outcome of surgery seems to be dependent on the amount of viable tissue, thus it is of utmost importance to be able to detect the presence of viable myocardium before surgery. Different approaches have been proposed for detection of ischaemic but viable myocardium.

Reference	EF (%) < 40%	OM (%)	EF (%) > 40%	OM (%)
Kennedy 1981	<19	6.7	>50	1.9
Califf 1988	<40	5.1	>60	1.7
Christakis 1992	<40	4.8	>40	2.3
Christakis 1992	<20	9.8	-	-

EF = ejection fraction; OM = operative mortality

Table 3.2 - Operative mortality according to ejection fraction.

3.5 Methods to assess myocardial viability

In order to anticipate the results of revascularization in this subset of patients a general classification may be used:

1. Measurements of regional function abnormalities (Contractile reserve).
2. Evaluation of the extent of perfusion and metabolism abnormalities (Membrane integrity).
3. Determination of the extent of the metabolic abnormality (Metabolic activity).

3.5.1. Contractile reserve

This approach is based on the observation that hibernating and stunned myocardium can be forced to contract (table 3.3). In several studies, cardiac systolic function was monitored by echocardiography (Marzullo 1993), radionuclide ventriculography (Cucchini 1978), or magnetic resonance imaging following a challenge to stimulate contractility, such as inotropic drug administration or postextrasystolic potentiation (Hambly 1975 and Popio 1977).

Methods to assess viability by measuring systolic function

1. Postextrasystolic potentiation
 2. Stimulation
 - isoproterenol
 - dopamine, dobutamine (low dose)
-

Table 3.3 - Methods to assess viability by measuring systolic function

Briefly, postextrasystolic potentiation is typically carried out in the cardiac catheterization laboratory by inducing premature ventricular contractions. This technique is very accurate. However, it relies on repeated ventriculography for the assessment of wall motion and it is linked to an invasive procedure (coronary angiography).

The stimulation alternative is based on the pharmacological action of different substances, such as, isoproterenol, that is a sympathomimetic agent with a very powerful inotropic and chronotropic effect. Often it increases cardiac output and myocardial oxygen requirements despite the frequent reduction in blood pressure caused by peripheral vascular dilation. However, its major drawback is that it may cause life-threatening arrhythmias that might be difficult

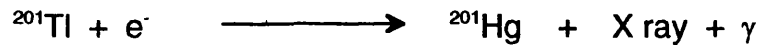
to control. Another substance used is dopamine, that is a precursor of norepinephrine. Its inotropic effect increases cardiac output, myocardial work and indirectly myocardial oxygen demand, thus precipitating ischaemia. Dobutamine may also be used for this purpose. Dobutamine increases heart rate, contractility and after load (blood pressure). It simulates exercise when used in high doses (up to 50µg/kg/min), and acts by inducing ischaemia as happens with dopamine. Nevertheless, when dobutamine is used in low doses (5 to 10µg/kg/min) chronotropic and inotropic effect increase modestly, and afterload may be decreased, causing an increase in contractility in the affected and nonaffected areas of the myocardium.

The studies using these three agents were generally done in small patient populations, which makes extrapolation to larger patient groups difficult (Marcovitz 1992 and Peshock 1992). Apart from the restricted number of patients studied, all these techniques had their safety questioned despite few complications had been reported. The concern raised is about the conceptual possibility that in the setting of a critically stenosed coronary artery, the administration of an inotropic agent could worsen ischaemia and regional dysfunction.

3.5.2. Membrane integrity

Because cell survival ultimately depends on the preservation of cell integrity, its measurement is used as an index of viability. Tracers like the potassium analogue ²⁰¹Tl (Mullins 1960 and Gehring 1967), whose uptake and retention require not only tracer delivery (perfusion), but also integrity of the sarcolemma

(that indirectly reflects metabolic function), have been used to assess viable tissue. Thallium-201 is a cyclotron produced radioisotope with a physical half-life of 72 hours. It decays by electron capture to mercury-201 emitting gamma photons of 135 and 167 keV (12% abundance) and 80 keV X-ray from mercury (95% abundance) (Strauss 1975).



After intravenous injection, approximately 87% is cleared from the blood in the first circulation. The myocardium reaches its maximum tissue concentration of about 4% of the total injected dose in the first 10 to 25 minutes after the injection (Bradley-Moore 1975) and once within the heart, thallium-201 is eliminated in two phases. The first phase eliminates 78% of the thallium in 4.4 hours and the remaining 22% is eliminated in 40 hours (Bradley-Moore 1975). This slow "washout" leads to an equilibrium between the intracellular and intravascular compartment. This means that thallium-201 redistributes along the time, with "washout" different rates in normal and ischaemic regions. Areas of ischaemia show slow washout, so much that with time they reach similar activity to areas with normal perfusion that have faster wash out.

In practical terms, the image immediately after injection (during stress) reflects myocardial perfusion and the late image (redistribution image) reflects primarily the distribution of viable cells and myocardial perfusion at rest. In regions with no thallium-201 activity during stress that did not change in the routine redistribution images were believed to represent an infarcted tissue. However, several studies (table 3.4) have shown that these regions with no thallium-201 redistribution occurred frequently in severely ischaemic, but viable myocardium (hibernating myocardium). In addition, it was shown that they recovered

inotropic function after revascularization. Thus, in these particular cases, thallium-201 was overestimating the extent of infarcted myocardium and consequently underestimating viable myocardium. When PET studies were carried out in patients showing fixed perfusion defects with thallium-201 it was demonstrated that 40 to 47% of these myocardial regions had preserved glucose metabolism, indicating that they were not scarred but contained viable tissue (Tamaki 1988 and Brunken 1987 and 1989) .

In order to solve the problem of detecting viable tissue missed by the usual thallium-201 stress-redistribution technique a number of approaches have been proposed:

1. Late thallium-201 redistribution image (Kiat 1988)
2. Thallium-201 reinjection technique (Dilsizian 1990)
3. Thallium-201 reinjection and late redistribution image (Dilsizian 1991)
4. Rest- redistribution thallium-201 images (Mori 1991)

Reference	Patients(n)	Method	Comments
Berger (1979)	22	R-Red	72% of the fixed defects improved after surgery
Rozanski (1981)	25	S-Red	10% of fixed defects improved rwm and perfusion after revascularization
Gibson (1983)	47	S-Red QA	50% of the regions with fixed defect improved after surgery
Iskandrian (1983)	26	R-Red	80% of the fixed defects improved rwm and perfusion after revascularization
Brundage (1984)	23	S-Red	Tl-201 immediately after surgery may be abnormal (1/3 of the patients) and improve during follow-up (stunning and hibernating)
Liu (1985)	52	S-Red	75% of the fixed defects improved after surgery
Manyari (1988)	43	S-Red	Tl-201 improved progressively after revascularization in 12 out of 43 patients
Fioretti (1988)	25	S-Red	improvement of persistent defects after CABG
Kiat (1988)	21	S-Red	72% of the fixed defects (4 h) improved after surgery. 37% of the fixed defects at the late image (24h) improved as well
Ohtani (1990)	24	S-Red-Reinj	(14/30)47% of the regions with fixed defect improved rwm after surgery. (12/45) 27% with redistribution after reinjection did not improve
Dilsizian (1990)	20	S-Red-Reinj	none of the fixed defects improved perfusion and rwm after surgery
Takeishi (1991)	45	S-Red	10% of the fixed defects improved perfusion and rwm after revascularization
Mori (1991)	17	R-Red	38% of the fixed defects improved perfusion and rwm after revascularization.
Kuijper (1993)	26	S-Reinj	23% (7/30) of the fixed defects improved after revascularization
Ragosta (1993)	21	R-Red	19% of segments with <50% of peak tl-201 activity improved rwm after surgery.

S = stress; Red = redistribution; Reinj = reinjection; R = rest; QA = qualitative assessment; CABG = coronary artery by-pass graft; rwm = regional wall motion

Table 3.4 - Thallium-201 studies with follow-up after revascularization

3.5.2.1 Late thallium-201 redistribution image

Late thallium-201 redistribution was proposed as an alternative. It consisted of post-stress imaging acquisition (delayed 12 to 36 hours). It was initially demonstrated with planar thallium (Gutman 1983), and confirmed afterwards with both planar (Takemoto 1991 and Kayden 1991) and SPET (Kiat 1988 and Cloninger 1988) that substantial thallium redistribution occurred in defects that seemed to be irreversible (or fixed) in the 3 to 4 hours redistribution study. This was consistent with the presence of viable myocardium (table 3.5).

Reference	Patients (n)	Comments
Gutman (1983)	59	late redistribution on 21% of Tl-201 fixed defects at 4 hours
Kiat (1988)	21	late redistribution on 61% of Tl-201 fixed defects at 4 hours
Cloninger (1988)	40	late redistribution on 60% of the incomplete redistributed segments at 4 hours
Yang (1990)	118	late redistribution on 22% of the Tl-201 fixed defects at 4 hours
Takemoto (1991)	90	late redistribution on 9% of the Tl-201 fixed defects at 4 hours
Kayden (1991)	41	27% had reversibility detected by 24h redistribution image

Table 3.5 - Studies using late thallium-201 redistribution image

The explanation for this late reversal of thallium defects at 4 hour is believed to be related to the coronary blood flow, first in terms of the severity of ischaemia induced during exercise. The ischaemic insult might be still significant even when exercise is finished, limiting the delivery of thallium. Second, it may, as well, be related to the level of thallium concentration in the serum in the interval between exercise and redistribution images (Budinger 1986). That means that even if late images are taken, some ischaemic regions may never redistribute unless serum thallium levels are augmented (Budinger 1987). This was

demonstrated in a study by Kiat in 1988. He showed that 37% of the late nonreversible segments improved function after surgery. However, it should still be taken into account that this approach requires: 1) a longer acquisition time for the third set of images and, 2) frequently the quality of the images obtained with a single thallium-201 injection after 24 hours is suboptimal (Kayden 1991).

3.5.2.2 Thallium-201 reinjection technique

The second alternative approach proposed is the reinjection of thallium-201.

There are several variations for this approach:

1. Slow intravenous infusion of thallium after stress images (Burns 1990).
2. Reinjection after completion of initial postexercise images (Kiat 1990).
3. Stress-reinjection and no redistribution images (Van der Wall 1993).
4. Stress-redistribution and reinjection images (Dilsizian 1990).

Preliminary results show that the first three methods do not only produce suboptimal results but may underestimate myocardial viability and/or are unpractical to be performed. For this reason the fourth variation is going to be focused. It consists of injecting thallium at rest immediately after the standard 3 to 4 hours redistribution study followed by another acquisition. The image obtained is a composite of two distribution patterns: redistribution and regional myocardial blood flow at rest. This approach has been used in clinical environment more than the others (slow intravenous infusion of thallium (Burns 1990) or reinjection after completion of initial postexercise images (Kiat 1990). The stress-redistribution and reinjection technique (Dilsizian 1990) shows

about 30 to 50% improvement in the thallium uptake on previous fixed or irreversible defects (table 3.6).

Reference	Patients (n)	Comments
Dilsizian (1990)	92	49% of the fixed defects improved after reinjection
Tamaki (1990)	60	32% of the fixed defects showed new fill-in after reinjection
Ohtani (1990)	24	47% improvement in fixed defects after reinjection
Rocco (1990)	41	31% improvement in fixed defects after reinjection
Cuocolo (1992)	20	47% improvement in fixed defects after reinjection
Lekakis (1993)	20	32% improvement in fixed defects after reinjection

Table 3.6 - Studies using stress-redistribution and reinjection

From the studies using the reinjection technique only two (Dilsizian 1990 and Ohtani 1990) correlated the new fill-in after reinjection and recovery of function after surgery. In the first study they predicted improvement in 13 out of 15 segments (positive predictive accuracy = 87%) and they predicted no improvement in none of the segments with fixed defects (negative predictive accuracy = 100%). In the second study (Ohtani 1990), they have predicted recovery in 12 out of 15 segments (positive predictive accuracy = 80%) and they have predicted no improvement in 14 out of 17 segments (negative predictive accuracy = 82%). The main problem with these figures are that they have been generated from a small group of patients (n = 44) (Dilsizian 1990, n = 20; Ohtani 1990, n = 24). However, despite of the small number these data have provoked interest and it has being compared with PET, as a golden standard (table 3.7).

Reference	Patients (n)	Method	Comments
Bonow (1991)	16	S-Red-Reinj	Tl-201 identified (31/35) 89% and (29/33) 88% of metabolic and nonmetabolic active segments
Perroni-Filardi (1992)	25	S-Red-Reinj	Tl-201 identified all metabolic active segments (100%) and (30/35)86% of nonmetabolic active segments
Perroni-Filardi (1994)	23	S-Red-Reinj	Tl-201 identified 39 fixed defects, of these (29/39) 74% had normal FDG uptake, the remaining 26% had reduced tl-201 uptake
Dilsizian (1994)	25	S-Red-Reinj	Tl-201 identified 94% of the viable regions by PET

Table 3.7 - Comparison between ^{201}Tl and ^{18}F -Fluorodeoxyglucose uptake in fixed defects (<50% of maximal activity).

Although, it seems that thallium reinjection results are comparable with those of [^{18}F]2-fluoro-2-deoxy-D-glucose (^{18}F -FDG) PET imaging, especially if quantitative thallium (normalised to maximum uptake is used), it became apparent from these studies above that not all thallium defects are alike, and that the severity of reduction in thallium activity is importantly related to the likelihood of metabolic assessment by ^{18}F -FDG uptake. From the available data it was thought that one potential limitation of the reinjection protocol would be the short time period between the reinjection and repeated imaging, that would not allow for further redistribution of the reinjected dose.

3.5.2.3 Thallium-201 reinjection and late redistribution image

For this purpose, it was introduced the protocol of thallium-201 reinjection and late redistribution image. Dilsizian (1991) showed that only 4 of the 35 (11%) myocardial regions without thallium uptake on the early post-reinjection study showed evidence of late post-reinjection thallium uptake. This involved 3 of the 50 patients (6%). The same observation has been confirmed later by a subsequent study (McCallister 1991). With this evidence there was no point in keeping with this protocol.

However, even with the thallium reinjection technique with early images there was a logistic problem of performing three sets of images in patients if the clinical question was myocardial ischaemia at rest. To overcome this issue, it has been proposed thallium imaging to be performed at rest, and thus the introduction of the resting-redistribution protocol.

3.5.2.4 Rest- redistribution thallium-201 images

This approach (table 3.8), however, still underestimates the amount of viable tissue, especially if compared with the stress-redistribution with early reinjection images. One possible reason for that is that the image derived from exercise or pharmacological stress could create more flow heterogeneity and hence have more potential for demonstrating reversal on subsequent images in regions with reduced perfusion at rest (Dilsizian 1993).

Reference	Patients (n)	Comments
Berger (1979)	22	72% of the fixed defects improved after CABG
Gerwitz (1979)	20	resting MBF in the presence of severe CS may or may not be normal
Iskandrian (1983)	26	22% of the patients with fixed defect improved rwm after surgery but not thallium images (QA)
Mori (1991)	17	100% of the segments with fixed defects with initial Tl-201 uptake of $72 \pm 6\%$ did not improve after surgery
Ragosta (1993)	21	23% of the segments with >50% reduction of peak Tl-201 uptake and no redistribution improved after surgery

MBF = Myocardial blood flow, CS = Coronary stenosis, QA= qualitative assessment, rwm = regional wall motion

Table 3.8 - Rest-redistribution studies

From the results above, there is still a percentage of patients that will have improvement in dysfunctional left ventricular segments despite the presence of fixed defects.

The third general approach used to assess viability and the one considered to be the more accurate is tracing the pathophysiological aspects of myocardial metabolism.

3.6 Metabolic activity

3.6.1 Myocardial Metabolism

Bing and coworkers in 1947 used coronary sinus catheterization to perform what is considered the first study of myocardial metabolism. Their procedure is based on the combined catheterisation of the coronary sinus and artery with measurements of substrate concentrations in simultaneously drawn blood samples. This approach, however, has several limitations: the spatial resolution is very crude and temporal resolution modest; regional information is limited to the territory of distribution of the left anterior descending artery.

The introduction of PET has made it possible to study regional myocardial metabolism in humans noninvasively (Figure 3.2). PET has been used to study different metabolic processes in myocardium such as amino acids utilization and protein turnover, but the main focus attention has been the study of energy metabolism. Techniques using single photon emission tomography (SPET) have also been used to assess oxidative metabolism by labelling free fatty acids (FFA) with radioiodine, ¹²³I.

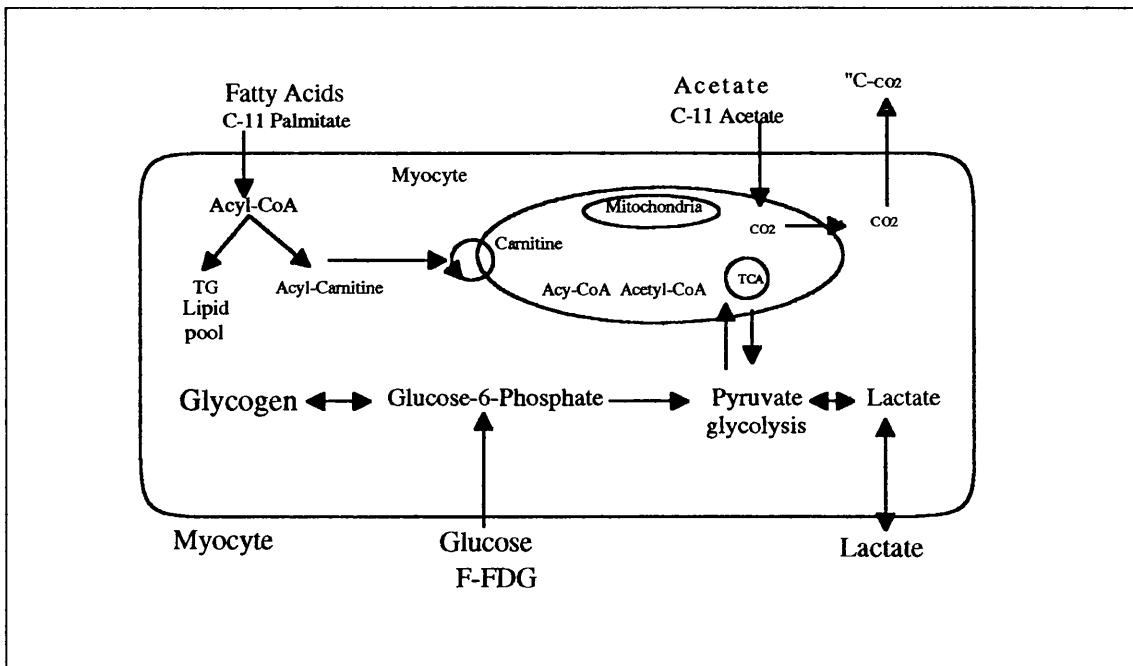


Figure 3.2 - Cardiac Metabolism (Adapted from Schwaiger 1991).

3.6.2 Oxidative Metabolism

In the postabsorptive state the normoxic heart relies mainly upon oxidation of the free fatty acids (FFA) as its main source of high energy phosphates while the uptake and oxidation of carbohydrates (glucose, lactate and pyruvate) is low (figure 3.2).

In the fed state, the uptake of carbohydrate is high and accounts for virtually all of the concurrent oxygen uptake (Camici 1989). This change from predominantly carbohydrate to predominant lipid usage is explained by the glucose free fatty acids cycle of Randle. An important observation was that the oxidation of glucose by the isolated rat heart was markedly inhibited by the concurrent provision of free fatty acids (Camici 1989). The factors that regulate myocardial substrate utilization are complex and depend, in addition to arterial substrate concentration, upon the hormonal milieu. Insulin which stimulates

myocardial glucose uptake and utilization also inhibits adipose tissue lipolysis, so that the circulating free fatty acids are low (Camici 1989). Catecholamines decrease rather than increase glycolysis in the heart together with a greatly increased uptake and oxidation of free fatty acids (Camici 1989). Myocardial utilization of carbohydrates is also affected by cardiac workload, and oxidation of carbohydrates accounts for more than 50% of energy produced during conditions of maximal stress (Camici 1989 and Marraccini 1989). Finally, glucose utilization is increased during conditions of reduced oxygen supply; under these circumstances exogenous glucose uptake and glycogen breakdown are increased, glycolysis and ATP can be produced from the anaerobic catabolism of glucose with concomitant formation of lactate (Camici 1989).

To measure the flux of free fatty acids during normoxic and ischaemic condition, the natural free fatty acid palmitate has been labelled with carbon-11 (^{11}C -palmitate).

3.6.2.1 ^{11}C -palmitate

Free fatty acids are transported in plasma loosely bound to serum albumin. Extraction of fatty acids by myocardium is dependent on the ratio of free fatty acids to albumin, the chain length of the fatty acids and their saturation. In general, extraction of long-chain fatty acids is higher than of short-chain fat acids. Palmitic acid and oleic acid are most avidly extracted by the myocardium. Although the clearance of ^{11}C -palmitate from the myocardium was related to the degree of oxidative metabolism, quantification of utilisation rates was not

possible due to the over-complexity of the model required to explain the behaviour of ^{11}C -palmitate in tissue (Schelbert 1983). Apart from this problem, interpretation of myocardial uptake and clearance of ^{11}C -palmitate is further complicated by the dependence of these two parameters on the prevailing blood flow and dietary state. During ischaemia, oxidation of fatty acid is reduced disproportionately to the reduction in oxygen consumption and approximately 50% of intact ^{11}C -palmitate (not metabolized) back-diffuses. Therefore, in this condition, the external detection of the clearance of ^{11}C -palmitate from the heart could overestimate myocardial oxidative metabolism of fatty acids. For this reason its value in differentiating viable from nonviable myocardium appears to be limited (Fox 1985).

3.6.2.2 ^{11}C -acetate

^{11}C -palmitate reflects only part of the oxidative metabolism, for this reason an alternative approach by using ^{11}C -acetate has been proposed, in order to evaluate the overall oxidative metabolism. Carbon-11 labelled acetate (^{11}C -acetate) has been advocated as a tracer of tricarboxylic acid cycle (TCA) activity (Buxton 1988) and has been used as an indirect marker of myocardial oxygen consumption (MVO_2) by positron emission tomography in both experimental animals (Brown 1988, Buxton 1989 and Armbrecht 1990) and humans (Armbrecht 1989 and Walsh 1989). A number of studies have shown that the rate constant describing the clearance of ^{11}C -acetate from the myocardium correlates well with catheter measurements of oxygen extraction fraction from analysis of arterio-venous differences of blood oxygen content using the Fick Principle (Buxton 1989, Armbrecht 1989 and Walsh 1989).

However, the lack of appropriate models which accurately describe the complex tissue kinetics of ^{11}C -acetate have prevented absolute quantification of myocardial oxygen consumption using this tracer. In addition, measurements of myocardial oxygen consumption using this tracer will be subject to blood flow constraints similar to those encountered during measurements made using labelled free fatty acids. However, the initial results of the use of this tracer are promising and seems to differentiate viable from nonviable myocardium (Gropler 1993). An important consideration when using this tracer is that the standardisation of substrate environment is not a crucial problem (Brown 1989) as it is with free fatty acids. This seems to be a promising approach to come.

3.6.2.3 Iodophenylpentadecanoic acid (IPPA) and beta-methyliodopentadecanoic acid (BMIPP)

These two tracers are labelled with radioiodine and can be detected by conventional single photon emission tomography imaging equipment. As all the previous free fatty acids they exchange across the sarcolemmal membranes along a concentration gradient, possibly through facilitated transport. They are trapped into the cell by a reaction that requires energy and then converted to acyl-Coenzyme A (figure 3.3). At this level their fate are different: BIMPP is stored into the lipid pool of glycerides and phospholipids. IPPA is oxidated and clears from the myocardium bound to benzoic acid, which is excreted by the kidney.

Although their kinetic properties are different, both trace the initial energy requiring step, thus providing a measure of viability.

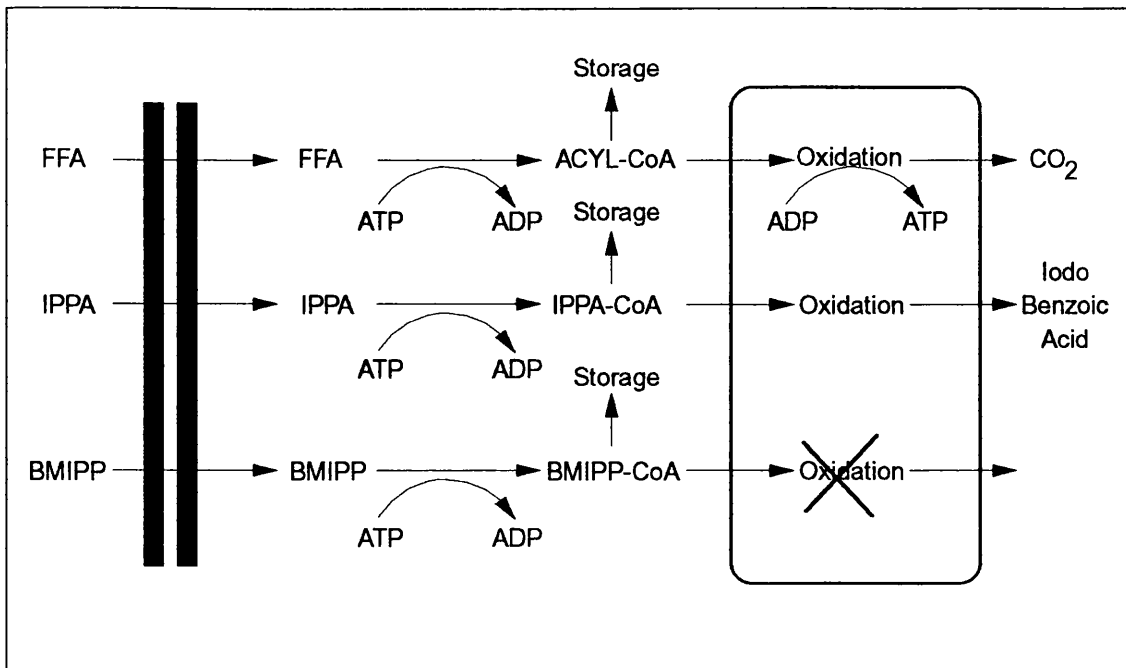


figure 3.3 - Schematic representation of major metabolic fate of free acid (FFA) and iodinated analogs in myocardium. ADP, Adenosine diphosphate; CoA, coenzyme A.

3.6.3 Glucose Utilisation

The utilization of exogenous glucose by the myocardium can be assessed with [¹⁸F]-2-fluoro-2-deoxyglucose (¹⁸F-FDG) as a tracer (Gallagher 1978). ¹⁸F-FDG is a glucose analogue that has a hydroxyl group substituted by a hydrogen atom in the second carbon; it traces the initial components of the metabolism of glucose by the heart, including transmembranous transport and hexokinase phosphorylation (figure 3.4). ¹⁸F-FDG transport and phosphorylation is essentially a unidirectional reaction and results in ¹⁸F-FDG-6-phosphate accumulation within the myocardium, as no glucose-6-phosphatase (the enzyme that can hydrolyse ¹⁸F-FDG-6-phosphate back to free ¹⁸F-FDG and free phosphate) has yet been identified in cardiac muscle (Gallagher 1978). Thus, measurement of the myocardial uptake of ¹⁸F-FDG is proportional to the overall rate of trans-sarcolemmal transport (Ratib 1982) and hexokinase-phosphorylation of exogenous (circulating) glucose by heart muscle. Measurement of myocardial

^{18}F -FDG uptake by PET, however, does not provide any information about the further intracellular disposal of glucose (i.e. glycogen synthesis, glycolysis or pentose shunt).

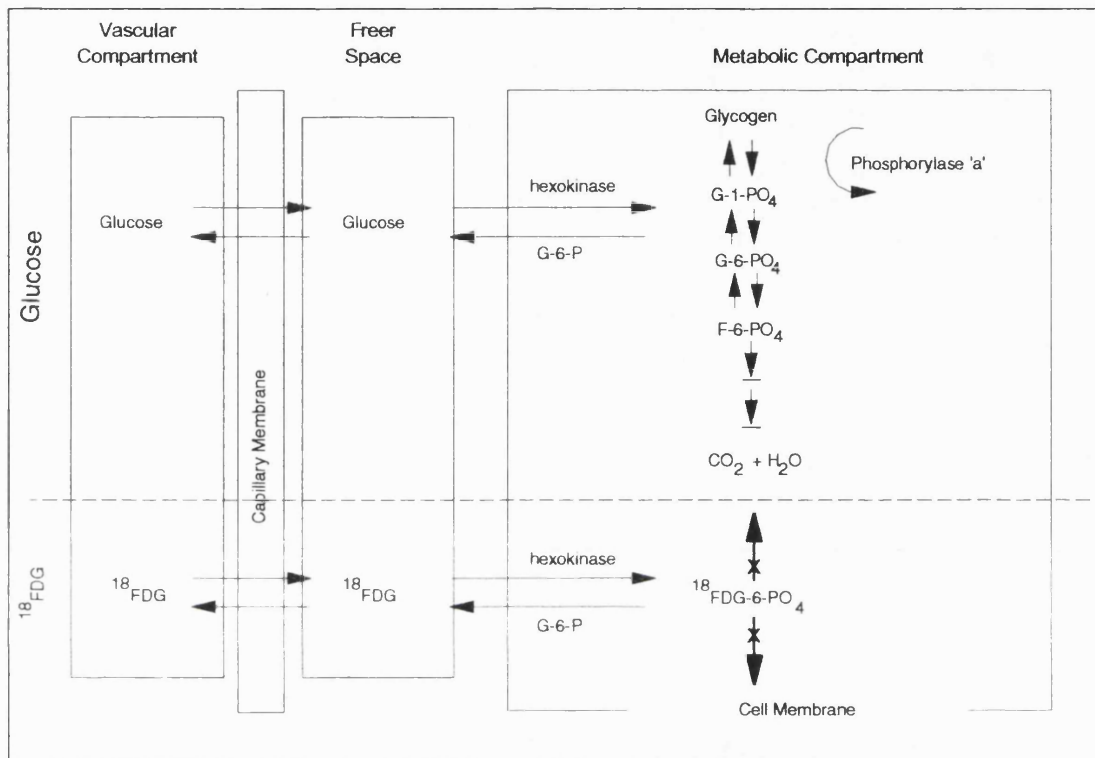


figure 3.4 - Simplified schematic representation of myocardial utilization of glucose and a physiologic analog, 2-deoxyglucose labelled with F-18 (^{18}F -FDG). G-6- PO_4 is glucose-6- PO_4 ; G-1- PO_4 is glucose-1- PO_4 ; F-6- PO_4 is fructose-6- PO_4 . ^{18}F -FDG competes with glucose for transport sites in the capillary and cell membrane and for hexokinase, the enzyme for converting glucose to glucose-6- PO_4 . ^{18}F -FDG is trapped in myocardial cells as ^{18}F -FDG-6- PO_4 , since the enzymatic conversion to G-1- PO_4 and F-6- PO_4 is inhibited by the 2-deoxy analog of glucose and low membrane permeability to DG-6- PO_4 . Slow tissue clearance of ^{18}F -FDG-6- PO_4 , shown in this work indicates that cellular concentration of glucose-6-phosphatase (G-6-P), which converts ^{18}F -FDG-6- PO_4 back to ^{18}F -FDG, must be low. Note that glycolysis can occur from both exogenous (cellular glycogen) sources, whereas ^{18}F -FDG is specific to the exogenous route.

Until recently, PET-derived glucose uptake measurements have been qualitative or semiquantitative because of the difficulty in estimating a value known as the lumped constant (table 3.9).

A number of kinetic modelling approaches have been used for the quantification of glucose utilization rates using ^{18}F -FDG (Huang 1986). The model applied in this thesis is the one proposed by Gambhir and coworkers in 1989. The major limitation of all these approaches is:

1. that quantification of glucose metabolism requires the knowledge of the lumped constant, a factor which relates the kinetic behaviour of FDG to naturally occurring glucose in terms of the relative affinity of each molecule for trans-sarcolemmal transporter and for hexokinase. Unfortunately, the value of the lumped constant in humans under different physiological and pathophysiological conditions is not known, thus making true in vivo quantification of myocardial metabolic rates of glucose very difficult. The lumped constant for this study has been defined as 1.0.
2. These models also assume that metabolic conditions such as plasma glucose and metabolic rate of glucose utilization remains constant during all the data acquisition. However, oral glucose loading, widely used in PET studies does not produce metabolic steady state, what might produce errors in the calculated metabolic rate of glucose utilization. An alternative approach to tackle this problem is to quantitate the uptake of ^{18}F -FDG under standardized dietary conditions using the insulin clamp (Ferrannini 1993) that allows comparison of absolute values from different individual and might help to establish rates of glucose utilization (in ^{18}F -FDG units) in normal and pathologic myocardium.

Reference	Number and type of subjects	Dietary state	Analysis of images	Comparison to other methods	follow up	Comments
Marshall 1983	15 recent MI, 1 DM	glucose load	Circumferential ¹⁸ F-FDG/ flow profile	¹³ N-ammonia	no	-
Tillisch 1986	17, 14 post MI, 2 recent MI	glucose load	Circumferential ¹⁸ F-FDG/ flow profile	¹³ N-ammonia	yes	¹⁸ F-FDG uptake relative to flow predicts late recovery
Camici 1986a,b	22, 12 CAD, 10 normal	Fasting, post-exercise	semiquantitative	⁸² Rb	no	¹⁸ F-FDG uptake is enhanced in previously ischaemic regions
Brunken 1986	20, post MI, 2 with DM	glucose load	Circumferential ¹⁸ F-FDG/ flow profile	¹³ N-ammonia	no	54% of Q-wave regions show preserved ¹⁸ F-FDG uptake
Schwaiger 1986	13, acute MI	fasting	Circumferential ¹⁸ F-FDG/ flow profile	¹³ N-ammonia	no	Half of segments with reduced flow and impaired function show ¹⁸ F-FDG uptake
Brunken 1987	12, CAD, fixed ²⁰¹ Tl defects	glucose load	Circumferential ¹⁸ F-FDG/ flow profile	¹³ N-ammonia	no	58% of fixed ²⁰¹ Tl defects show ¹⁸ F-FDG uptake
Fudo 1988	22, post MI	after 5 hours fasting	Circumferential ¹⁸ F-FDG/ flow profile + visual analysis	¹³ N-ammonia	no	Increase of ¹⁸ F-FDG uptake is common in hypoperfused areas
Tamaki 1988	28, post MI	fasting	visual analysis	¹³ N-ammonia, ²⁰¹ Tl SPECT	no	40% of fixed ²⁰¹ Tl defects show ¹⁸ F-FDG uptake
Hashimoto 1988	22, CAD, 11 post MI	fasting	Circumferential ¹⁸ F-FDG/ flow profile + visual analysis	¹³ N-ammonia	no	Preserved ¹⁸ F-FDG uptake is common in Q-wave regions
Tamaki 1989	22, CAD, 17 post MI	fasting	Circumferential ¹⁸ F-FDG/ flow profile + visual analysis	¹³ N-ammonia	yes	¹⁸ F-FDG uptake relative to flow predicts the late recovery
Brunken 1989	26, post MI	post-prandial	Circumferential ¹⁸ F-FDG/ flow profile	¹³ N-ammonia ²⁰¹ Tl SPECT	no	Preserved ¹⁸ F-FDG uptake common in perfusion defects
Grople 1990	9, normal	fasting and glucose loading	semiquantitative	¹¹ C- acetate, ¹⁵ O-water	no	Heterogeneity in ¹⁸ F-FDG uptake at fast
Nienaber 1991	12, 8 stable, 4 unstable angina	glucose load (25g)	Circumferential ¹⁸ F-FDG/ flow profile + visual analysis	¹³ N-ammonia	yes	¹⁸ F-FDG uptake relative to flow predicts the late recovery

Table 3.9 - Studies using ¹⁸F-FDG and positron emission tomography.

Reference	Number and type of subjects	Dietary state	Analysis of images	Comparison to other methods	follow up	Comments
Hicks 1991	9, normal	insulin clamp	quantitation	¹¹ C-acetate	no	Lower rMGU in septum compared to lateral wall
Tamaki 1991a	18, 14 post MI, 11 with follow-up	fasting	semiquantitative	²⁰¹ Tl SPECT, reinjection	yes	Reinjection of ²⁰¹ Tl identifies viable tissue
Tamaki 1991b	31, 10 normal, 21 CAD, 3 with DM	fasting (7 after glucose loading)	semiquantitative vs quantitative	-	no	Simple quantitation. Heterogenous uptake at fast
Bonow 1991	16, CAD and LV dysfunction	glucose load	semiquantitative (normalization)	²⁰¹ Tl SPECT, reinjection	no	Reinjection of ²⁰¹ Tl identifies viable tissue
Gropler 1992	16, CAD, 11 post MI, 3 recent MI	post-prandial	¹⁸ F-FDG uptake relative to flow	¹⁵ O-water, ¹¹ C-acetate	yes	Variable ¹⁸ F-FDG uptake in viable and non-viable regions
Eizman 1992	82, CAD LV dysfunction	glucose load	visual analysis	¹³ N ammonia	yes	¹⁸ F-FDG predicts clinical outcome
de Silva 1992	12 post MI (8 with ¹⁸ F-FDG)	glucose load	semiquantitative (normalization)	¹⁵ O-water, echocardiography	yes	PTI correlates well with ¹⁸ F-FDG uptake and functional recovery
Althoefer 1992	46, CAD, 43 post mi	glucose load	semiquantitative (normalization)	^{99m} Tc-MIBI perfusion SPECT	no	Preserved ¹⁸ F-FDG uptake common in perfusion defects
Marwick 1992	16, post MI	fasting, post exercise	semiquantitative (normalization)	Rubidium-82, echocardiography	yes	
Perroni-Filardi 1992a	25, CAD and LV dysfunction	glucose load	semiquantitative (normalization)	Radionuclide ventriculography, NMR, ¹⁵ O-water	no	Preserved ¹⁸ F-FDG uptake common in dysfunctional and thinned myocardium
Perroni-Filardi 1992b	25, post MI	glucose load	semiquantitative (normalization) ¹⁸ F-FDG uptake relative to flow	¹⁵ O-water, ²⁰¹ Tl SPECT, NMR	no	Moderately reduced ¹⁸ F-FDG uptake represents viable myocardium
Vanovershelde 1992	15, acute MI no DM	glucose infusion	relation of ¹⁸ F-FDG uptake to flow + quantitation	¹³ N ammonia, ¹¹ C acetate	no	

CAD = Coronary artery disease, DM = Diabetes mellitus, MI = Myocardial infarction, SPECT = Single photon emission tomography

Table 3.9 - continuation - Studies using ¹⁸F-FDG and positron emission tomography.

3.6.3.1 [^{18}F]2-fluoro-2-deoxy-D-glucose (^{18}F -FDG) Imaging and Myocardial Ischaemia

An epicardial coronary artery stenosis reduces the increase in coronary blood flow available during stress when an increase in myocardial oxygen demand occurs. Most of our knowledge on myocardial metabolism comes from work on isolated perfused animal hearts in normoxic and anoxic conditions. Ischaemia is the commonest situation to reduced myocardial oxygen delivery in man, and many different factors determine the duration, severity and extent of ischaemia (Maseri 1983). ^{18}F -FDG is selectively taken up by the myocardial cells which have been rendered ischaemic, even for a few minutes (Camici 1986). This approach lends itself particularly well to the study of ischaemia caused by provocation tests that do not increase myocardial work, as this by itself stimulates glucose uptake in non-ischaemic myocardial cells.

During myocardial ischaemia, major changes occur in intracellular substrate metabolism: there is an increased glycogen breakdown and exogenous glucose uptake which fuel glycolysis (Camici 1989 and Opie 1973) (Figure 3.5). Accumulation of reduced coenzymes (NADH_2) stimulates the conversion of pyruvate to lactate by lactate dehydrogenase. With mild ischaemia, the transport of glucose into the cell is accelerated, as is glycolysis. However, the distal products of glycolysis, lactate and reduced coenzymes, will finally inhibit the enzyme glyceraldehyde 3-phosphate dehydrogenase lower down the Embden-Meyerhof pathway (Rovetto 1975). Although there is an increase in glucose uptake, carbohydrate oxidation is negligible. With the return of myocardial oxygen delivery, lactate is oxidised back to pyruvate with restoration

of depleted glycogen store to pre-ischaemic levels. The time required to return to the pre-ischaemic metabolic pattern is prolonged with persisting high glucose uptake, probably for glycogen re-synthesis, more in post-ischaemic than normal myocardium (Camici 1989b). This persistence of high glucose uptake in post-ischaemic myocardium is the underlying principle which allows the identification of transiently ischaemic myocardium using ^{18}F -FDG with PET.

With severe ischaemia, the rate of exogenous glucose delivery is also reduced. Under these circumstances, the ischaemic myocardium will rely almost exclusively on intracellular glycogen stores. However, the insufficient "washout" of accumulated hydrogen ions and the resulting intracellular acidosis will inhibit phosphofructokinase, and thus, glycolysis much earlier than with mild ischaemia. Thus, the uptake and intracellular utilisation of glucose is modulated by the presence and severity of ischaemia.

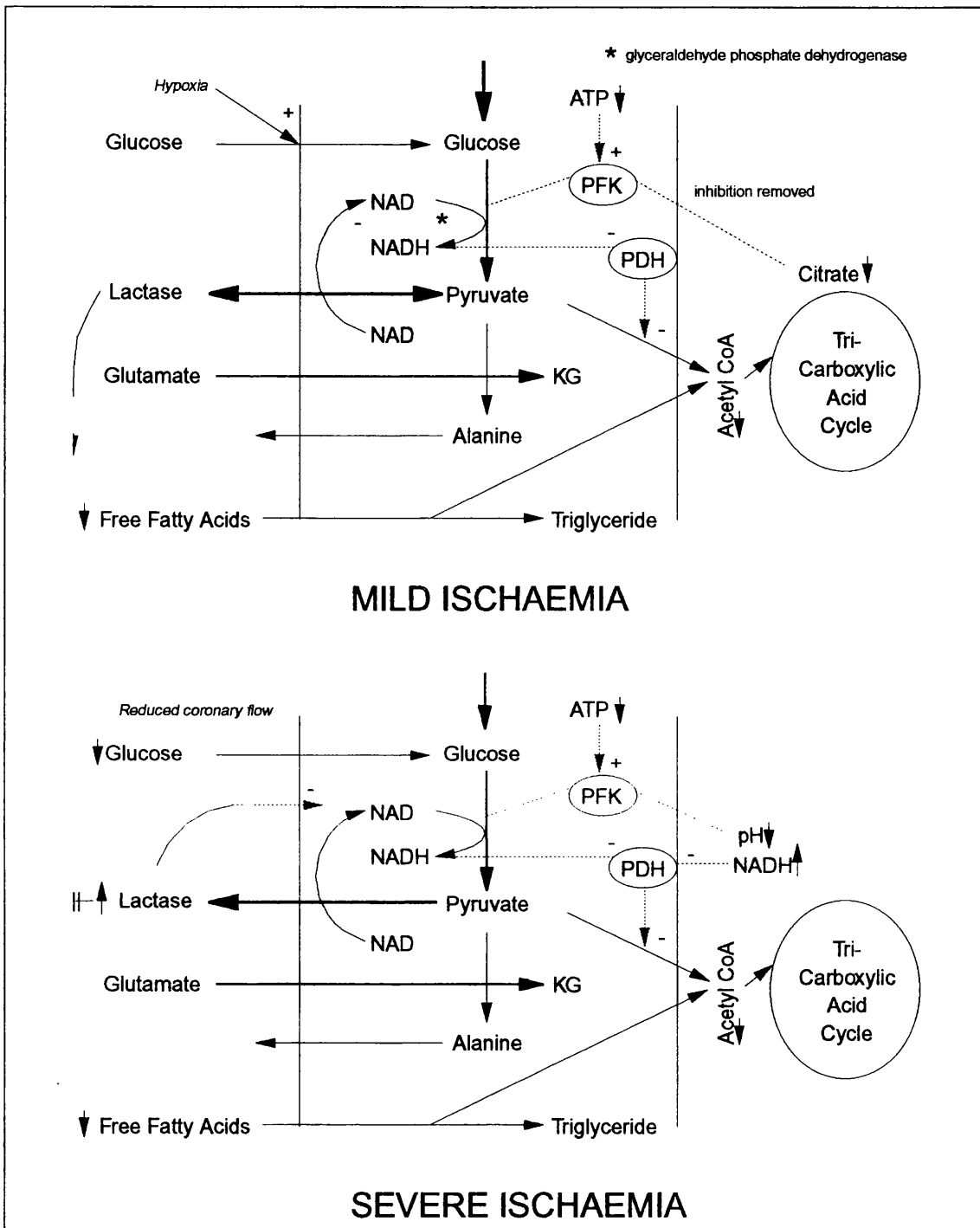


Figure 3.5 - **Upper panel)** During stress-induced myocardial ischaemia, there is a reduced oxidation of free fatty acid with an increased storage of triglycerides. Glucose utilisation is increased (both from exogenous glucose and from glycogen), but the extra pyruvate formed cannot be oxidised. Hypoxia stimulates glucose uptake and phosphofrutokinase (PFK) activity is accelerated due to adenosine triphosphate and creatine phosphate and a decrease of citrate. Pyruvate dehydrogenase is inhibited by increased amounts of NADH (reduced coenzyme nicotinamide dinucleotide). There is an increased production of alanine with a greater myocardial glutamate consumption. In addition, due to the accumulation of NADH, there is activation of the enzyme lactate dehydrogenase, with conversion of pyruvate to lactate that is then released, at the same time 1 mole of NADH is reoxidised to NAD. **Lower panel)** With severe myocardial ischaemia, glycolysis is inhibited. This because of a reduced delivery, inhibition of phosphofrutokinase by a low intracellular pH and inhibition of glyceraldehyde-3-phosphodehydrogenase by lactate and NADH. (Modified from Camici 1989a,b)

3.6.3.2 [¹⁸F]2-fluoro-2-deoxy-D-glucose (¹⁸F-FDG)

This approach is based on the demonstration of the relationship between metabolic uptake of ¹⁸F-FDG and regional myocardial blood flow in ischaemic myocardium (Marshall 1983). It has been demonstrated that the presence of glycolytic activity in myocardial hypoperfused areas with contractile dysfunction is an important index of preserved viable tissue (Camici 1989a). The methods that demonstrate the sustained glycolytic activity rely on the positron emission tomography (PET). This technique initially has used myocardial glucose metabolism (¹⁸F-FDG) in conjunction with measurements of blood flow (¹³N-ammonia or ¹⁵O-water) to demonstrate patterns suggestive of viable and nonviable myocardium (De Silva 1992). These patterns include:

1. Preserved flow and metabolism
2. Reduced flow with preserved glucose metabolism (Flow-metabolism "mismatch")
3. Reduced flow and metabolism (Flow-metabolism "match")
4. Preserved perfusion and reduced metabolism.

The first two patterns are more commonly found in viable myocardium, whereas the third is characteristic of nonviable tissue (figure 3.6). The physiological significance of the fourth pattern is not completely understood. It might reflect myocardial stunning, in which the metabolism is normal or reduced and flow is normal. Although the reduction in flow and perfusion seems to clearly indicate nonviable tissue, it is not clear if the increment of metabolism over flow is really indicative of hibernating myocardium or it is the result of repetitive episodes of stunning with prolonged alterations in metabolism. Several studies have been

Myocardial Viability Study

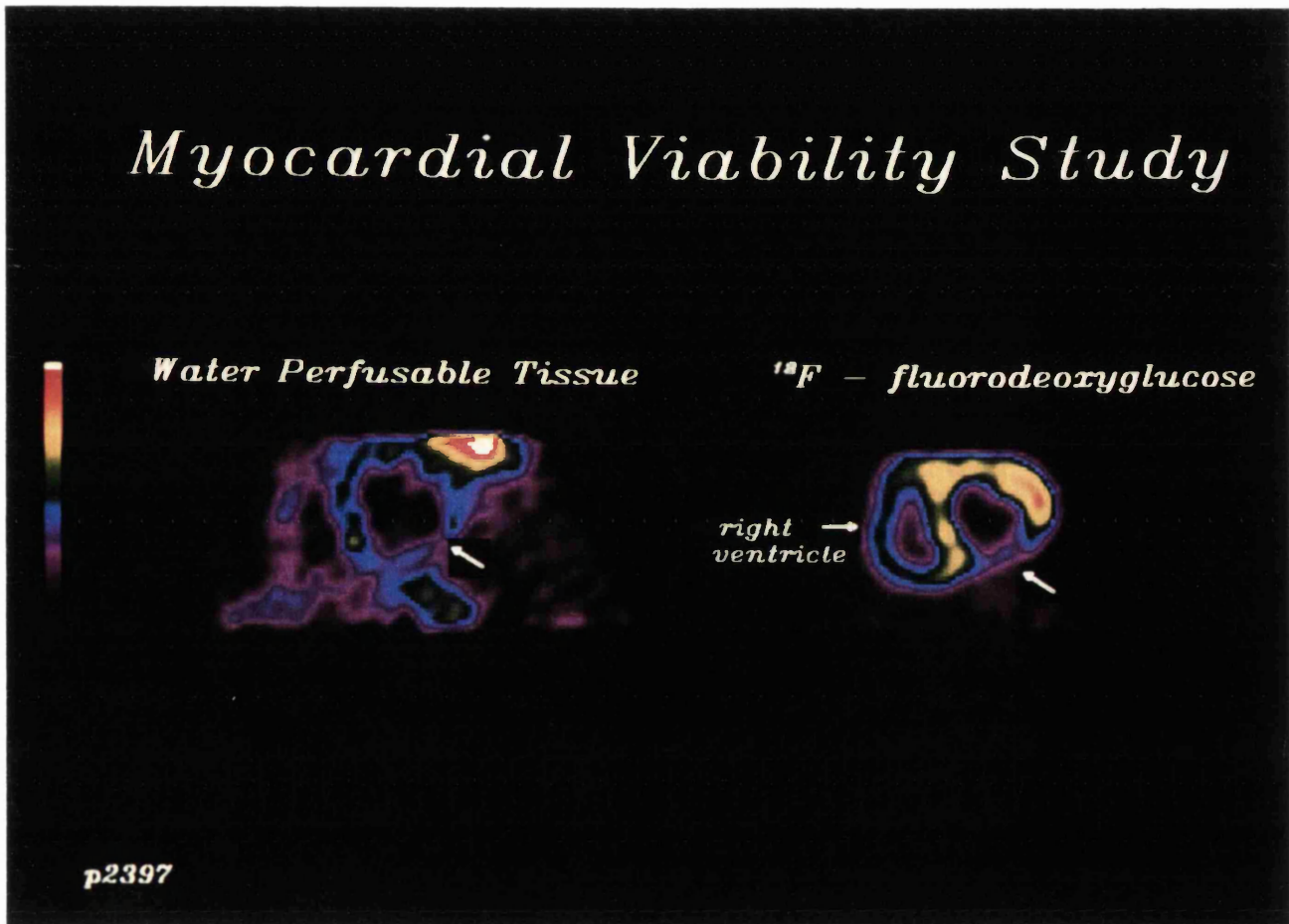


Figure 3.6 - Flow metabolism "match" in a patient assessed for myocardial viability before coronary artery by-pass surgery.

published comparing metabolic activity to different diagnostic tools, such as electrocardiography, ^{201}Tl and $^{99\text{m}}\text{Tc}$ MIBI scintigraphy, regional wall motion and/or myocardial wall thickening or thickness. In particular the predictive value of PET^{W02} compared with the outcome of revascularization (table 3.10).

Reference	Patients (n)	PPA(%)	NPA(%)	Comments
Tillisch (1986)	17	85	92	Improvement in EF related to number of viable segments
Tamaki (1989)	28	78	80	Functional recovery associated with resolution of perfusion and metabolic abnormalities
Schwaiger (1986)	13	50	90	72 hours after MI
Pierard (1990)	17	55	100	9 days after MI
Gropler (1992)	16	79	83	recent MI
Lucignani (1992)	14	95	80	perfusion studies with MIBI
Gropler (1993)	34	72	82	Criteria for viability comparing ^{18}F -FDG and ^{11}C -acetate

EF = ejection fraction; MI = myocardial infarction

Table 3.10 - Accuracy of ^{18}F -FDG metabolic criteria for detecting viable myocardium

One of the limitation of all the studies, again, is that they are semiquantitative, and although they indicate the presence of metabolically active tissue components, they do not accurately define the amount of viable tissue in an asynergic region of the left ventricle (Camici 1993), which is the most important determinant of functional recovery of that region after revascularization. It is possible that measurements of the metabolic rate of glucose ($\mu\text{mol}/\text{min}/\text{g}$) with ^{18}F -FDG during maximally stimulated metabolism (e.g. Hyperinsulinaemic euglycaemic clamp) will allow a more accurate evaluation of the amount of recoverable myocardium in a dysfunctional region.

3.7 New Developments in the Measurement of Myocardial Viability

In the clinical environment, most positron emission tomography scanning is done to demonstrate myocardial viability in patients with reduced left ventricular function prior to revascularization. All the approaches used at the moment rely on the metabolic changes present during ischaemia, however a new measurement not related to metabolism has been proposed.

3.7.1 The Perfusable Tissue Index

The water perfusable tissue index (PTI) is the new proposed measurement, which is independent of tissue metabolism and has been derived from the analysis of transmission, blood pool ($C^{15}O$) and dynamic ($H_2^{15}O$) scans (Yamamoto 1992). The concept of tissue fraction was first introduced to correct for the underestimation of myocardial radiotracer concentration caused by cardiac wall motion and the small transmural myocardial thickness relative to the spatial resolution of positron emission tomography scanners (the partial volume effect) (Iida 1988). Tissue fraction is the fractional volume of a given region of interest occupied by myocardium that is capable of rapidly exchanging water i.e. the $H_2^{15}O$ -perfusable tissue. It is dependent on the ability of the tissue to exchange $H_2^{15}O$ at a microvascular level as well as wall motion and partial volume effects. It may be referred to as perfusable tissue fraction (PTF). Using the anatomical tissue fraction (ATF) defined above it is possible to define the PTI as (figure 3.7):

$$PTI [g(H_2^{15}O\text{-perfusable tissue}).ml^{-1}]ROI \div ATF [g(\text{anatomical tissue}).ml^{-1}] ROI$$

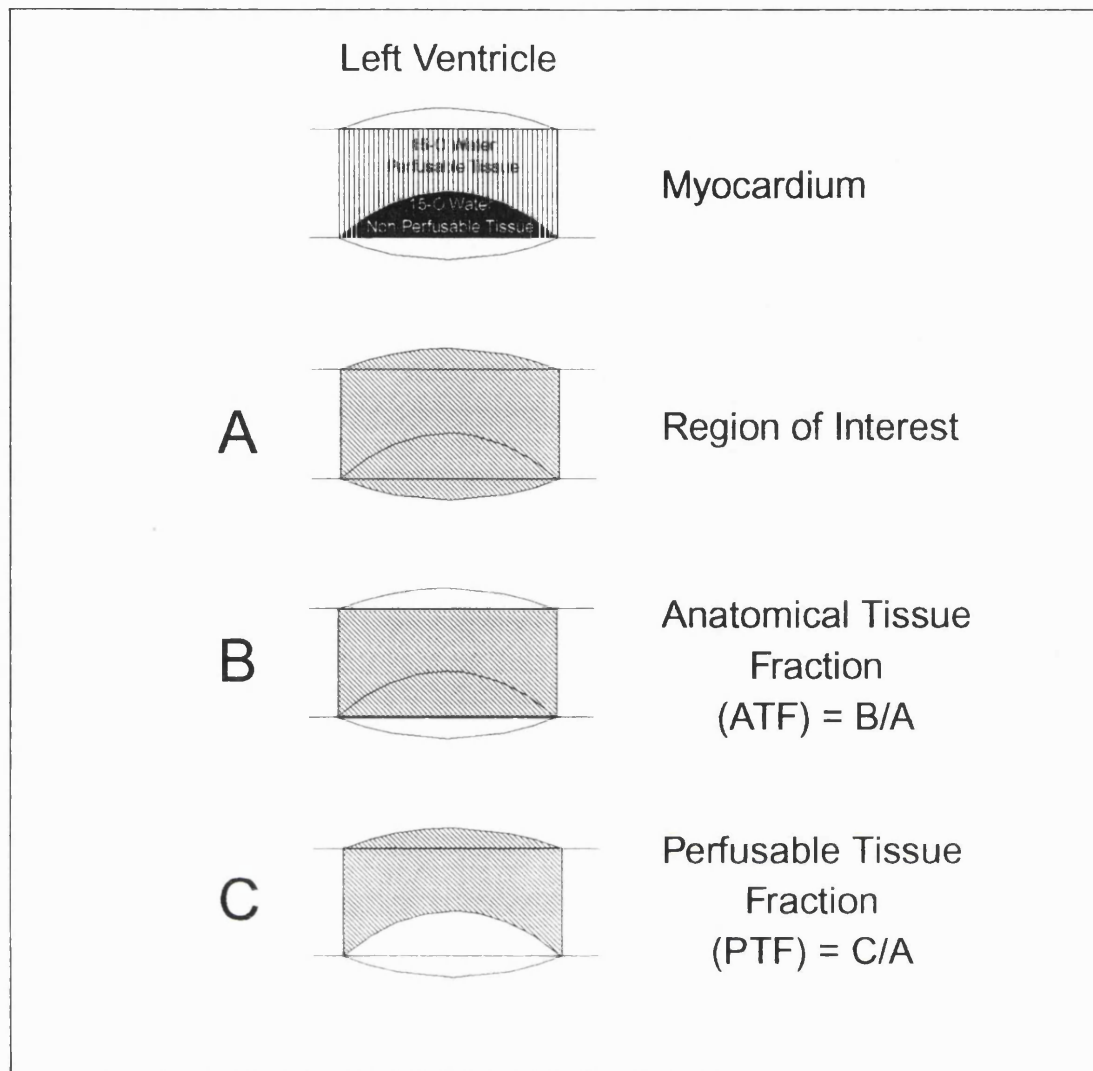


Figure 3.7 - Diagrammatic representation of a myocardial region of interest (ROI) containing a mixture of ^{15}O -water perfusable and non-perfusible tissue. **Panel A)** Volume of the ROI. **Panel B)** Anatomical tissue fraction (ATF) for the ROI produced by subtraction of the converted C^{15}O emission scan (blood pool) from the transmission data after normalisation of the latter to tissue density. ATF contains both perfusable and non-perfusible tissue components. **Panel C)** ^{15}O -water perfusable tissue fraction (PTF) for the ROI calculated from the dynamic H_2^{15}O study. Note that the non-perfusible or necrotic region is excluded from this parameter. The ^{15}O -water perfusable tissue index (PTI) is calculated by dividing PTF (C/A) by ATF (B/A) thus independent of ROI size, and represents the fraction of total anatomical tissue that is perfusable by water.

In normal myocardium, this value should be unity i.e. all myocardium should be perfused by water. Using H_2^{15}O as a flow tracer, this technique also allows absolute quantification of myocardial blood flow, in addition to a measure of myocardial viability.

In an initial study, patients were studied within 2-4 days and 4 months after successful thrombolysis for myocardial infarction who had asynergic myocardium (at echocardiography) and a regional reduction in myocardial blood flow (Yamamoto 1992). In the acute phase, the perfusable tissue index (PTI) was significantly lower in regions in which there was no subsequent contractile recovery, although myocardial blood flow was reduced to a similar extent in both recovery and non-recovery segments. These data also indicated that within a given region, 70% of the tissue should be capable of rapidly exchanging water to enable a subsequent improvement in contractile function. In patients with previous myocardial infarction, perfusable tissue index demonstrated good agreement with ^{18}F -FDG scanning in predicting reversibility of injury in these patients. Subsequently, this sensitivity in discriminating reversibly from irreversible injured myocardium has been confirmed in a group of 12 patients undergoing coronary by-pass surgery and angioplasty (de Silva 1992). In this study, contractile recovery only occurred in myocardial regions where perfusable tissue index was greater than 0.7.

Although the initial data seems to be promising there are some doubts about this approach. It seems unlikely that this index can distinguish between normal and functionally compromised although viable myocytes. Such discriminatory power seems critical for predicting the degree of potential functional recovery.

3.7.2 $^{99\text{m}}\text{Tc}$ -Labeled methoxyisobutylisonitrile (Sestamibi)

Sestamibi is a myocardial perfusion agent that is taken up by the myocardium in proportion to regional blood flow. Its mechanism of uptake is largely passive

(Maublant 1988), and related to its lipophilicity. Although it was demonstrated in animal models that retention of sestamibi depends on the presence of cell integrity (Bonow 1992), data from clinical studies (Cuocolo 1992 and Dondi 1993) in patients with coronary artery disease and left ventricular dysfunction do not support this. Cuocolo et al. 1992 studied 20 patients with exercise-redistribution-reinjection thallium imaging and stress-rest (2-day protocol) sestamibi. Of the 122 segments with fixed defects on stress-redistribution thallium imaging 47% improved after reinjection, whereas 82% (100/122) appeared fixed and 18% reversible with sestamibi. Dondi and co-workers 1993, confirmed these findings. One possible explanation for these findings is that sestamibi is bound to cytosol proteins and to cell membranes (Mousa 1987), preventing it from "washout" from normal tissue, thus decreasing its availability in the intravascular space, where it eventually would be taken up by the ischaemic cells. However, these two studies have been carried out in a small population group (n = 46), thus, no definitive conclusion can be made at the present.

Chapter 4

Positron Emission Tomography and the Assessment of Myocardial Function

4.1. Introduction

The first observation of penetrating radiation comes from Wilhelm Röntgen at Bavaria's University of Würzburg in 1895, who was posteriorly awarded the Nobel prize in 1901 for the discovery of the X-rays. However, it took several years, passing through the discovery of penetrating radiations arising from naturally occurring compounds in 1934 by Irene Curie and Frederic Joliot, the discovery of the positrons, the development of the first cyclotron in Berkeley by Ernest O. Lawrence between 1930 and 1936, until 1960, when single photon tomography and several types of positron scanners and cameras were developed (Ter-Pogossian 1992). Although the development of the positron emission tomographs required about 30 years for being clinically relevant, the usefulness of the positrons emitters radionuclides were realised shortly after the development of the first cyclotron in Berkeley. Nowadays, Positron Emission Tomography (PET) is actually the only radionuclide imaging technique which enables quantitative assessment of regional myocardial tissue function in vivo (Phelps 1986). Using the appropriate tracers, labelled with positron emitting isotopes, a variety of functional parameters can be investigated such as regional myocardial blood flow, metabolism and receptor density (De Silva 1992). Positron-emitting isotopes can be generated from some elements of the periodic table, and organic molecules may be labelled

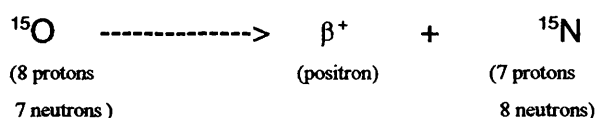
with radioisotopes such as carbon-11, nitrogen-13, and oxygen-15, without altering the chemical structure of the compound used. The short half-lives of the radionuclides used in PET studies enable multi-parametric imaging to be performed in the same patient in the same scanning session. In nuclear cardiology, PET has been a tool of constant evolution and has been proposed as a clinical routine investigation of physiological and pathological parameters. However, despite the unique characteristics of the PET, its acceptance by the scientific community is still restricted, mainly because PET scanners are expensive and it requires a number of different specialists and facilities to be operated. In this chapter, the principles and theory behind PET imaging and its application to the non-invasive measurement of myocardial blood flow and metabolism are described.

4.2 Physical Principles of Positron Emission Tomography

PET imaging involves the detection of radiation released from positron emitting radionuclides. Positron decay generally occurs in atomic nuclei which have an excess of positive charge. Two means of decay exist for such nuclei:

1. capture of an orbital electron by the nucleus, this type of decay is more frequent among heavier elements, since in heavy elements orbital electrons tend to be closer to the nucleus and are more easily captured (e.g. ^{18}F and ^{68}Ga)
2. emission of a positive electron (a positron) from the nucleus

For example, ^{15}O , by releasing a positron turns into stable ^{15}N :



Once released from their parent nucleus, positrons (which are anti-electrons) travel a limited distance away from the parent atom and collide with an electron in orbit and they annihilate to produce two 511 keV gamma photons which are emitted simultaneously at 180° to one another and they can be detected externally by taking advantage of this phenomenon (Sorenson 1987) figure 4.1. Imaging by PET relies on the detection of these annihilation gamma photons by a process known as annihilation coincidence detection (ACD). This system of detection takes advantage of the properties of the annihilation gamma photons. ACD relies on the use of pairs of detectors which are linked together by a coincidence circuit. Only when both detectors register a gamma photon simultaneously will a true count be deemed to have occurred. The site of the annihilation event can therefore be localized to the volume between the two detectors (Hoffman 1986).

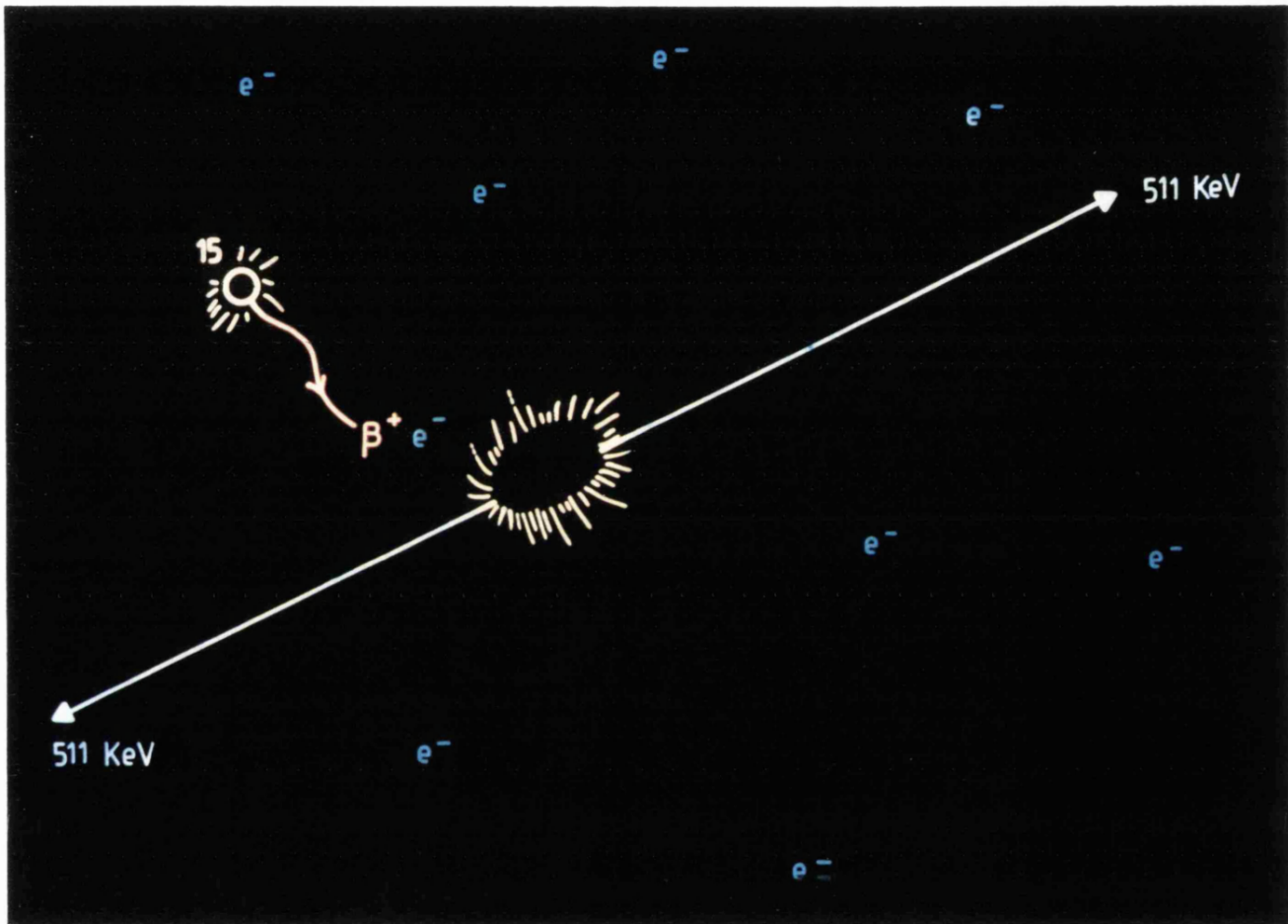


Figure 4.1 - Emission of a positron (β^+) from the nucleus of a molecule of 15-oxygen. Collision with an electron (e^-) leads to annihilation radiation of two 511keV photons of gamma radiation is always at 180° to each other.

To determine the three-dimensional isotope distribution, measurements must be taken from multiple directions. Thus, radiation detectors surround an object to obtain a count rate profile for a certain slice through the object. This allows reconstruction of an image of isotope concentrations. This reconstruction is dependent on the physics of positron decay, positron annihilation, gamma-ray interactions within the object, as well as the geometry and engineering of the system. There are several methods for reconstructing the data to minimize error from assumptions made from count detection, which is outside the scope of this chapter (Sorenson 1987). Suffice it to say, PET systems are designed to maximize the detection of coincidence events (unscattered photons) and minimize background events from scattered photons and high count rates from outside the field of view.

The aim of the ACD is to identify the site of the positron emitting isotope. In practice, this is limited due to two factors known as:

1. the positron range effect and
2. the non-collinearity effect (Hoffman 1986).

Positron range results from the distance a positron must travel away from its parent nucleus before annihilating with an electron: the further a positron travels before annihilating with an electron, the less precision with which the site of positron decay can be localized. The range of positron is dependent on the energy with which it is emitted from parent nucleus and varies for different radionuclides. The distance travelled by the positron before collision increases with the positron energy and thus localization of annihilation events by ACD is

less precise when using radionuclides with high positron energies e.g. positrons from ^{18}F nuclei have lower energy than those from ^{82}Rb nuclei.

The non-collinearity effect describes the phenomenon of the two annihilation gamma photons not being precisely at 180° to one another (Hoffman 1986). This could result in the inappropriate assignment of the time-of-flight of detection. This phenomenon is a consequence of the non-zero momentum of the positron at the time of its annihilation with an electron. These two factors limit the ability of PET to localize the site of radionuclide decay and thus set a theoretical limit on the spatial limit on the resolution of PET cameras (Hoffman 1986) of approximately 2 mm.

Although ACD provides a form of electronic collimation, the counts measured by the ACD circuit may not necessarily represent only true coincidence events which resulted from positron annihilation in the volume spanning the two detectors. Apparent coincidence events can be registered as a result of random or Compton scattered photons. These sources of inaccuracy can be minimized with the appropriate shielding and electronics (Hoffman 1986 and Spinks 1988).

4.3 The Block Detector Positron Emission Tomography

Modern PET systems are designed with regular polygonal or circular rings of detectors to maximize the detection efficiency per slice. These are isolated by lead or tungsten as shielding for off-plane activity, but are at the vertex of a fan beam of sensitivity across the field of view, thus increasing sensitivity. The advantage of the circular sampling system is that there is no longer a need for

detector banks (hexagonal or octogonal array of blocks) to rotate to compensate for under-sampling. High density detector materials and high spatial resolution have reduced the need for moving detector system, such as a "wobble" about the centre of the field of view to increase sampling, and thus improve resolution and reduce artifact.

The scanner used in these studies was the ECAT 931/08-12 (Siemens-CTI Inc. Knoxville, Tennessee, U.S.A.) (Spinks 1988). As described above, this scanner uses the principle of annihilation coincidence detection but has 8 rings of detectors each with 512 detector elements made of bismuth germanate. The detector elements are coupled to photomultiplier tubes in the ratio of 32 to 4 , and localisation of the detector in which the count is registered occurs through analysis of the peaks from all 4 multiplier tubes. Thus, any one detector is in coincidence with other detectors in the same ring and adjacent rings. There is an axial field of view of 10.8 cm consisting of 15 planar slices, 8 direct planes and 7 cross planes. Thus data acquisition occurs in direct planes between detector pairs in the same ring , and in cross planes between detector pairs in adjacent rings of detectors, giving better axial resolution and sensitivity in the latter case. The spatial resolution of the PET camera is assessed by the accuracy in localising a radioactive point source in the field of view of the camera. This is determined from the gaussian-shaped profile resulting from the measurement of a radioactive line source positioned axially in the camera. The width of the count profile at 50% of the peak is a commonly used determinant of the spatial resolution. Using the ECAT 931/08-12, transaxial spatial resolution is 8.4 mm at full width half maximum (FWHM) at the centre of the field of view (Spinks 1988).

4.4 Quantification

The quantity actually measured in PET is the local tissue concentration of positron emitter. This quantity can be related to a physiological or metabolic process through the application of an appropriate mathematical model of the process. With a uniform response from the annihilation coincidence detection system and attenuation correction, it becomes practical to do this with PET.

4.4.1. Calibration

The first step towards quantitation is accurate calibration of the system. This is done regularly by scanning a uniform cylindrical phantom much larger than the spatial resolution of the tomograph, containing a solution of positron emitting radionuclide at a known concentration. An aliquot of this solution is taken from the phantom and counted in a sodium iodide crystal well counter. The count rate measured by the scanner can be determined from the analysis of the image of the phantom acquired by the scanner and have units of counts per second per pixel ($\text{cts}\cdot\text{s}^{-1}\cdot\text{vx}^{-1}$), where a pixel represents a volume element on the PET image. The count rate measured by the well counter has units $\mu\text{Ci}\cdot\text{ml}^{-1}$. This cross-calibration experiment between the scanner and the well counter provides a factor which will convert the coincident count rate measured in the image into units of absolute radioactive concentration. Every picture element (or pixel) in the generated image may then be scaled by this calibration factor .

4.4.2 Image Reconstruction

Once the coincidence data are collected by the scanner they need to be reconstructed into images which quantitatively represent the distribution of the radiotracer within the field of view (FOV) of the camera. Image reconstruction is performed using the technique of filtered back projection (Hoffman 1986). This technique produces images which accurately represent radiotracer concentration independent of the size of the object from which the signal arose (Hoffman 1986). Image reconstruction by filtered back projection relies on a number of assumptions, in particular, that:

1. the transaxial resolution remains constant throughout the FOV;
2. that there is no absorption of emitted gamma photons by any material between coincident detector pairs;
3. that the measured counts are all true coincidences and are independent of coincidences arising from scattered and random photons; and finally,
4. there are no significant losses in counts due to detector dead time.

The main limitation lies with the loss of annihilation gamma photons due to their absorption or attenuation by the structures within the FOV of the camera (Hoffman 1986).

4.4.3 Attenuation correction

During imaging of the heart, annihilation gamma photons originating from the positron emitting radionuclides have a high chance of interacting with thoracic tissue structures. This can result in the photons deviating or being totally

absorbed from their original course due to Compton scattering, with a consequent loss in energy. Therefore, many of the annihilation gamma photons are absorbed by the body tissues, thus limiting the number of counts detected by the scanner (Hoffman 1986). These losses may be corrected for by the process of attenuation correction. It has been demonstrated that the attenuation of gamma photons emanating from within an uniformly dense object is dependent only on the thickness of the object and is independent of the depth of the source of the gamma photons within the object (Hoffman 1986). However, in cardiac imaging, the density of the thoracic structures is far from uniform as exemplified by the six-fold density difference between the heart and lungs. In this instance, rather than calculating the attenuation correction factors on the basis of the dimensions of the thoracic cavity, the correction factors should be measured directly. This is achieved by first performing a blank scan which is acquired with air in the FOV of the camera after exposure of an external ring source containing the positron emitting radionuclide germanium-68 (^{68}Ge , $t_{1/2}=287$ days). Positrons emanating from this ring source annihilate in air and give off pairs of 511 keV gamma photons which are detected. Afterwards, the patient can be positioned in the scanner and a transmission scan performed during which the same procedure as for the blank scan is repeated. By taking the ratio of the counts measured by each coincident detector pair in the absence (blank) and presence (transmission scan) of patient's body, a correction factor can be calculated for the degree of attenuation of annihilation gamma photons for each detector by the patient's body. These data are subsequently used to correct the emission scans, where positron emitting radionuclides are administered to the patient by either intravenous injection or inhalation, for tissue attenuation.

4.4.4 Tracer Kinetic modelling

The definition of a tracer is that of a measurable compound which can follow or trace a chemical process under study without markedly disturbing the process itself (Huang 1986). This is made possible by:

1. the high sensitivity of PET imaging which enables the measurements of radiolabelled tracers administered in picomolar concentrations which are sufficiently low so as not to disturb the process under study; and
2. the ability of current PET cameras to perform rapid dynamic imaging, i.e. to provide good temporal resolution.

Positron emitting radionuclides are incorporated into tracers by rapid radiochemical procedures. These can be administered to subjects either by intravenous injection or inhalation. The tracer substitutes for natural or endogenous substrate and gives information on the cellular pathway that would have been followed by that substrate. After administration of a known amount of the tracer, the myocardial concentration (tissue response) and arterial concentration (arterial input) of the tracer can be measured as a function of time using the PET camera. Indirect measurement of the radiotracer concentration in arterial blood can be made from regions of interest positioned in either the left atrium (Araujo 1991 and Bergmann 1989) (Figure 4.2) or left ventricle (Weinberg 1988 and Iida 1992) of the PET images and provide information on the supply of tracer to the myocardium over the time course of the PET study.

THE SHORTAXIS VIEW OF THE BLOOD VOLUME IMAGE AS A TEMPLATE FOR LEFT ATRIAL ROI

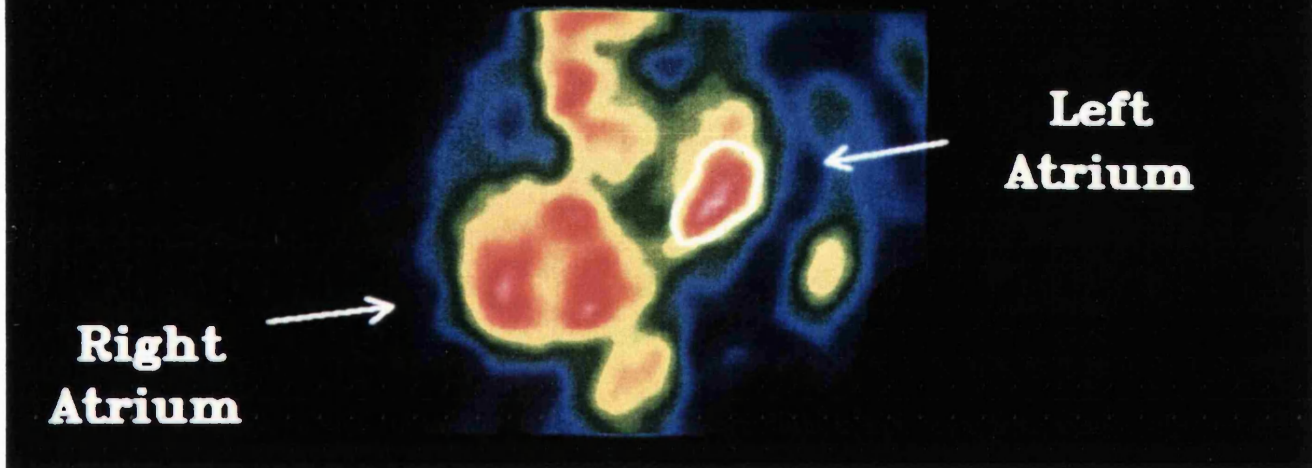


Figure 4.2 - Region of interest for arterial input function. Regions of interest positioned in the left atrium are used to measure the tracer concentration in the arterial blood, in order to provide information on the supply of tracer to the myocardium over the time course of the PET study.

The tissue response to an arterial input function can be derived using a tracer kinetic model, which describes the dynamic biological behaviour of the tracer in tissue in mathematical terms, in order to make a quantitative assessment of the biological process of interest. These kinetic models are based upon the findings of previous biochemical and physiological experiments on the behaviour of the tracer in vitro and in vivo using animal models. The mathematical relation between the tissue response and the arterial input function is usually achieved by non-linear least squares regression analysis of an operational equation which describes the biological behaviour of the tracer. Biochemical and kinetic validations of tracer kinetic models should be obtained before they are used for data interpretation.

4.5 Limitations of PET scanning

With an ideal imaging technique, the value in each pixel of a PET image is equal to the concentration of a positron-emitting radioisotope at that point in the tissue under study. However, no technique is free from a degree of error although with particular interpretation of images allowing for known sources of error, it is possible to minimize this.

4.5.1 Resolution

The primary limitation in PET is spatial resolution. The term line spread function (LSF) is used to define the spatial accuracy of a PET camera and refers to a narrow line source of positron emitter between a pair of coincidence detectors

to give a count rate profile as a function of position. In cylindrical detectors, the LSF is approximately gaussian in shape with a full width at half maximum (FWHM) of 40-50% of the diameter of the detectors at the midpoint of the detectors. Thus, LSF measurements taken over the central third of the region between coincidence detectors are remarkably constant, and that region constitutes the most useful field of view for accurate measurements in PET. When two line sources of activity are exactly one FWHM apart, it is not possible to tell that there are two sources, and when they are two FWHM apart the lines should be clearly separated, with the valley between going to the background level.

The limiting resolution due to the physics of the beta annihilation is of the order of 2-3 mm. Poor resolution can affect quantitative measurements by:

1. causing difficulty in interpretation of the anatomy for the identification of the structure of interest
2. failing to resolve two structures close to each other and incorrectly attributing activity from one structure to the other
3. reducing the apparent isotope concentration in structures that are smaller than about twice the system resolution
4. causing overestimation in size of structures smaller than twice the resolution distance of the PET system, and
5. low sensitivity in the detection of small low contrast lesions.

Resolution may also be lost if the patient moves during any stage of the scan. This is reduced by placing the patient on a comfortable bed, using a head restraint to remove axial movement, and employing short scan times.

The partial volume effect is another limitation of scanner resolution that is discussed below (section 4.6.1)

4.5.2. Accidental and scatter coincidences

Accidental and scatter coincidences are the two primary sources of background noise in PET. Accidental coincidence occurs due to the nature of detection of emitted gamma rays. To establish that annihilation photons are in coincidence, timing measurements need to be performed for thousands of combinations of detector pairs. The detector, a scintillation crystal such as bismuth germanate, absorbs a photon and generates an electronic pulse (timing signal) of precise width (through emission of light to a photomultiplier), which is summed with other pulses from other detectors possibly in coincidence. When in coincidence, the pulses sum to twice the amplitude, identified by a pulse height discriminator and store as image data. Because of the decay time of bismuth germanate (300nsec), there is an inherent delay between the annihilation event and the timing signal. The width of the timing signal is chosen so that most of the signal from true coincidences falls into the electronic coincidence time window. Inevitably, unrelated photons may also produce timing signals which overlap accidental coincidences. These may be corrected for and subtracted from the total coincidences either by measuring the single event of the individual detectors or using parallel timing circuit to delay one of the signals (Hoffman 1986) figure 4.3. Scatter coincidences occur through photons being deflected by the tissue of the subject, with very little energy lost as a consequence and detected similarly to true events by the detectors. It is dependent on:

1. the cross-sectional geometry of the patient,

2. the distribution of activity, and
3. the design of the PET system

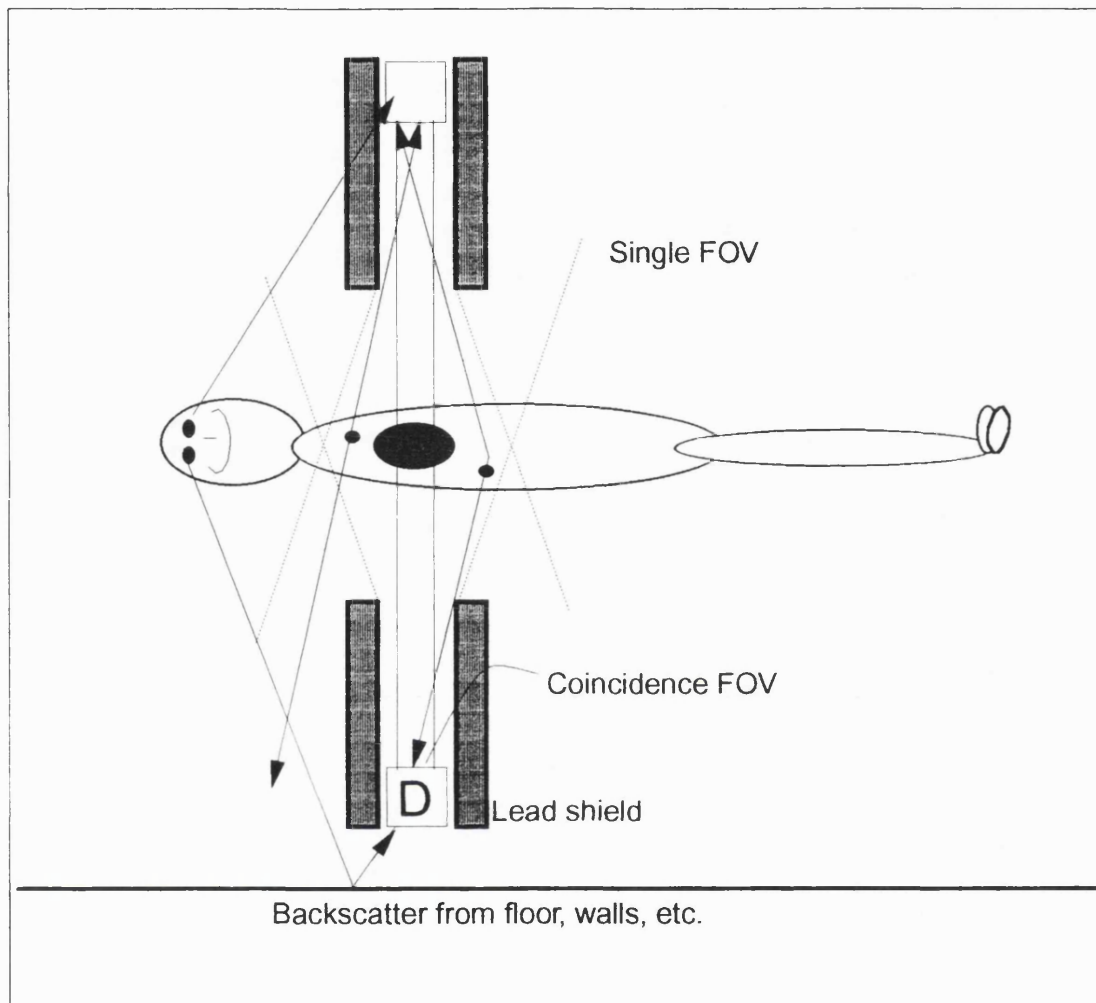


figure 4.3 - Sources of true, accidental, and scatter coincidences. True coincidences are those which are detected simultaneously in the region between the two detectors (d), the coincidence field of view (FOV). Accidental coincidences originate in areas of the subject which is in the direct field of view of one of the detectors (single FOV within either set of the dashed lines). Such coincidences can also arise from poor shielding, back scatter, and non-annihilation photons from the radioisotope. scatter coincidences originate in a region that is viewed simultaneously by both detectors (between two sets of dashed lines) (modified from Hoffman & Phelps, 1986).

Although scatter can be measured in detail using line sources placed in the field of view, an estimate can usually be made from the edges of the field of view and correction made accordingly (Hoffman 1986).

Design of the PET system is of utmost importance in minimising these artifacts. A larger system diameter increases the ratio of true to background events and allows the use of longer lead side shielding. The sources of true, accidental and scatter coincidences are shown in figure 4.3.

4.5.3 Dead-time Losses

Dead-time losses can be estimated for a particular distribution of activity by taking a series of PET measurements of that distribution as a function of time until the total number of events per data acquisition is decaying with the true physical half-life of the isotope. Extrapolation to earlier times, with the physical half-life of the isotope, allows calculation of the true data rate. The difference between the true and measured rates is an estimate of data losses at higher count rates. Dead-time corrections in PET require simultaneous measurements of the single event rate of each detector and the coincidence rate.

4.6 Myocardial PET scanning

The anatomical and physiological nature of the heart impose specific requirements on the acquisition and analysis of images generated by positron-emitting isotopes. Because of this, there are several considerations which need to be taken into account in order to improve image quality and tissue quantitation. It is important to ensure that the patient under study remain still during imaging so as to achieve optimum time-activity curves in each region of interest during each individual component of the study. In addition with

multiple studies during the scan, it is important that comparability is not lost between studies because of patient movement. To avoid this, a neon laser beam is used to demonstrate the patient's position in relation to the field of view, and temporary marks applied to maintain position from scan to scan.

The block detectors are positioned in a circumference around the long axis of the patient. However, the long axis of the heart is oblique to this such that images when reconstructed are transaxial limiting complete evaluation of the left ventricle, particularly with respect to the inferior wall, cutting a tangential plane through this region. This problem is less apparent when restricting analysis to mid-ventricular sections with equally sized regions of interest from all wall of the ventricle. It is now possible to reslice the reconstructed PET images along the axis of the heart to create short axis images from base to apex, without the need for tilting of the imaging gantry as was previously done in some centres.

Because the position of the heart in relation to other thoracic structures is asymmetrical, surrounded by tissue of different density, the degree and extent of photon attenuation by these tissues requires measurement before delivery of tracer, which has the advantage of conferring quantitation on the technique. This has led to the initial transmission scan generated by external irradiation which allows determination of the attenuation coefficients of the soft tissues and correction for photon attenuation, as well as defining the thoracic anatomy.

Cardiac and respiratory wall motion are potential causes of image degradation with problems of motion artifacts causing apparent heterogeneity in myocardial

tissue tracer uptake. PET images may be taken gated to the electrocardiogram (ECG), so that the apparent changes in regional tracer concentration caused by regional wall motion and due to partial volume effect may be minimized.

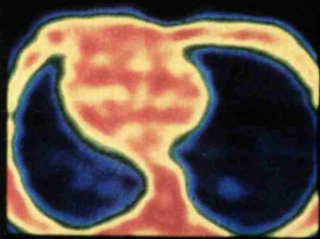
In addition to the potential problems caused by the physical nature of the scanning, there are other considerations in relation to the analysis of images when determining true tissue concentration of tracer such as the partial volume effect, bidirectional cross contamination of activity between myocardium and blood, so-called "spillover" activity, and blood activity in the vascular space of myocardium.

4.6.1 Partial volume effect

Tissue concentrations of tracer are underestimated if the object size (e.g. left ventricular wall thickness), is less than twice the spatial resolution of the imaging camera ($2 \times \text{FWHM}$), and the image is only partially occupying the sensitive volume of the detectors viewing that dimension, as after reconstruction, the concentration seen in the image is proportional to the concentration in the object. This leads to an underestimation of the isotope concentration in the object. Previously the resolution was of the order of 15-20 mm, causing underestimation of up to 50% of tissue tracer concentration. With improved resolution, currently at 6.6 mm, this error has declined. In order to correct for the partial volume effect, correction can be derived from scanning of different-sized phantoms containing a positron-emitting radioisotope allowing measurement of count recovery (the recovery coefficient) against object size.

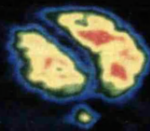
In the method employed in this thesis, partial volume may be corrected for by manipulating the transmission and $C^{15}O$ blood pool images (Figure 4.5). This involves pixel-by-pixel subtraction of a blood density image from the transmission after normalization of the latter for tissue density (Iida 1991). This provides a quantitative image of extravascular tissue density (Figure 4.4). Using phantom studies, this method has been validated over a range of wall thickness of 3 to 27 mm (Spinks 1991). The value of extravascular tissue density measurements is dependent only on cardiac wall motion and the physical dimensions of the heart wall and is termed the anatomical tissue fraction (ATF).

CREATION OF THE EXTRAVASCULAR VOLUME IMAGE



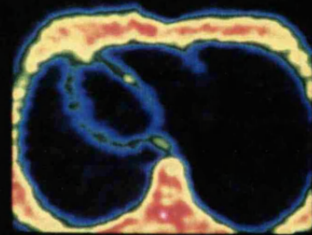
**Normalized
Transmission
Image**

—



**Blood Volume
Image**

=



**Extravascular
Volume Image**

HBOMRC

Figure 4.4 - Creation of extravascular volume image from the normalized transmission image and the blood volume image.

4.6.2 Spillover

The resolution of the scanner determines the amount of spillover of activity from the ventricular chamber i.e. blood pool to the myocardium and vice versa. With the improvement in resolution with the newer generation of scanners, spillover has become less a problem.

4.6.3 Arterial Activity

In man, the coronary vascular space occupies an average of 10% of myocardial volume. High activity in this compartment contaminates the data from tissue activity, particularly early in tracer uptake.

4.7 Measurement of Myocardial Blood Flow Using PET

A number of tracers have been used for measurements of regional myocardial blood flow using PET, in particular oxygen-15 labelled water (Araujo 1991, Bergmann 1984, Bergmann 1989 and Iida 1989), nitrogen-13 labelled ammonia (Schelbert 1979, Bellina 1990 and Hutchins 1990), the cationic potassium analogue rubidium-82 (Herrero 1990 and Green 1992), ^{62}Cu -PTSM (Green 1992), and carbon-11 and gallium-69 labelled albumin microspheres (Beller 1979 and Wilson 1984).

Agent	Physical half-life	Route of administration	Comments
⁶⁸ Ga microspheres	68 min	LA, LV	generator produced
⁶² Cu microspheres	9.7 min	LA, LV	generator produced
¹¹ C microspheres	20.4 min	LA, LV	generator produced
¹³ N ammonia	9.8 min	IV	cyclotron produced
Potassium-38	7.7 min	IV	cyclotron produced
Rubidium-82	1.3 min	IV	generator produced
¹⁵ O water	2.0 min	IV, IH	cyclotron produced

Table 4.1 Positron-emitting tracers for myocardial blood flow measurements.

LA = left atrium, LV = left ventricle, IV = intravenous, IH = inhalation

These myocardial blood flow tracers can be divided in two general groups:

1. microspheres and
2. diffusible radiotracers.

1. Microspheres

Microspheres are trapped in capillary bed in direct proportion to blood flow. Regional concentration in tissue correlates linearly with blood flow. This technique is widely used in animal experiments, and is considered to be the "gold standard" of blood flow measurements. However, it requires tracer administration into left atrium or left ventricle and myocardial blood flow is calculated from the withdraw rate and microsphere activity of the arterial reference blood sample, and microsphere activity concentration in tissue. This in an invasive procedure that is confined to the cardiac catheterization laboratory and thus precludes its widespread use.

2. Diffusible tracers

Diffusible tracers circumvent these limitations. They are administered intravenously or by inhalation. Several diffusible tracers of blood flow are

available with PET (table 4.1). Each possesses certain virtues and also some drawbacks. Early work investigating the effect of coronary artery stenoses on MBF distribution used rubidium-82 (Selwyn 1982), and nitrogen-13-labelled ammonia ($^{13}\text{NH}_3$) (Krivokapich 1989). However, they observed accumulation of $^{13}\text{NH}_3$ in ischaemic areas, which may reflect altered metabolism rather than perfusion alone (Bergmann 1985). This has led to the use of oxygen-15 labelled water (H_2^{15}O), which is a pure flow marker, free from the distortion attributable to the effects of ischaemia or metabolism (Bergmann 1984 and Iida 1988). Currently H_2^{15}O , nitrogen-13 labelled ammonia ($^{13}\text{NH}_3$) and rubidium-82 (^{82}Rb) are the most widely used PET perfusion tracers.

4.7.1 ^{13}N -ammonia

Nitrogen-13 labelled ammonia is administered intravenously as boluses. It clears rapidly from blood and distributes in proportion to regional myocardial blood flow in myocardium, where it becomes trapped for several hours. Initial extraction approaches 100%, however there is some back diffusion leading to an extraction fraction of 82%. The long biological half-life of $^{13}\text{NH}_3$ in tissue and its rapid clearance from blood pool yields excellent image quality. However, at high flow rates there is a decline in the extraction fraction of $^{13}\text{NH}_3$, leading to a non-linear tissue response curve (the linear relationship only holds to myocardial blood flows of up to 2.5 ml/min/g). $^{13}\text{NH}_3$ diffuses across the cell membrane in the NH_4^+ form equilibrating to $^{13}\text{NH}_3$ which is trapped by the enzyme glutamine synthetase, which converts glutamic acid to glutamine. Because of the dependence on an enzyme involved in tissue metabolism, it has been suggested that tracer fixation may be affected by the underlying metabolic

state of the myocardium (Bergmann 1980). Under the presence of chronic myocardial ischaemia is difficult to evaluate if the relationship between net extraction of $^{13}\text{NH}_3$ and regional myocardial blood flow is significantly affected. Another drawback is that using $^{13}\text{NH}_3$, arterial blood samples are required within two minutes of injection to allow well count activity.

4.7.2 Rubidium-82 (^{82}Rb)

Rubidium-82 like $^{13}\text{NH}_3$ is a cation and its uptake by the myocardium is a product of flow and extraction, for this reason exactly like $^{13}\text{NH}_3$, a systematic underestimation occurs when measuring high flows. ^{82}Rb is transported by diffusion and by active transport dependent on Na-K ATPase pump present in the cell membrane. Two methods are used for quantitation of myocardial blood flow using ^{82}Rb . The first is the equilibrium technique, that relies on an image taken during constant ^{82}Rb infusion, followed by another image after the infusion has been stopped. These two images allow calculation of the arterial and myocardial ^{82}Rb concentrations and thus extraction fraction. The second method employs a rapid injection over 10-30 seconds along with sequential PET image acquisition. Although kinetic models have been proposed for quantification of regional myocardial blood flow using ^{82}Rb (Herrero 1992 and Huang 1989), these are limited by the dependence of the myocardial extraction of this tracer on the prevailing flow rate and myocardial metabolic state (Araujo 1984). Therefore, quantification of regional myocardial blood flow either under hyperaemic conditions or in metabolically impaired myocardium may be inaccurate. Furthermore, the high positron energy of this radionuclide results in

relatively poor image quality and in a reduced spatial resolution due to the relatively long positron track of ^{82}Rb (Araujo 1984).

4.7.3 ^{15}O -water

^{15}O -water is freely diffusible with an extraction fraction approaching 100% which is unaffected by tissue metabolism. With a half-life of only 123 seconds, serial studies may be performed. Problems with this tracer originally occurred because of the high ^{15}O content of the blood pool and the myocardial vascular space. However, by recording blood pool images during ^{15}O -labelled carbon monoxide, it is possible to subtract blood pool activity from tissue activity. ^{15}O -water has been given as an intravenous bolus along with fast PET scanning, although this required intra-arterial sampling to determine the arterial input function (Iida 1988). By giving a ^{15}O -labelled carbon monoxide (C^{15}O_2) inhalation which is rapidly converted to ^{15}O -water in the lung capillaries, the delivery to the myocardium is achieved without need for rapid scanning levels of activity. The advantages of this method of delivery is that C^{15}O_2 is easy to produce and may be delivered to the PET laboratory without the need for direct handling by the radiochemist, and may be controlled by the scanner operator. The slow inhalation, by providing a slow input function, reduces the artefact seen with bolus injections.

The main disadvantage is the high level of activity in the cardiac chambers which interferes with the myocardial signal, because of the limited resolution of the scanners. To correct for this, the V_a , representing the arterial blood volume and the spillover fraction has been introduced into the model. Myocardial blood

flow is calculated by fitting the arterial input and tissue time-activity curves to a single tissue compartment tracer kinetic model, which includes corrections for the underestimation of tissue activity due to partial volume effect and the spillover of activity from the left ventricular chamber into the myocardial wall. The model estimates myocardial blood flow, the fraction of exchangeable tissue, and the V_a with the region of interest measured. The fraction of exchangeable tissue is the fraction of the region of interest that consists of tissue capable of exchanging water within the time period of the study. This tissue fraction accounts for different wall thickness and thus corrects for myocardial tracer underestimation because of the partial volume effect, obviating the need for an independent measurement of wall thickness. Another minor disadvantage is that image quality is poorer than that seen with $^{13}\text{NH}_3$ or ^{82}Rb because of the kinetic characteristics of the tracer and the rapid dynamic scanning involved. However, the ability to quantify myocardial blood flow, with a correlation coefficient of 0.91 against microspheres, makes up for this minor disadvantage. The non-invasive measurement of the arterial input function is also affected by the partial volume and spillover effects, although these effects may be minimized by using the left atrial chamber which has a recovery of over 90%.

Chapter 5

Materials and methods

5.1 Introduction

This chapter describes the entire protocol followed in this thesis. The study population (patients and normal controls) and the study protocol.

One hundred patients and all the controls underwent the first phase of the protocol (before surgery assessment). It included coronary angiography and radionuclide ventriculography (only for the patients). Positron emission tomography for the assessment of myocardial blood flow and myocardial glucose utilization using hyperinsulinaemic euglycaemic clamp for all the subjects enrolled (patients and normal controls). However, only thirty patients had their follow-up studies performed at the time of this these was being written (Chapter1; section 1.1).

5.2 Methods

5.2.1 Study population

5.2.1.1 Patients

The patient population consisted of 30 patients [2 women and 28 men, mean (\pm SD) age 56 ± 11 years, range 34 to 72 years] with chronic coronary artery disease and at least one dysfunctional left ventricular region subtended by a diseased coronary artery amenable to revascularization. All had myocardial infarction at least six months before the scan, 5 had Diabetes mellitus and 4 had hypertension.

5.2.1.2 Normal controls

A group of 25 normal volunteers (16 men, mean age 56 ± 12 , range 33 to 77 years; $p=NS$ vs patients) served as controls for the measurements of myocardial blood flow (control-MBF). A second group of 9 normal volunteers (all males, mean age 47 ± 7 , range 31 to 56 years, $p=NS$ vs patients) served as controls for the measurements of the myocardial metabolic rate of glucose during hyperinsulinaemic euglycaemic clamp (control-MRG). The normal volunteers were selected, since their clinical history and physical examination had indicated them to be at low risk for coronary artery disease. All had normal resting electrocardiograms and negative exercise tests in response to a high workload.

5.3 Study protocol

5.3.1 Coronary Arteriography

Selective arteriography of the right and left coronary arteries in multiple views was performed in all patients using the Judkins technique (Braunwald 1988). The percent reduction of the internal luminal diameter, in the projection with maximal severity, was assessed visually.

5.3.2 Radionuclide Ventriculography

All patients underwent radionuclide ventriculography (Zaret 1993) before and 4 to 6 months after coronary by-pass. Briefly, after red blood cells had been labelled in vivo with 740 MBq of technetium-99m sodium pertechnetate, the intracardiac blood pool was imaged using a gamma camera (GE 400 XCT) equipped with a low energy all-purpose collimator and interfaced with a dedicated computer system (S3000). Data for each cardiac cycle, synchronized to the R-wave on the electrocardiogram were divided into 21 frames. Six million counts per view were acquired. Planar blood pool imaging was performed in 2 projections (Prvulovich 1994):

1. in the left anterior oblique projection (best septal separation) with a 20° caudal tilt;
2. in the left posterior oblique projection.

The percentage of left ventricular ejection fraction was obtained from the left anterior oblique projection of the planar acquisition. Regional wall motion was assessed qualitatively from an endless loop cine format. The wall motion was graded as 0 (normal), 1 (hypokinetic), 2 (akinetic) and 3 (dyskinetic).

5.3.3 Hypersinulinaemic euglycaemic glucose clamp

Prior to PET scanning, with the patient lying on the scanner bed, a 20G polyethylene cannula was inserted in a superficial forearm vein for infusion of glucose and insulin as described by De Fronzo et al (1979). A second cannula was inserted retrogradely into a superficial vein of the wrist or hand which had been arterialized using a commercially available heating pad set at 50° C. The degree of arterialization was checked by measuring respiratory gases on a blood sample drawn towards the end of the 30 minute heating period. At time zero, the insulin infusion was started. Insulin was given at 4 times the final constant rate (calculated according to De Fronzo et al (1979) for the first 4 minutes, then at two times the final constant rate for the following 3 minutes, and then at a constant rate for the remainder of the study. At 4 minutes, exogenous glucose infusion was started at an initial rate of 1.5 mg/min/kg of body weight. The blood glucose concentration was measured, from arterialized vein, at baseline (>30 minutes after the insertion of the cannula) and every five minutes during the clamp. The glucose infusion rate was adjusted according to the change in plasma glucose over the preceding five minutes. Samples for insulin assay were taken from the arterialized line immediately before starting insulin infusion and 60 minutes into the clamp.

5.3.4 Positron emission tomography (PET)

The PET study for the measurement of myocardial blood flow and glucose utilization was carried out within a week of radionuclide ventriculography. All

PET scans were performed using an ECAT 931-08/12 scanner (CTI Inc., Knoxville, TN, USA), which consists of eight rings of bismuth germanate crystal detectors. This scanner enables the acquisition of 15 planes of data over an axial field of view of 10.5 cm, thus allowing the whole heart to be imaged. All emission and transmission sinograms were reconstructed with a Hanning filter with a cut-off frequency of 0.5 maximum. This resulted in a spatial resolution of 8.4 mm full width at half maximum (FWHM) for the emission and 7.7 mm FWHM for the transmission data at the centre of the field of view, with a slice thickness of 6.6 mm FWHM (Spinks 1988). All subjects lay supine on the scanner bed. The optimal imaging position was determined using a 5 minutes rectilinear scan after exposure of the external ^{68}Ge ring source. A 20 minutes transmission scan was then performed. These data were used to correct subsequent emission scans for tissue attenuation of the annihilation gamma photons.

After the transmission scan, the blood pool was imaged by inhalation of ^{15}O -labelled carbon monoxide (C^{15}O), which labels erythrocytes through the formation of carboxyhemoglobin. C^{15}O was administered for 4 minutes at a concentration of 3 MBq/ml and a flow rate of 500 ml/min. A 6 minute single-frame emission scan was initiated 1 minute after the end of C^{15}O inhalation to allow for equilibration (Araujo 1991). Venous blood samples were taken every minute during the scan, and the C^{15}O concentration in whole blood was measured using a NaI well counter cross-calibrated with the scanner.

After a 15 minutes period, to allow for decay of ^{15}O radioactivity to background levels, myocardial blood flow was measured using inhaled C^{15}O_2 which is

rapidly converted to ^{15}O -labeled water (H_2^{15}O) by carbonic anhydrase in the lungs (Araujo 1991). C^{15}O_2 was inhaled for a period of 3.5 minutes (4 MBq/ml at a flow rate of 500ml/min). A 25 frames dynamic PET scan, covering a period of 7 minutes, was started 30 seconds before the start of C^{15}O_2 delivery (Figure 5.1). The images generated from C^{15}O_2 and C^{15}O (Blood volume image) were used for the creation of a template for drawing regions of interest to be used for myocardial blood flow measurements (Figure 5.1).

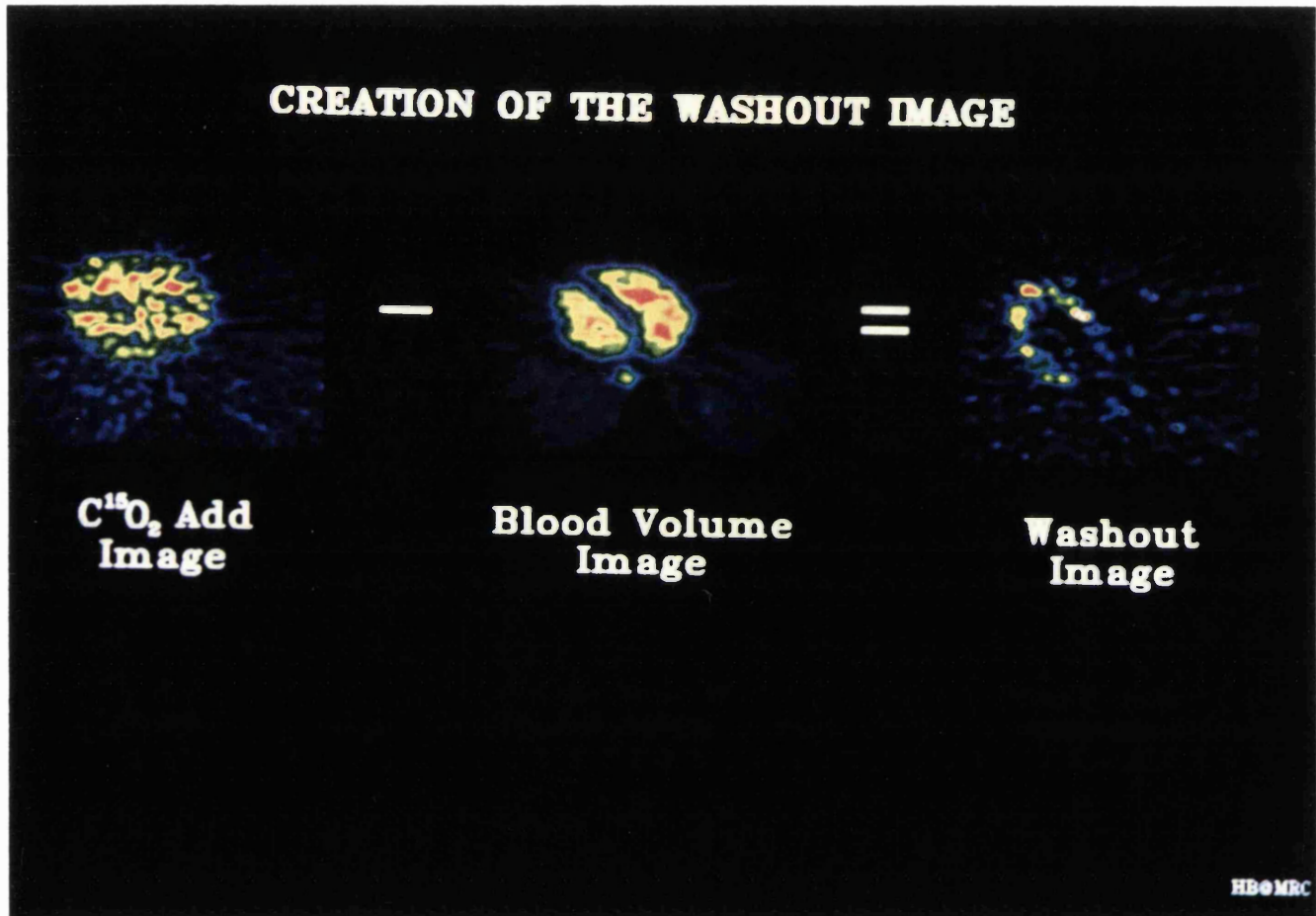


Figure 5.1 - Generation of myocardial blood flow image

Myocardial glucose utilization, during hyperinsulinaemic euglycaemic clamp, was measured with the glucose analogue [^{18}F]2-fluoro-2-deoxy-D-glucose (^{18}F -FDG). ^{18}F -FDG (185 MBq) was infused intravenously over 2 minutes. A 36-frame dynamic PET scan, with progressive increase in frame duration, was performed for a period of 65 minutes. Arterialized whole blood was withdrawn continuously at a rate of 5 ml/min for the first 10 minutes and 2.5 ml/min thereafter. The on-line detection system, cross-calibrated against the PET scanner, has been described previously (Lammertsma 1991). At set times (5, 10, 20, 45 and 60 min after start of the ^{18}F -FDG infusion) continuous blood withdrawal was interrupted briefly for the collection of blood samples which were used to estimate plasma to whole blood ratios of radioactivity using a NaI well counter cross-calibrated with the scanner. After each sample, the line was flushed with heparinised saline.

5.3.4.1 PET data analysis

All sinograms were corrected for tissue attenuation and reconstructed on a Micro Vax II computer (Digital Equipment Corp., Marlboro, Mass) using dedicated array processors and standard reconstruction algorithms. Images were transferred to SUN 3/60 workstation (Sun Microsystems, Mountain View, Califor.) for further analysis. Image manipulation and data handling were performed using ANALYZE (Version 3.0, Biodynamics Research Unit, Mayo Foundation, Rochester, Minnesota) (Robb 1990) and the MATLAB (The MathWorks Inc., Natick, Massachusetts) software packages. All images were reconstructed in the short axis orientation.

A myocardial blood volume (MBV) image was generated by dividing the $C^{15}O$ image by the product of the average concentration of the blood samples on a pixel by pixel basis. Appropriate corrections for decay were applied to both the $C^{15}O$ image and the blood samples. The resultant quantitative images of blood volume have units of millimetres of blood per image volume element. These images were used to position two to four regions of interest (ROI) in the left atrial chamber, such that myocardial blood volume, and thus the recovery of counts, was greater than 90%. These regions of interest were then projected onto the dynamic $H_2^{15}O$ images in order to generate arterial time-activity curves. The average of these atrial curves was used as the arterial input function for the subsequent kinetic of myocardial blood flow analysis (Araujo 1991).

The above mentioned atrial regions of interest were not used to generate the input function for the kinetic ^{18}F -FDG analysis. Due to the high tissue to blood ratio at late times even a limited amount of spill-over would significantly affect the tail of the blood curve. Instead, the continuously monitored arterialized venous whole blood curve was used. This curve was multiplied by the average plasma to whole blood ratio obtained from the discrete samples, in order to obtain a plasma input function. A correction for the delay of this curve (arm and tubing) was made by shifting it so that the initial rise coincided with that from the atrial regions of interest. Four equally spaced sectors corresponding to the anterior, septal, lateral and inferior myocardium were drawn on each plane of the last ^{18}F -FDG frame. Within each sector 3 to 4 elliptical regions of interest (6 x 6 pixels each) (figure 5.2) were drawn. These regions of interest were also

projected onto the entire dynamic ^{18}F -FDG and H_2^{15}O data set, and tissue time-activity curves were generated for each region of interest.

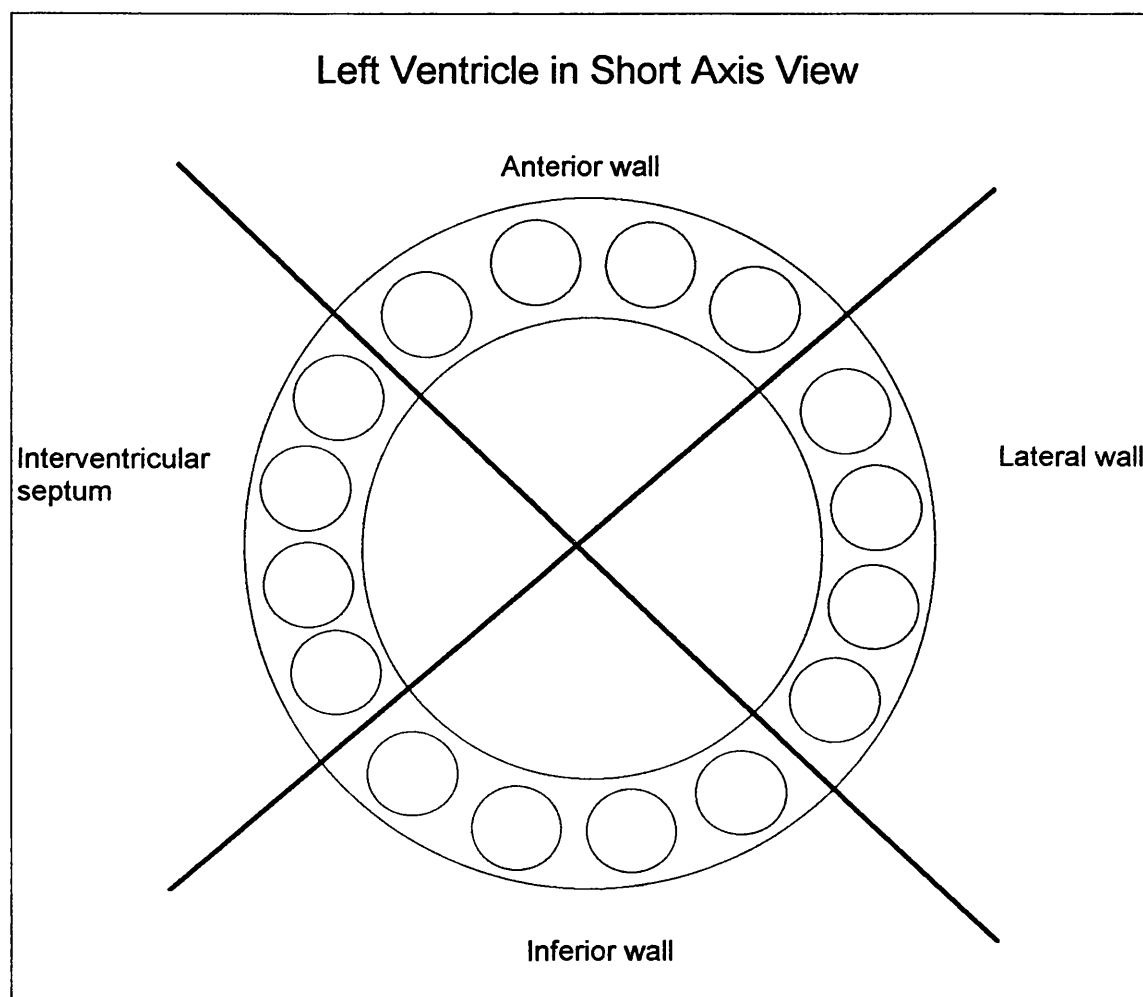


Figure 5.2 - Regions of interest drawn to be projected onto the dynamic ^{18}F -FDG and H_2^{15}O data set.

The tissue H_2^{15}O time-activity curves were fitted for myocardial blood flow (MBF) and fraction of perfusable tissue (tf) using standard non-linear regression techniques and a tracer kinetic model described previously (Araujo 1991). It is important to note that, unlike other methods the myocardial blood flow values obtained are not expressed per ml of region of interest, but per ml of perfusable tissue, i.e. the method contains an intrinsic correction for partial volume effect. The latter point implies that H_2^{15}O will rapidly diffuse into perfusable tissue excluding scar. Therefore, in a myocardial region consisting

of an admixture of normal and necrotic tissue, $H_2^{15}O$ only measures flow to residual normal myocardium (Iida 1991). At variance, the flow measured with other tracers, e.g. ^{13}N -labelled ammonia, represents an average flow per unit mass of tissue as with the microspheres technique (Bellina 1990).

Tissue ^{18}F -FDG time-activity curves were analysed using the linear approach proposed by Patlak (1983), for irreversible processes. The ratio of tissue concentration over plasma concentration was plotted against the ratio of the integral of the plasma concentration over the plasma concentration and a linear regression was performed for all data points corresponding to times greater than ten minutes post injection. The slope of this line provides the net influx rate of ^{18}F -FDG. The myocardial metabolic rate of glucose (MRG) was then obtained by multiplying these regional influx rate by the plasma concentration of stable glucose, assuming a lumped constant of 1, and by dividing the corresponding tissue fraction values obtained from the kinetic of myocardial blood flow analysis. This last step was performed in order to correct for partial volume effects, thereby, allowing for a comparison with corresponding myocardial blood flow values. A conversion from millilitres to grams of perfusable tissue was made by dividing by the density of tissue (1.04 g/ml). Thus myocardial blood flow values are expressed as ml/min/g and metabolic rates of glucose values as $\mu\text{mol}/\text{min}/\text{g}$ of perfusable tissue.

5.4 Statistical analysis

All the data are represented as mean \pm SD. Student's t test was used to compare any pair of mean group values. Simultaneous comparison of more

than two mean values was performed using one-way analysis of variance (ANOVA) for repeated measures, and Fisher's least significant different method was subsequently applied to localize the source of the difference (Godfrey 1985). Regression analysis was performed according to standard techniques. A value of $P < 0.05$ was considered significant.

Chapter 6

Results

6.1 Introduction

All the results are presented as mean plus or minus one standard deviation for all the variables assessed. Left ventricular function was assessed in terms of ejection fraction (%) and regional wall motion scores before and after surgery in all patients. Metabolic profile measured blood glucose (mmo/l) and plasma insulin (mU/l) concentration in the patients and normal controls at baseline. Regional myocardial blood flow (ml/min/g) and metabolic rate of glucose utilization ($\mu\text{mol}/\text{min}/\text{g}$) was measured before surgery in the patients and at baseline in the normal volunteers.

6.2 Ventricular function and metabolic profile

6.2.1 Before surgery

Global left ventricular ejection fraction was $35\pm 11\%$ (range 12 to 55%). A total of 295 segments were analyzed in the 30 patients. Of these 107 were dysfunctional and 188 had a normal function. Regional wall motion average score was 5.3 ± 3.1 (range 1 to 11). Regional wall motion was graded as: normal = 0; hypokinetic = 1; akinetic = 2; dyskinetic = 3. Blood glucose concentration,

measured before the beginning of the clamp, was 7.1 ± 3.4 mmol/l (range 4 to 22 mmol/l). Five of these patients were known diabetics (three had insulin dependent diabetes and two had non insulin dependent diabetes). Baseline plasma insulin concentration was 16 ± 12 mU/l (range 2 to 40 mU/l). During clamp, euglycaemia was achieved in all but one patient and blood glucose concentration was 5.8 ± 1.3 mmol/l (range 4 to 11, $p < 0.01$ vs baseline). Plasma insulin during clamp was 88 ± 17 mU/l (range 68 to 133 mU/l, $p < 0.0001$). In the nine normal subjects baseline blood glucose was 5.3 ± 0.9 mmol/l (range 4.1 to 6.7 mmol/l, $p = \text{NS}$ vs patients) and plasma insulin was 19 ± 1 mU/l (range 17 to 21 mU/l, $p = \text{NS}$ vs patients) (table 6.1). During clamp blood glucose was 6.1 ± 0.9 (range 4.8 to 7.6 mmol/l, $p = \text{NS}$ vs patients) and plasma insulin was 139 ± 92 mU/l (range 79 to 250 mU/l, $p = \text{NS}$ vs patients) .

	RWM pre-op	RWM post-op	Glucose baseline	glucose clamp	EF (%) pre-op	EF (%) post-op
normals	-	-	5.3 ± 0.9	6.1 ± 0.9	-	-
patients	5.3 ± 3.1	3.4 ± 3.0	7.1 ± 3.4	5.8 ± 1.3	35 ± 11	36 ± 12

RWM = regional wall motion; pre-op = before surgery; pos-op = after surgery;
EF = ejection fraction; RWM = regional wall motion average score (0=normal; 1=hypokinetic; 2= akinetic; 3=dyskinetic)

Table 6.1 -Results of ventricular function and metabolic profile

6.2.2 After surgery

Global left ventricular ejection fraction after coronary bypass was 36 ± 12 (range 12 to 60%, $p = \text{NS}$ vs baseline). Fifty nine out of 107 (55%) dysfunctional segments had a functional improvement after bypass surgery while 48 were

unchanged. Ten segments (originally 3 normals and 7 dysfunctional) that became worse probably due to technical surgical problems were excluded from the analysis. Regional wall motion average score improved to 3.4 ± 3.0 (range 0 to 11, $p < 0.001$)

Patient	Age	LAD	LCx	RCA	EF% (pre-op)	EF% (post-op)	RWM (pre-op)	RWM (post-op)
1	70	>75	>75	>75	32	22	1	4
2	45	50-75	>50	100	37	28	2	1
3	57	>75	nor	nor	37	38	8	5
4	58	>75	dis	>75	34	35	4	4
5	62	>75	>75	100	41	38	3	2
6	58	<50	100	100	24	49	9	1
7	53	>75	nor	nor	40	43	2	0
8	60	nor	nor	100	55	55	2	0
9	34	>75	>75	100	49	51	2	2
10	62	nor	50-75	100	54	60	3	0
11	54	>75	>75	>75	41	38	2	1
12	60	>75	nor	100	12	25	9	3
13	52	100	nor	nor	19	36	11	5
14	54	>75	>75	>75	36	52	6	0
15	61	>75	>75	100	38	29	11	11
16	55	>75	>75	nor	49	40	3	3
17	52	100	>75	>75	23	20	10	10
18	40	>75	nor	nor	25	28	7	7
19	46	nor	100	>75	46	45	2	1
20	59	>75	nor	100	28	37	5	3
21	70	100	nor	>75	32	29	5	9
22	59	>75	>75	>75	54	59	7	4
23	72	nor	nor	100	32	28	4	5
24	54	100	nor	nor	41	39	9	3
25	58	>75	100	nor	42	38	1	1
26	53	>75	nor	nor	21	12	4	4
27	72	100	100	100	22	26	6	2
28	34	100	nor	100	15	21	9	8
29	69	>75	>75	100	27	28	8	2
30	71	>75	>75	>75	30	44	5	1

LAD = left anterior descending; LCx = left circumflex coronary artery; RCA = right coronary artery; nor = angiographically normal artery; <50 = less than 50% diameter reduction; >50 = greater than 50% diameter reduction; >75 = greater than 75% diameter reduction; 50-75 = diameter reduction between 50 and 75%; 100 = total occlusion; EF = left ventricular ejection fraction percent; Pre-op = before bypass surgery; post-op = after by-pass surgery; RWM = regional wall motion score (0 = normal; 1 = hypokinetic; 2 = akinetic; 3 = dyskinetic)

Table 6.2 - Patient characteristics

6.3 Myocardial blood flow

In the 25 normal volunteers, myocardial blood flow (MBF) was homogeneously distributed in the different ventricular regions and mean left ventricular myocardial blood flow was 1.11 ± 0.28 ml/min/g (range 0.75 to 1.64 ml/min/g). After correction for the rate-pressure (RPP) product mean left ventricular myocardial blood flow was 1.13 ± 0.27 ml/min/g (range 0.74 to 1.77 ml/min/g). In the patients, myocardial blood flow in the 130 segments with normal function was 0.92 ± 0.26 ml/min/g (range 0.43 to 1.56, $p=0.001$ vs normal subjects) and 1.00 ± 0.33 ml/min/g (range 0.37 to 2.45, $p=NS$ normal subjects) after correction for RPP. In the 107 dysfunctional segments corrected for rate pressure product, myocardial blood flow was 0.93 ± 0.51 ml/min/g (range 0.17 to 4.40, $p=NS$ vs both segments with normal function and vs normal subjects). Myocardial blood flow in the 59 segments that improved after bypass was 0.95 ± 0.41 ml/min/g and myocardial blood flow in the 48 segments that were unchanged after surgery was 0.91 ± 0.61 ml/min/g $p=NS$ vs normal segments and normal subject (table 6.3). To identify dysfunctional segments, with abnormally low myocardial blood flow a cutoff value of 0.67 ml/min/g was used (this corresponds to the mean MBF - 1SD in normal segments. In 23/107 segments MBF was less than 0.67ml/min/g. After surgery, regional wall motion improved in 11/23 while was unchanged in 12/23. In 84/107 dysfunctional segments (79%) myocardial blood flow was greater than 0.67 ml/min/g and regional wall motion improved in 48/84 (57%) and was unchanged in 36/84 despite comparable myocardial blood flow (0.95 ± 0.41 versus 0.91 ± 0.61 ml/min/g) (figure 6.1).

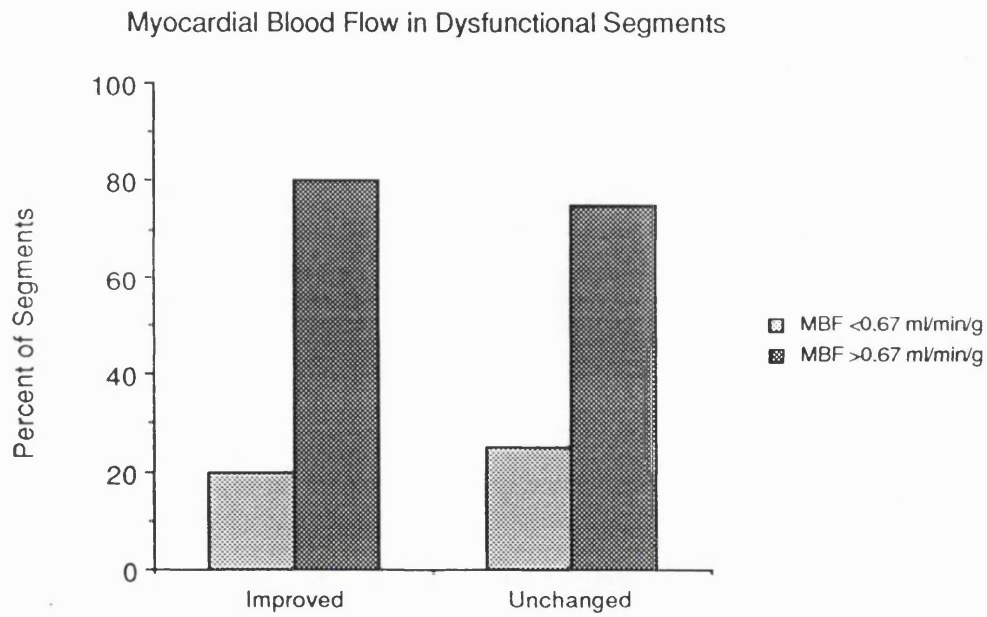


Figure 6.1 - Myocardial Blood Flow in Dysfunctional Segments.

Segments	Myocardial blood flow (ml/min/g)	Metabolic rate of glucose (μ mol/min/g)
Normal volunteers	1.13 \pm 0.27	0.71 \pm 0.14
Normal segments (n=130)	1.00 \pm 0.33	0.45 \pm 0.19
Improved segments (n=59)	0.95 \pm 0.41	0.44 \pm 0.14
Unchanged segments (n=48)	0.91 \pm 0.61	0.34 \pm 0.17 *

*Table 6.3 - Results of myocardial blood flow and metabolic rate of glucose. Myocardial blood flow values are RPP corrected. * = $P < 0.05$ versus normal and improved segments*

6.4 Metabolic rate of glucose

In the nine normal volunteers, metabolic rate of glucose (MRG) was 0.71 \pm 0.14 μ mol/min/g (range 0.46 to 1.02 μ mol/min/g). In patients, metabolic rate of glucose in the 130 segments with normal function was 0.45 \pm 0.19 μ mol/min/g (range 0.10 to 1.02 μ mol/min/g, $p < 0.0001$ vs normal subjects). Metabolic rate of glucose in the 59 segments that improved after bypass was 0.44 \pm 0.14 μ mol/min/g (range 0.04 to 0.71 μ mol/min/g, $p = \text{NS}$ vs normal segments), and metabolic rate in the 48 segments that were unchanged after surgery was 0.34 \pm 0.17 μ mol/min/g, (range 0.09 to 0.78 μ mol/min/g, $p < 0.0001$ vs normal segments and normal subjects (figure 6.2). The MRG in the 23/107 dysfunctional segments with abnormally low myocardial blood flow was 0.40 \pm 0.16 μ mol/min/g (range 0.04 to 0.78 μ mol/min/g) In the 84/107 dysfunctional segments with MBF greater than 0.67 ml/min/g, the MRG was 0.41 \pm 0.16 μ mol/min/g (range 0.09 to 0.79 μ mol/min/g, $p = \text{NS}$ vs segments with MBF greater than 0.67 ml/min/g) (Figure 6.3)

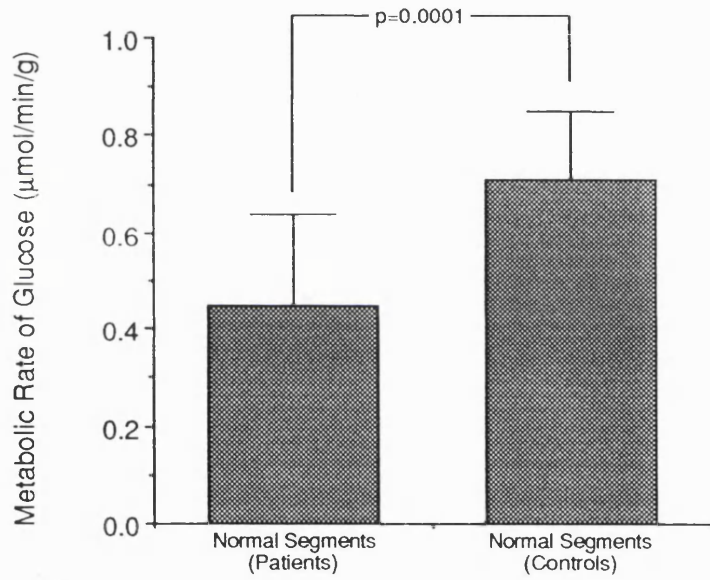


Figure 6.2 - Metabolic Rate of Glucose in Normal Segments in Patients and in Controls.

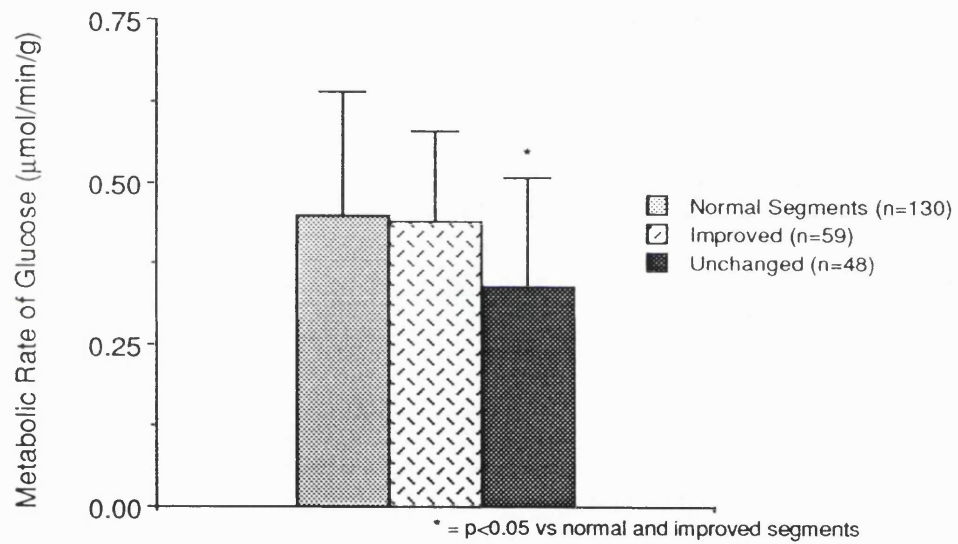


Figure 6.3 - Metabolic Rate of Glucose in Patients.

Chapter 7

Discussion

7.1 Introduction

It is now well established that myocardial regions with chronic wall motion abnormalities, subtended by stenotic arteries, may improve their function after coronary revascularisation. To describe this condition, the term "hibernating myocardium" was introduced by Rahimtoola in 1985. On the basis of a retrospective analysis of 3 studies, which included a large number of patients with coronary artery disease randomized to receive either medical or surgical treatment (Rahimtoola 1985), he concluded that:

"there is a prolonged subacute or chronic stage of myocardial ischaemia that is frequently not accompanied by pain and in which myocardial contractility and metabolism are reduced to match the reduced blood supply" .

However, the hypothesis that a chronic reduction of myocardial blood flow is the cause of myocardial hibernation, has recently been challenged by Vanovershelde 1992, who demonstrated that baseline myocardial blood flow was normal in chronically dysfunctional myocardium subtended by occluded coronary arteries in patients with angina and no previous infarction. These

authors suggested that repeated episodes of ischaemia, rather than chronic hypoperfusion, might form the basis of myocardial hibernation in these patients.

Nonetheless, in most cases chronic myocardial dysfunction is detected in patients with previous infarction. In these patients wall motion abnormalities may be the result of permanent anatomical damage and/or be due to a state of hibernation. It has been demonstrated that the simultaneous assessment of myocardial blood flow and metabolism with positron emission tomography , allows the differentiation between scarred and viable myocardium in patients with chronic left ventricular dysfunction, who are potential candidates for coronary revascularization (Tillisch 1986, Tamaki 1989, Marwick 1992 and Gropler 1993). In this context, however, positron emission tomography has been used mainly to provide qualitative or semiquantitative information rather than to exploit its capability to give absolute measurements. In addition, no effort has been made to standardize the dietary state of patients undergoing the positron emission tomography studies, thereby precluding a reliable assessment of the metabolic data (Choi 1993). The latter point is particularly relevant given the high prevalence of insulin resistance amongst patients with coronary artery disease .

Therefore, the aim of the present study was to measure, using PET, absolute regional myocardial blood flow and glucose utilization during hyperinsulinaemic euglycaemic clamp in patients with hibernating myocardium and previous infarction before coronary artery by-pass graft.

7.2 Discussion

This thesis has demonstrated that most of the chronically dysfunctional myocardial segments which improve following coronary revascularization have myocardial blood flow values within the normal limits. Although, the way in which "low flow" was defined in the present work (i.e. mean myocardial blood flow minus one standard deviation in normally contracting myocardium) is arbitrary, the chosen cut-off value of myocardial blood flow (0.67 ml/min/g) is identical to that proposed by Bergmann (1989) and very similar to that (0.70 ml/min/g) proposed by Perroni-Filardi (1994), both obtained using $H_2^{15}O$ and positron emission tomography. The findings of this thesis indicate that, in most of the patients with previous myocardial infarction, hibernating myocardium was not due to chronically reduced myocardial blood flow. This is consistent with the findings of Vanoverschelde (1993) in patients without previous infarction and suggests that additional mechanisms are responsible for this condition. In patients with coronary artery disease, coronary flow reserve decreases as the degree of stenosis is increased and is abolished for stenosis equal to 80% or more of the luminal diameter (Uren 1994). Under these circumstances, any increase in cardiac workload above baseline conditions cannot be met by an adequate increase in myocardial blood flow, leading to myocardial ischaemia. Therefore, it is possible that in patients with severe coronary artery disease the limited flow reserve leads to the development of myocardial ischaemia even for small increases of oxygen demand as those associated with ordinary daily activities. In this case, frequently repeated bouts of ischaemia, rather than chronically reduced myocardial blood flow, could be the mechanism of hibernation. In several other studies myocardial blood flow has been assessed

using positron emission tomography in patients with sub-acute or chronic myocardial infarction. In 22 patients 86±38 hours after acute myocardial infarction (Czernin 1993), flow in the infarcted segments that were shown to be metabolically active with ^{18}F -FDG imaging was higher (0.6 ± 0.2 ml/min/g) than in non viable ones (0.3 ± 0.1 ml/min/g, $p < 0.05$). In another series of 15 patients with reperfused anterior infarction that were studied 42±25 days after the acute event, transmural flow averaged 0.8 ± 0.1 ml/min/g in remote segments, 0.7 ± 0.2 ml/min/g in adjacent and 0.5 ± 0.1 ml/min/g in segments located in the centre of the infarcted area (Vanoverschelde 1992). Similar findings have recently been reported in 26 patients with chronic healed infarction studied 44±65 months after the event (Gerwitz 1994). However, it is worth noting that in all these positron emission tomography, studies myocardial blood flow was measured using $^{13}\text{NH}_3$ as flow tracer. As discussed earlier, it is important to consider that in a myocardial region consisting of an admixture of normal and necrotic tissue H_2^{15}O only measures flow to the residual myocardium (Iida 1991) while $^{13}\text{NH}_3$ gives an average flow value within the entire region of interest.

Another major finding of this thesis was that the rate of myocardial ^{glucose} utilization in normally contracting segments in patients was 35% lower than that measured in the myocardium of normal subjects. This was observed despite comparable values of circulating glucose and insulin were achieved in patients and controls during hyperinsulinaemic euglycaemic clamp. Insulin resistance has been demonstrated principally in insulin sensitive tissues (Skeletal muscle and adipose tissue) in patients with different diseases including diabetes (Lillioja 1993), arterial hypertension (Ferrannini 1987) and coronary artery disease, but it is not clear whether myocardial tissue is equally resistant to the action of this

hormone. In two different studies, performed during hyperinsulinaemic euglycaemic clamp, the myocardial utilization of glucose, measured with positron emission tomography, in patients with type 1 diabetes was found to be similar to that in non diabetic controls (Nuutila 1993 and Vom Dahl 1993). By contrast, glucose utilization in skeletal muscle as well as whole body glucose uptake were significantly reduced in diabetic patients compared to controls (Voipio-Pulkki 1993). Some differences in the absolute values of myocardial utilization exist between these studies and the data presented here. These differences can be explained by the fact that it was used a "lumped constant" value of 1 compared to the value of 0.67 used in the above mentioned reports. It must be emphasised, however, that the 0.67 value derives from animal studies (Ratib 1982) and it is not known whether this is also applicable to human myocardium. In addition, it is not known whether the same "lumped constant" value can be used for normal subjects and patients. However, taking into account the different "lumped constant" values, myocardial glucose utilization rates measured in the control group are comparable with those obtained in other studies (Nuutila 1993, Vom Dahl 1993 and Hicks 1991). A similar study was performed in patients with type 2 diabetes demonstrating that, during clamp, myocardial utilization was reduced 39% in these patients compared to controls (Voipio-Pulkki 1993). In summary, the results of this thesis indicated that the myocardium of patients with coronary artery disease is more resistant to insulin than myocardium of normal controls. This seems to be true even in the absence of other conditions known to be associated with insulin resistance. In fact, the difference between normals and patients was still significant after exclusion of the five patients with diabetes and the four with arterial hypertension (0.71 ± 0.14 vs 0.46 ± 0.18 $\mu\text{mol}/\text{min}/\text{g}$, $p=0.0001$).

This thesis demonstrates that absolute quantification of the metabolic rates of glucose utilization in the myocardium during hyperinsulinaemic euglycaemic clamp allows to differentiate between segments which will improve after surgery from those that will not. Using a cut-off point of $0.26 \mu\text{mol}/\text{min}/\text{g}$ (calculated as the mean metabolic rate of glucose minus one standard deviation in patient's normal segments), one gets a positive accuracy of 62% and a negative predictive accuracy of 73% (Figure 7.1, top panel). It is worth noting, however, that at this cut-off value already 90% of the viable segments have been correctly identified (Figure 7.1, bottom panel). This figure presents the number of segments correctly identified for every cut-off (increments of $0.1 \mu\text{mol}/\text{min}/\text{g}$), e.g. if a segment presents a value of $0.2 \mu\text{mol}/\text{min}/\text{g}$ it can be compared with our results, in which nearly 98% of the segments that improved after surgery had values of glucose utilization equal or greater than $0.2 \mu\text{mol}/\text{min}/\text{g}$. It is important to emphasize that the number of patients enrolled in this thesis was limited by the time of the research and that studies based on larger patient population may provide more accurate values of positive and negative predictive accuracy.

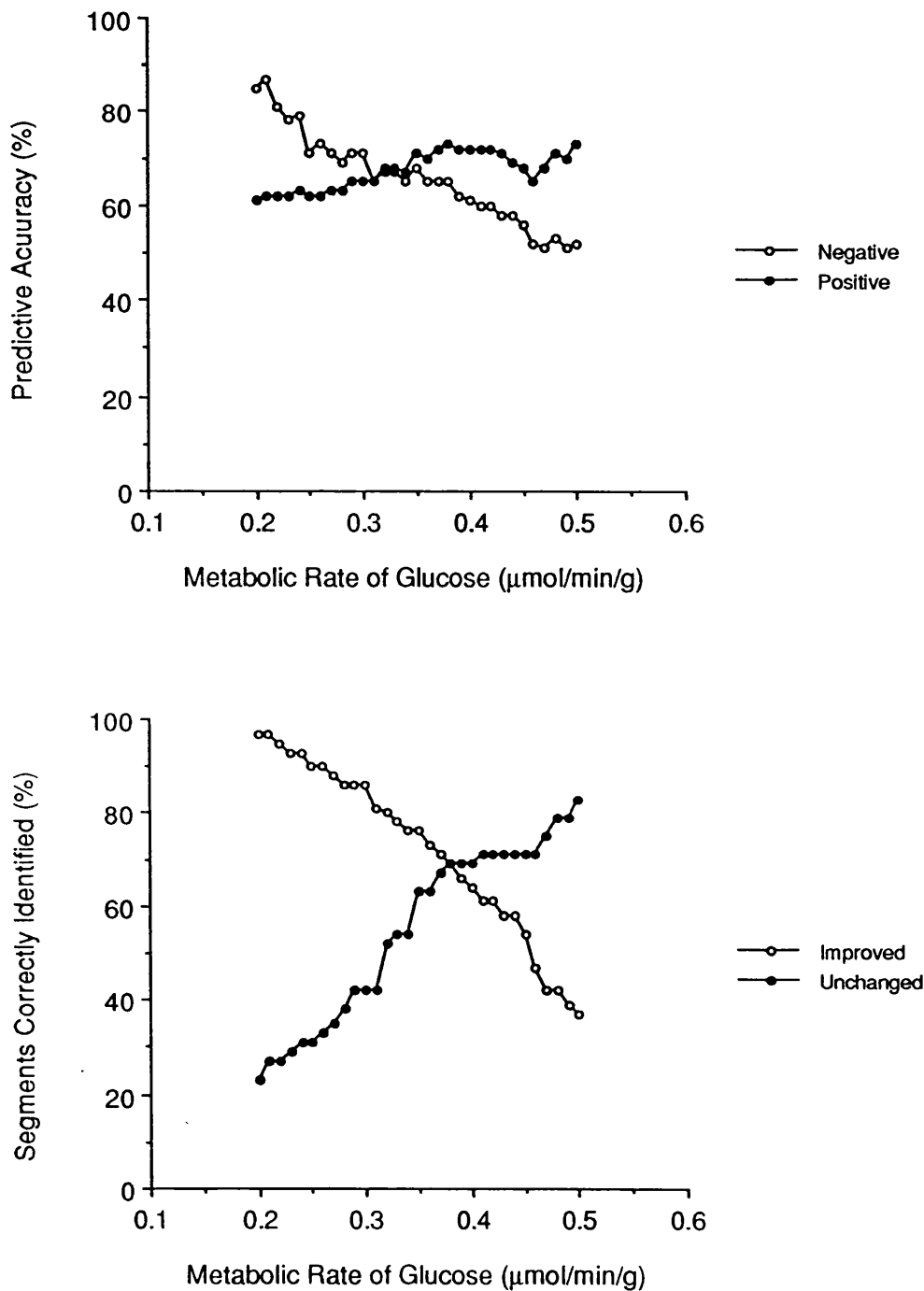


Figure 7.1 **Top panel:** Positive and negative predictive accuracy of the PET scan according to the value of the myocardial metabolic rate of glucose. The percentage of dysfunctional segments that improved (positive predictive accuracy) and those that did not improve after surgery (negative predictive accuracy) is shown as a cumulative function of the metabolic rate of glucose. Thus, for example about 65% of segments that recovered after surgery (improved) had a metabolic rate of glucose greater than $0.25\mu\text{mol}/\text{min}/\text{g}$ whereas about 80% of those which did not recover (unchanged) had a metabolic rate of glucose lower than $0.25\mu\text{mol}/\text{min}/\text{g}$.

Bottom panel: Number of segments correctly identified (either improved or unchanged) as a function of the metabolic rate of glucose.

7.3 Conclusions

The results of the present thesis have provided evidence that:

1. Viable "hibernating myocardium" in patients with previous infarction is not chronically hypoperfused in most cases.
2. The myocardium of patients with coronary artery disease is less sensitive to insulin than the myocardial tissue of normal subjects.
This is a global condition not confined to regions with wall motion abnormalities
3. The use of hyperinsulinaemic euglycaemic clamp allowed to produce high quality metabolic (^{18}F -FDG) images in all subjects; this is particularly important in view of the insulin resistance demonstrated in the myocardium of these patients,
4. The use of the clamp allowed adequate standardization of the dietary state making possible the comparison of absolute metabolic rate of glucose values amongst different individuals.

Chapter 8

Recommendations for Future Research

8.1 Future Research

Due to time constraints the work carried out investigated the prediction power of flow ($H_2^{15}O$) and its behaviour in the hypothesis of "low flow" that was believed to occur in hibernating myocardium. It also investigated myocardial glucose utilization ^{18}F -FDG, under controlled dietary conditions, in the identification of myocardial areas which may deserve revascularization treatment. The definition of improvement was based upon pre and post surgical assessment of regional wall motion.

Future research should compare similar findings in larger groups, and with more widely available technique, such as thallium-201, in order to establish an organogram for pre-revascularization assessment of patients with coronary artery disease. Other techniques, i.e. magnetic resonance mapping, receptor studies, free fatty acids metabolism and anti-myosin, as well as echocardiography should be employed in larger samples of patients with hibernating myocardium, in order to establish which patients would clearly benefit from revascularization procedures.

References

- Altehoefer C, Kaiser H-J, Dorr R, Feinendegen C, Beilin I, Uebis R, Buell U : Fluorine -18 deoxyglucose PET for assessment of viable myocardium in perfusion defects in ^{99m}Tc-MIBI SPET : a comparative study in patients with coronary artery disease. *Eur J Nucl Med* 1992;**19**:334-342
- Arai AE, Pantley GA, Anselone CG, Bristow J, Bristow JD : Active downregulation of myocardial energy requirements during prolonged moderate ischemia in swine. *Circ Res* 1991;**69**:1458-1469
- Araujo LI, Lammerstma AA, Rhodes CG, McFallas EO, Iida H, Rechavia E, Galassi AR, De Silva R, Jones T, Maseri A : Non-invasive quantification of regional myocardial blood flow in normal volunteers and patients with coronary artery disease using oxygen-15 labeled carbon dioxide and positron emission tomography. *Circulation* 1991;**83**:875-885
- Armbrecht JJ, Buxton DB, Brunken RC, Phelps ME, Schelbert HR : Regional myocardial oxygen consumption determined noninvasively in humans with [1-¹¹C]acetate and dynamic positron tomography. *Circulation* 1989;**80**:936-872
- Armbrecht JJ, Buxton DB, Schelbert HR : Validation of [1-¹¹C] acetate as a tracer for noninvasive assessment of oxidative metabolism with positron emission tomography in normal, ischemic, postischemic, and hyperemic canine myocardium. *Circulation* 1990;**81**:1594-1605
- Bartenstein P, Schober O, Hasfeld M, Schäfers M, Matheja P, Breithard G : Thallium-201 single photon emission tomography of myocardium: Additional information in reinjection studies is dependent on collateral circulation . *Eur J Nucl Med* 1992;**19**:790-795
- Beller GA, Alten WJ, Cochavi S, Hnatowich D, Brownell GL : Assessment of regional myocardial perfusion by positron emission tomography after

- intracoronary administration of Ga-69 labeled albumin microspheres. J Comp Assist Tomogr 1979;**3**:447-452
- Bellina CR, Parodi O, Camici P, Salvadori PA, Taddei L, Fusani L, Guzzardi R, Klassen GA, L'Abbate A, Donato L : Simultaneous in vitro and in vivo validation of nitrogen-13 ammonia for the assessment of regional myocardial blood flow : J Nucl Med 1990;**31**:1335-1343
- Berger BC, Watson DD, Burwell LR, Crosby IK, Wellons HA , Teates CD, Beller GA : Redistribution of thallium at rest in patients with stable and unstable angina and the effect of coronary bypass artery surgery. Circulation 1979;**60**:1114-1125
- Bergmann SR, Fox KAA, Rand AL, McElvany KD, Welch MJ, Markham J, Sobel BE : Quantification of regional myocardial blood flow in vivo with H₂¹⁵O. Circulation 1984;**70**:724-733
- Bergmann SR, Herrero P, Markham J, Weinheimer CJ, Walsh MN : Noninvasive quantification of myocardial blood flow in human subjects with O-15 labelled water and positron emission tomography. J Am Coll Cardiol 1989;**14**:639-652
- Berne RM : The role of adenosine in the regulation of coronary blood flow. Circ Res 1980;**47**:807-813
- Bing RJ: The metabolism of the heart. Orlando, Fla/New York, Academic Press, Inc. Harvey Lecture Series 50, 1954, pp 27-70
- Blumgart HL, Gilligan R, SchlesingerMJ : Experimental studies on the effect of temporary occlusion of coronary arteries. II. The production of myocardial infarction. Am Heart Journal 1941;**22**:374-389
- Bolli R : Mechanism of myocardial "stunning". Circulation 1990;**82**:723-738

- Bonow RO, Dilsizian V : Thallium-201 and technetium-99m-sestamibi for assessing viable myocardium. *J Nucl Med* 1992;**33**:815-818
- Bonow RO, Dilsizian V, Cuocolo A, Bacharach SL : Identification of viable myocardium in patients with chronic coronary artery disease and left ventricular dysfunction. Comparison of thallium scintigraphy with reinjection and PET imaging with ¹⁸F-Fluorodeoxyglucose. *Circulation* 1991;**83**:26-37
- Bounous EP, Mark DB, Pollock BG, Hlatky MA, Harrel Jr FE, Lee KL, Rankin JS, Wechsler AS, Pryor DB, Califf RM : Surgical survival benefits for coronary disease patients with left ventricular dysfunction. *Circulation* 1988;**78**(suppl I):I-151-I-157
- Bradley AB, Baim DS : Evaluation of myocardial blood flow and metabolism. In: *Cardiac Catheterization and Angiography*, edited by W Grossman. Philadelphia: Lea & Febiger, 1986,pp320-338
- Bradley-Moore PR, Lebowitz E, Greene MW, Ansari AN : Thallium for medical use. II : Biologic behavior. *J Nucl Med* 1975;**16**:156-160
- Braunwald E (editor) : *Heart disease. A textbook of cardiovascular medicine.* W.B. Saunders Company 1988 pages 268-270
- Braunwald E, Kloner RA : The stunned myocardium: Prolonged, postischemic ventricular dysfunction. *Circulation* 1982;**66**:1146-1149
- Bristow JD, Arai AE, Anselone CG, Pantely GA : Response to myocardial ischemia as a regulated process. *Circulation* 1991;**84**:2580-2587
- Brown MA, Myears DW, Bergmann SR : Noninvasive assessment of canine myocardial oxidative metabolism with carbon-11 acetate and positron emission tomography. *J Am Coll Cardiol* 1988;**12**:1054-1036

- Brown MA, Myears DW, Bergmann SR : Validity of estimates of myocardial oxidative metabolism with carbon-11 acetate positron emission tomography despite altered patterns of substrate utilization. *J Nucl Med* 1989;**30**:187-193
- Brundage BH, Massie BM, Botvinick EH : Improved regional ventricular function after successful surgical revascularization. *J Am Coll Cardiol* 1984;**3**:902-908
- Brunken RC, Kottou S, Nienaber CA, Schwaiger M, Ratib OM, Phelps ME, Schelbert HR : PET detection of viable tissue in myocardial segments with persistent defects at TI-201 SPECT. *Radiology* 1989;**172**:65-73
- Brunken R, Schwaiger M, Grover-McKay M, Phelps ME, Tillisch J, Schelbert HR : Positron emission tomography detects tissue metabolic activity in myocardial segments with persistent thallium perfusion defects. *J Am Coll Cardiol* 1987;**10**:557-567
- Brunken R, Tillisch J, Schwaiger M, Child JS, Marshall R, Mandelkern M, Phelps ME, Schelbert HR : Regional perfusion, glucose metabolism, and wall motion in patients with chronic electrocardiographic Q wave infarctions: evidence for persistence of viable tissue in some infarct regions by positron emission tomography. *Circulation* 1986;**73**:951-963
- Budinger TF, Pohost GM : Thallium "redistribution" - an explanation. *J Nucl Med* 1986;**27**:996 [Abstract]
- Budinger TF, Knittel BL : Cardiac thallium redistribution and model. *J Nucl Med* 1987;**28**:588 [Abstract]
- Burns RJ, Galligan L, Wright L : Thallium infusion scintigraphy improves detection of viable myocardium. *Circulation* 1990;**82**(suppl III):III-544[Abstract]

- Buxton DB, Nienaber CA, Luxen A, Ratib O, Hansen H, Phelps ME, Schelbert HR : Noninvasive quantitation of regional myocardial oxygen consumption in vivo with [1-¹¹C]acetate and dynamic positron emission tomography. *Circulation* 1989;**79**:134-142
- Buxton DB, Schwaiger M, Nguyen A, Phelps MR, Schelbert HR : Radiolabeled acetate as a tracer of myocardial tricarboxylic acid cycle flux. *Cir Res* 1988;**63**:628-634
- Califf RM, Harrel Jr FE, Lee KL, Rankin JS, Mark DB, Hlatky MA, Muhlbaier LH, Wechsler AS, Jones RH, Oldham Jr HN, Pryor DB : Changing efficacy of coronary revascularization. Implications for patient selection. *Circulation* 1988;**78**(suppl I):I-185-I-191)
- Camici PG, Araujo LI, Spinks T, Lammerstma AA, Kaski JC, Shea MJ, Selwyn AP, Jones T, Maseri A : Increased uptake of ¹⁸F-fluorodeoxyglucose in postischemic myocardium of patients with exercise-induced angina. *Circulation* 1986b;**74**:81-88
- Camici PG, Araujo LI, Spinks T, Lammerstma AA, Sohanpal SK, Jones T, Maseri A : Prolonged metabolic recovery allows late identification of ischemia in the absence of electrocardiographic and perfusion changes in patients with exertional angina. *Can J Cardiol* 1986a;**(suppl A)**:131A-135A
- Camici PG, Ferrannini E and Opie LH : Myocardial metabolism in ischemic heart disease: basic principles and applications to imaging by positron emission tomography. *Prog Cardiovasc Dis* 1989a;**32**:217-238
- Camici PG, Marinho NVS : Assessment of myocardial viability and the role of surgery. *Cur Opin Cardiol* 1993;**8**:927-931

- Camici PG, Marraccini P, Lorenzoni R, Buzzigoli G, Pecori N, Perissinotto A, Ferrannini E, L'Abbate A, Marzilli M : Metabolic markers of stress-induced myocardial ischemia. *Circulation* 1991;**83**:III8-III13
- Camici PG, Marraccini P, Marzilli M, Lorenzoni R, Buzzigoli G, Puntoni R, Boni C, Bellina CR, Klassen GA, L'Abbate A : Coronary hemodynamics and myocardial metabolism during and after pacing stress in normal humans. *Am J Physiol* 1989b;**257**:E309-E317
- Chambers J, Bass C : Chest pain with normal coronary anatomy: A review of natural history and possible etiologic factors. *Prog Cardiovasc Dis* 1990;**33**:161-184
- Chilian WM, Eastham CL, Layne SM, Marcus ML : Small vessel phenomena in the coronary microcirculation: Phasic intramyocardial perfusion and microvascular dynamics. *Prog Cardiovasc Dis* 1988;**31**:17-38
- Chilian WM, Eastham CL, Marcus ML : Microvascular distribution of coronary vascular resistance in beating left ventricle. *Am J Physiol* 1986;**251**:H779-H788
- Chilian WM, Layne SM, Eastham CL, Layne SM, Marcus ML : Heterogeneous microvascular coronary -adrenergic vasoconstriction. *Circ Res* 1989;**64**:376-388
- Choi Y, Brunken RC, Hawkins RA, Huang S-C, Buxton DB, Hoh CK, Phelps ME, Schelbert HR : Factors affecting myocardial 2-[F-18]fluoro-2-deoxy-D-glucose uptake in positron emission tomography studies of normal humans. *Eur J Nucl Med* 1993;**20**:308-318
- Christakis GT, Weisel RD, Fremes SE, Ivanov J, David TE, Goldman BS, Salerno TA, Cardiovascular surgeons of the University of Toronto :

- Coronary artery bypass grafting in patients with poor left ventricular function. *J Thorac Cardiovasc Surg* 1992;**103**:1083-1092
- Clarke JG, Davies GJ, Kerwin R, Hackett D, Larkin S, Dawbarn D, Lee Y, Bloom SR, Yacoub M, Maseri A : Coronary artery infusion of neuropeptide Y in patients with angina pectoris. *Lancet* 1987;**I**:1057-1059
- Cloninger KR, DePuey EG, Garcia EV, Roubin GS, Robbins WL, Nody A, De Pasquale EE, Berger HJ : Incomplete redistribution in delayed thallium-201 single photon emission tomographic (SPECT) images: An overestimation of myocardial scarring. *J Am Coll Cardiol* 1988;**12**:955-963
- Cole JS, Hartley CJ : The pulsed doppler coronary artery catheter. Preliminary report of a new technique for measuring rapid changes in coronary flow velocity in man. *Circulation* 1977;**56**:18-25
- Cucchini F, Di Donato M, Ferrari R, Visioli O : Dynamic ventriculography with K-strophanthin. *Eur J Cardiol* 1978;**81**:75-84
- Cuocolo A, Pace L, Ricciardelli B, Chiariello M, Trimarco B, Salvatore M : Identification of viable myocardium in patients with chronic coronary artery disease: Comparison of thallium-201 scintigraphy with reinjection and technetium-99m-methoxyisobutyl isonitrile. *J Nucl Med* 1992;**33**:505-511
- Czernin J, Porenta G, Brunken R, Krivokapich J, Chen K, Bennet R, Hage A, Fung C, Tillisch J, Phelps ME, Schelbert HR : Regional blood flow, oxidative metabolism, and glucose utilization in patients with recent myocardial infarction. *Circulation* 1993;**88**:884-895
- De Fronzo RA, Jordan DT, Reubin A : Glucose clamp technique: a method for quantifying insulin secretion and resistance. *Am J Physiol* 1979;**237**:E214-E223

- De Silva R, Camici PG : Assessment of myocardial perfusion, metabolism and pharmacology using positron emission tomography. *Cardioscience* 1992;**3**:205-216
- De Silva R, Yamamoto Y, Rhodes CG, Iida H, Maseri A, Jones T : Noninvasive quantification of regional myocardial oxygen consumption in anaesthetized greyhounds. *J Physiol* 1992;**446**:219P (Abstract)
- Dilsizian V, Arrighi JA, Diodati JG, Quyyumi AA, Alavi K, Bacharach SL, Marin-Neto JA, Katsiyannis PT, Bonow RO : Myocardial viability in patients with chronic coronary artery disease. Comparison of ^{99m}Tc-sestamibi with thallium reinjection and [¹⁸F]Fluorodeoxyglucose. *Circulation* 1994;**89**:578-587
- Dilsizian V , Bonow RO : Current diagnostic techniques of assessing myocardial viability in patients with hibernating and stunned myocardium. *Circulation* 1993;**87**:1-20
- Dilsizian V, Rocco TP, Freedman NM, Leon MB, Bonow RO : Enhanced detection of ischemic but viable myocardium by the reinjection of thallium after stress-redistribution imaging. *N Engl J Med* 1990;**323**:141-146
- Dilsizian V, Smeltzer WR, Freedman NMT, Dextras R, Bonow RO : Thallium reinjection after stress-redistribution imaging. Does 24-hour delayed imaging after reinjection enhance detection of viable myocardium? *Circulation* 1991;**83**:1274-1255
- Dondi M, Tartagni F, Fallani F, Fanti S, Marengo M, Di Tommaso I, Zheng Q-F, Monetti N : A comparison of rest sestamibi and rest-redistribution thallium single photon emission tomography: possible implications for myocardial viability detection in infarcted patients. *Eur J Nucl Med* 1993;**20**:26-31

Duling BR : Microvascular responses to alterations in oxygen tension. *Circ Res* 1972;**31**:481-488

Duling BR : Changes in microvascular diameter and oxygen tension induced by carbon dioxide. *Circ Res* 1973;**32**:370-376

Eitzman D, Al-Aouar Z, Kanter HL, Vom Dahl J, Kirsh M, Deeb GM, Schwaiger M : Clinical outcome of patients with advanced coronary artery disease after viability studies using positron emission tomography. *J Am Coll Cardiol* 1992;**29**:559-565

Elefteriades JA, Tolis Jr G, Levi E, Mills LK, Zaret BL : Coronary artery bypass grafting in severe left ventricular dysfunction: Excellent survival with improved ejection fraction and functional state. *J Am Coll Cardiol* 1993;
:1411-1417

Epstein SE, Cannon III RO: Site of increased resistance to coronary flow in patients with angina pectoris and normal epicardial coronary arteries. *J Amer Coll Cardiol* 1986;**8**:459-461

Ferrannini E, Santoro D, Bonadonna R, Natali O, Parodi O, Camici PG : Metabolic and hemodynamic effects of insulin on human hearts. *Am J Physiol* 1993;**264**:E308-E315

Fioretti P, Reijns EM, Neumann D, Taams M, Kooij PPM, Bos E, Reiber JHC : Improvement in transient and persistent perfusion defects on early and late post-exercise thallium-201 tomograms after coronary artery bypass grafting. *Eur Heart J* 1988;**9**:1332-1338

Fox KAA, Abendschein DR, Ambos HD, Sobel BE, Bergmann SR : Efflux of metabolized and nonmetabolized fatty acid from canine myocardium. Implications for quantifying myocardial metabolism tomographically. *Circ Res* 1985;**57**:232-243

- Fudo T, Kambara H, Hashimoto T, Hayashi M, Hobara R, Tamaki N, Yonekura Y, Senda M, Konishi J, Kawai C : F-18 deoxyglucose and stress N-13 ammonia positron emission tomography in anterior wall healed myocardial infarction. *Am J Cardiol* 1988;**60**:1191-1197
- Gallagher BM, Fowler JS, Gutterson NI, MacGregor RR, Wan C-N, Wolf AP : Metabolic trapping as a principle of radiopharmaceutical design: Some factors responsible for the biodistribution of [¹⁸F] 2-deoxy-2-fluoro-D-glucose. *J Nucl Med* 1978;**19**:1154-1161
- Gallagher KP, Kumala T, Koziol JA et al : Significance of regional wall thickening abnormalities relative to transmural myocardial perfusion in anesthetized dogs. *Circulation* 1980;**62**:1266-1274
- Gambhir SS, Schwaiger M, Huang S-C, Krivokapich J, Shelbert HR, Nienaber CA, Phelps ME : A simple non-invasive quantification method for measuring myocardial glucose utilization in humans employing positron emission tomography and ¹⁸F-deoxyglucose. *J Nucl Med* 1989;**30**:359-366
- Ganz W, Tamura K, Marcus HS, Donoso R, Yoshida S, Swan HJC. Measurement of coronary sinus blood flow by continuous thermodilution in man. *Circulation* 1971;**44**:181-195
- Gasser R, Furian C, Grisold M, Dusleag J, Kein W : Myocardial hibernation. *The Lancet* 1992;**340**:796-797
- Gehring PJ, Hammond PB : The interrelationship between thallium and potassium in animals. *J Pharmacolo Exp Ter* 1967;**155**:187-201
- Gellai M, Norton JM, Detar R : Evidence for direct control of coronary vascular tone by oxygen. *Circ Res* 1973;**32**:279-289
- Gewirtz H, Fischaman AJ, Abraham S, Gilson M, Strauss HW, Alpert NM : Positron emission tomographic measurements of absolute regional

myocardial blood flow permits identification of nonviable myocardium in patients with chronic myocardial infarction. J Am Coll Cardiol 1994;**23**:851-859

Gewirtz H, Beller GA, Strauss HW, Dinsmore RE, Zir LM, McKusick KA, Pohost GM: Transient defects of resting thallium scans in patients with coronary artery disease. Circulation 1979;**59**:707-713

Gibson RS, Watson DD, Taylor GJ, Crosby IK, Wellons HL, Holt ND, Beller GA : Prospective assessment of regional myocardial perfusion before and after coronary revascularization surgery by quantitative thallium-201 scintigraphy. J Am Coll Cardiol 1983;**1**:804-815

Godfrey K : Comparing the means of several groups. N Engl J Med 1985;**313**:1450-1456

Goldstein RA, Kirkeeide RL, Demer LL, Merhige M, Nishikawa A, Smalling RW, Mullani NA, Gould KL : Relation between geometric dimensions of coronary artery stenoses and myocardial perfusion reserve in man. J Clin Invest 1987;**79**:1473-1478

Gould KL : Dynamic coronary artery stenosis. Am J Cardiol 1980;**45**:286-292

Gould KL, Lipscomb K, Hamilton GW : Physiologic basis for assessing critical coronary stenosis. Instantaneous flow response and regional distribution during coronary hyperemia as measures of coronary flow reserve. Am J Cardiol 1974; **33**:87-94

Gree MA : Myocardial perfusion imaging with copper-62 labelled Cu-PTSM. In: What's new in cardiac imaging? edited by van de Waal EE, Sochor H, Righetti A, Niemeyer MG. Dordrecht: Kluwer Academic Publishers,1992,pp165-177

- Gropler RJ, Getman EM, Sampathkumaran K, Perez JE, Moerlein SM, Sobel BE, Bergmann SR, Siegel BA : Functional recovery after revascularization for chronic coronary artery disease is dependent on maintenance of oxidative metabolism. *J Am Coll Cardiol* 1992;**20**:569-577
- Gropler RJ, Siegel BA, Lee KJ, Moerlein SM, Perry DJ, Bergmann SR, Geltman EM : Nonuniformity in myocardial accumulation of fluorine-18-fluorodeoxyglucose in normal fasted humans. *J Nuc Med* 1990;**31**:1749-1756
- Gropler RJ, Getman EM, Sampathkumaran K, Perez JE, Schechtman KB, Conversano A, Sobel BE, Bergmann SR, Siegel BA : Comparison of carbon-11-acetate with fluorine-18-fluorodeoxyglucose for delineating viable myocardium by positron emission tomography. *J Am Coll Cardiol* 1993;**22**:1587-1597
- Gutman J, Berman DS, Freeman M, Rozanski A, Maddahi J, Waxman A, Swan HJC: Time to completed redistribution of thallium-201 in exercise myocardial scintigraphy: Relationship to the degree of coronary artery stenosis. *Am Heart J* 1983;**106**:989-995
- Hambly RI, Aintablian A, Wisoff BG, Harstein MI : Response of the left ventricle in coronary artery disease to postextrasystolic potentiation. *Circulation* 1975;**51**:428-435
- Hamlin RI, Levesque MJ, Kettleson MD : Intramyocardial pressure and distribution of coronary blood flow during systole and diastole in the horse. *Cardiovasc Res* 1982;**16**:256-262
- Hartley CJ, Cole JS : An ultrasonic pulsed doppler system for measuring blood flow in small vessels. *J Appl Physiol* 1974;**37**:626-629

- Hashimoto T, Kambara H, Fudo T, Hayashi M, Tamaki S, Tokunaga S, Tamaki N, Yonekura Y, Konishi J, Kawai C : NonQ wave versus Q wave myocardial infarction: Regional metabolism and blood flow assessed by positron emission tomography. *J Am Coll Cardiol* 1988;**12**:88-93
- Herrero P, Markham J, Shelton ME, Bergmann SR : Implementation and evaluation of a two-compartment model for the quantification of myocardial perfusion with rubidium-82 and positron emission tomography. *Cir Res* 1992;**70**:496-507
- Herrero P, Markham J, Shelton ME, Weinheimer CJ, Bergmann SR : Noninvasive quantification of regional myocardial perfusion with rubidium-82 and positron emission tomography. *Circulation* 1990;**82**:1377-1386
- Hicks RJ, Herman WH, Kalff V, Molin E, Wolfe ER, Hutchins G, Schwaiger M : Quantitative evaluation of regional substrate metabolism in the human heart by positron emission tomography. *J Am Coll Cardiol* 1991;**18**:101-111
- Hoffmann JIE : Transmural myocardial perfusion. *Prog Cardiovasc Dis* 1987;**29**:429 -464
- Hoffman EJ, Huang SC, Phelps ME : Quantitation in positron emission tomography: I Effect of object size. *J Comput Assist Tomogr* 1979;**3**:299-308
- Hoffman EJ, Phelps ME : Positron emission tomography: Principles and quantitation. In: *Positron Emission Tomography and Autoradiography. Principles and Applications for the Brain and the Heart* edited by Phelps ME, Mazziota JC, Schelbert HR. New York, 1986, pp113-148

Huang SC, Phelps ME :Principles of tracer kinetic modelling in positron emission tomography and autoradiography. In Positron Emission Tomography and Autoradiography. Principles and Applications for the Brain and the Heart edited by Phelps ME, Mazziota JC, Schelbert HR. New York, 1986, pp 287-346

Hutchins GD, Schwaiger M, Rosempire KC, Krivokapich J, Schelbert H, Kuhl DE : Noninvasive quantification of regional blood flow in the human heart using N-13 ammonia and dynamic positron emission tomographic imaging. J Am Coll Cardiol 1990;**15**:1032-1042

Iida H, Kanno I, Takahashi A, Miura S, Murakami M, Takahashi K, Ono Y, Shishido F, Inugami A, Tomura N, Higano S, Fujita H, Sasaki H, Nakamichi H, Mizusawa S, Kondo Y, Uemura K : Measurement of absolute myocardial blood flow with H₂¹⁵O and dynamic positron emission tomography : Strategy for quantification in relation to the partial-volume effect. Circulation 1989;**78**:104-115

Iida H, Rhodes CG, De Silva R, Araujo LI, Jones T : Use of a left ventricular time-activity curve as a noninvasive input function in H₂¹⁵O dynamic positron emission tomography. J Nucl Med 1992;**33**:1669-1677

Iida H, Rhodes CG, De Silva R, Yamamoto Y, Araujo LI, Maseri A, Jones T : Myocardial tissue fraction: Correction for partial volume effects and measure of tissue viability. J Nucl Med 1991;**32**:2169-2175

Iida H, Rhodes CG, Yamamoto Y, Jones T, De Silva R, Araujo LI: Quantitative measurements of myocardial metabolic rate of oxygen (MMRO₂) in man using positron emission tomography. Circulation 1990;**82**:III-614 (Abstract)

Iskandrian AS, Hakki A, Kane SA, Goel IP, Mundth ED, Segal BI : Rest and redistribution thallium-201 myocardial scintigraphy to predict improvement

in left ventricular function after coronary arterial bypass grafting. *Am J Cardiol* 1983;**51**:1312-1316

Jordan CD, Flood JG, Laposata M, Lewandrowski KB : Normal reference laboratory values. *N Engl J Med* 1992;**327**:718-724

Kanatsuka H, Lamping KG, Eastham CL, Marcus ML : Heterogeneous changes in epimyocardial microvascular size during graded coronary stenosis. Evidence of the microvascular site for autoregulation. *Circ Res* 1989;**66**:389-396

Kayden DS, Sigal S, Soufer R, Mattera J, Zaret BL, Wackers FJTh : Thallium-201 for assessment of myocardial viability: Quantitative comparison of 24-hour redistribution image with imaging after reinjection at rest. *J Am Coll Cardiol* 1991;**18**:1480-1486

Kawaguchi T, Morris CK, Ribick PM, Ueshima K, Myers J, Froelicher VF : Predictors of disease severity and survival in patients with coronary artery disease. *Coronary Artery Disease* 1993;**4**:971-980

Kennedy JW, Kaiser GC, Fisher LD, Fritz JK, Myers W, Mudd JG, Ryan TJ : Clinical and angiographic predictors of operative mortality from the collaborative study in coronary artery surgery (CASS). *Circulation* 1981;**63**:793-802

Kiat H, Berman DS, Maddahi J, De Yang L, Van Train K, Rozanski A, Friedman J : Late reversibility of tomographic myocardial thallium-201 defects: an accurate marker of myocardial viability. *J Am Coll Cardiol* 1988;**12**:1456-1463

Kiat H, Berman D, Wang F, Friedman J, Maddahi J : Frequency of late reversibility in stress TI-201 SPECT using a reinjection protocol. *Circulation* 1990;**82**(supplIII):III-544 [Abstract]

- Krivokapich J, Smith GT, Huang SC, Hoffman EJ, Ratib O, Phelps ME, Schelbert HR : Nitrogen-13 ammonia myocardial imaging at rest and with exercise in normal volunteers : Quantification of coronary flow with positron emission tomography. *Circulation* 1989;**80**:1328-1337
- Kuijper AFM, Niemeyer MG, D'Haene EG, Van der Wall EE, Paulwels EKJ : Stress-reinjection thallium-201 scintigraphy: Prediction of effect of coronary artery bypass grafting on regional myocardial perfusion (Abstract). *J Am Coll Cardiol* 1993;**21**:389A
- Kuijper AFM, Vliegen HW, Van der Wall EE, Oosterhuis WP, Zwinderman AH, Van Eck-Smit BLF, Niemeyer MG, Paulwels EKJ : The clinical impact of thallium-201 reinjection scintigraphy for detection of myocardial viability. *Eur J Nucl Med* 1992;**19**:783-789
- Kuo L, Davis MJ, Cannon MS, Chilian WM : Pathophysiological consequences of atherosclerosis extend into the coronary microcirculation. Restoration of endothelium-dependent responses by L-arginine. *Circ Res* 1992;**70**:465-476
- L'Abbate A, Maseri A : Xenon studies of myocardial blood flow: Theoretical, technical and practical aspects. *Sem Nucl Med* 1980;**10**:2-15
- Lammerstma AA, Bench CJ, Cremer JE, Luthra SK, Turton D, Wood ND, Frackowiack RSJ : Measurement of cerebral monoamine oxidase B activity using L-[11C]deprenyl and dynamic positron emission tomography. *J Cereb Blood Flow Metab* 1991;**11**:545-556
- Larkin SW, Clarke JG, Keogh BG, Araujo L, Rhodes C, Davies GJ, Taylor KM, Maseri A. Intracoronary endothelin induces myocardial ischemia by small vessel constriction in the dog. *Am J Cardiol* 1989;**64**:956-958

- Lee J-D, Tajimi T, Guth B, Seitelberger R, Miller M, Ross JJr: Exercise-induced regional dysfunction subcritical coronary stenosis. *Circulation* 1986;**73**:596-605
- Lekakis J, Vassilopoulos N, Germanidis J, Theodorakos A, Nanas J, Kostamis P, Mouloupoulos S : Detection of viable tissue in healed infarcted myocardium by dipyridamole thallium-201 reinjection and regional wall motion studies. *Am J Cardiol* 1993;**71**:401-404
- Lerch RA, Bergamnn SR, Ambos HD, Welch JM, Ter-Pogossian MM, Sobel BE : Effect of flow-independent reduction of metabolism on regional myocardial clearance of ¹¹C-palmitate. *Circulation* 1982;**65**:731-738
- Lerch RA, Ambos HD, Bergamnn SR, Welch JM, Ter-Pogossian MM, Sobel BE : Localization of viable, ischemic myocardium by positron-emission tomography with ¹¹C-palmitate. *Circulation* 1981;**64**:689-699
- Lewis SJ, Sawada SG, Ryan T, Segar DS, Armstrong WF, Feigenbaum H : Segmental wall motion abnormalities in the absence of clinically documented myocardial infarction: Clinical significance and evidence of hibernating myocardium. *Am Heart J* 1991;**121**:1088-1093
- Lipscomb K, Gould KL: Mechanism of the effect of coronary artery stenosis on coronary flow in the dog. *Am Heart J* 1975;**89**:60-67
- Liu P, Kiess MC, Okada RD, Block PC, Strauss HW, Pohost GM, Charles AB : The persistent defect on exercise thallium imaging and its fate after myocardial revascularization: Does it represent scar or ischemia? *Am Heart J* 1985;**110**:996-1001
- Lucignani G, Paolini G, Landoni C, Zuccari M, Paganelli G, Galli L, Di Credico G, Vanoli G, Rosseti C, Mariani MA, Gilardi MC, Colombo F, Grossi A, Fazio F : Presurgical identification of hibernating myocardium by combined

use of technetium-99m hexakis 2-methoxyisotylisonitrile single photon emission tomography tomography and fluorine-18 fluoro-2-deoxyglucose-d-glucose positron emission tomography in patients with coronary artery disease.. Eur J Nucl Med 1992;**19**:874-881

Manyari DE, Knudtson M, Kloiber R, Roth D : Sequential thallium-201 myocardial perfusion studies after successful percutaneous transluminal coronary artery angioplasty: Delayed resolution of exercise induced scintigraphic abnormalities. Circulation 1988;**77**:86-95

Marban E : Myocardial stunning and hibernation. The physiology behind the colloquialisms. Circulation;1991;**83**:681-688

Marcovitz PA, Armstrong WF : Assessing myocardial viability with magnetic resonance imaging. Am J Cardiac Imag 1992;**6**:214-218

Marcus ML, Chilian WM, Kanatsuka H, Dellsperger KC, Eastham CL, Lamping KG : Understanding the coronary circulation through studies at the microvascular level. Circulation 1990;**82**:1-7

Marcus ML Wilson RF, White CW : Methods of measurements of myocardial blood flow in patients: A critical review. Circulation 1987;**76**:245-253

Marshall RC, Tillisch JH, Phelps M, Huang SC, Carson R, Henze E, Schelbert HR : Identification and differentiation of resting myocardial ischemia and infarction in man with positron computed tomography, 18-F-labeled fluorodeoxyglucose and N-13 ammonia. Circulation 1983;**67**:766-788

Marzullo P, Reisenhofer B, Sambucete G, Picano E, Distanto A, Gimelli A, L'Abbate A : Value of the rest thallium-201/technetium-99m sestamibi scans and dobutamine echocardiography for detecting myocardial viability. Am J Cardiol 1993;**71**:166-172

- Marwitz TH, McIntyre WJ, Lafont A, Nemecek JJ, Salcedo EE : Metabolic response of hibernating and infarcted myocardium to revascularization. A follow-up study of regional perfusion, function, and metabolism. *Circulation* 1992;**85**:1347-1353
- Maseri A : Coronary vasoconstriction: visible and invisible. *N Engl J Med* 1991a;**325**:1579-1580
- Maseri A, Crea F, Cianflone D : Myocardial ischemia caused by distal coronary vasoconstriction. *Am J Cardiol* 1992;**70**:1602-1605
- Maseri A, Crea F, Kaski JC, Crake T : Mechanism of angina in syndrome X. *J Am Coll Cardiol* 1991;**17**:499-506
- Matsuzaki M, Gallagher KP, Kemper WS, White F, Ross Jr. : Sustained regional dysfunction produced by prolonged coronary stenosis: gradual recovery after reperfusion. *Circulation* 1983;**68**:170-182
- Maublant JC, Gachon P, Moins N : Hexakis (2-Methoxy Isobutylisocyanide) technetium-99m and thallium-201 chloride: Uptake and release in cultured myocardial cells. *J Nucl Med* 1988;**29**:48-54
- McCallister Jr BD, Clemmets IP, Hauser MF, Gibbons RJ : The limited value of 24-hour images following 4-hour reinjection thallium imaging. *Circulation* 1991;**84**(suppl II):II-533 [Abstract]
- McFadden EP, Clarke JG, Davies GJ, Haider AW, Kaski JC, Maseri A : Coronary vasomotor effects of serotonin on coronary vessels in patients with stable and variant angina. *N Engl J Med* 1991;**324**:648-654
- Mock MB, Ringvist I, Fisher LD, Davis KB, Chaitman BR, Kouchoukos NT, Kaiser GC, Alderman E, Ryan TJ, Russell RO, Mullin S, Fray D, Killip III T, and participants in the Coronary Artery Surgery Study : Survival of

medically treated patients in the coronary artery surgery study (CASS) registry. *Circulation* 1982, **66**:562-568

Montalescot G, Faraggi M, Drobinski G, Messian O, Evans J, Grosogoeat Y, Thomas D : Myocardial viability in patients with Q wave myocardial infarction and no residual ischemia. *Circulation* 1992;**86**:47-55

Mori R, Minamiji K, Kurogane H, Ogawa K, Yoshida Y : Rest-injected thallium-201 imaging for assessing viability of severe asynergic regions. *J Nucl Med* 1991;**32**:1718-1724

Mousa SA, Williams SJ, Sands H : Characterization of in vivo chemistry of cations in the heart. *J Nucl Med* 1987;**28**:1351-1357

Mullins LJ, Moore RD : The movement of thallium ions in muscle. *J Gen Physiol* 1960;**43**:759-773

Nabel EG, Ganz P, Gordon JB: Atherosclerosis and endothelial function influence the coronary response to exercise. *J Clin Invest* 1989;**83**:1946-1952

Nabel EG, Ganz P, Gordon JB, Alexander RW, Selwyn AP : Dilatation of normal and constriction of atherosclerotic coronary arteries caused by cold pressor test. *Circulation* 1988;**73**:43-52

Neely JR, Feuvray D : Metabolic products and myocardial ischemia. *Amer J Pathology* 1981; **241**:282-291

Neely JR, Morgan HE : Relationship between carbohydrate and lipid metabolism and the energy balance of heart muscle. *Ann Rev Physiol* 1974;**36**:413-459

Nellis SH, Liedtke AJ, Whitesell L : Small coronary vessel pressure and diameter in an intact beating rabbit using fixed-position and free-motion techniques. *Cir Res* 1981;**48**:342-353

- Newman CM, Maseri A, Hackett DR, El-Tamimi HM, Davies GJ : Response of angiographically normal and atherosclerotic left anterior descending coronary arteries to acetylcholine. *Am J Cardiol* 1990;**66**:1070-1076
- Nienaber CA, Brunken RC, Sherman CT, Yeatman LA, Gambhir SS, Krivokapich J, Demer LL, Ratib OM, Child JS, Phelps ME, Schelbert HR : Metabolic and functional recovery of ischemic human myocardium by positron tomography. *J Am Coll Cardiol* 1991;**18**:966-978
- Ohtani H, Tmaki N, Yonekura Y, Mohiuddin IH, Hirate K, Ban T, Konishi J : Value of thallium-201 reinjection scintigraphy after delayed SPECT imaging for predicting reversible ischemia after coronary bypass grafting. *Am J Cardiol* 1990;**66**:394-399
- Okada RD, Lim YL, Boucher CA, Pohost GM, Chesler DA, Block PC : Clinical, angiographic, hemodynamic, perfusional and functional changes after one-vessel left anterior descending coronary angioplasty. *Am J Cardiol* 1985;**55**:347-356
- Opherk D, Zebe H, Weihe E, Mall G, Dürr C, Gravert B, Mehmenl HC, Schwarz F, Kübler W : Reduced coronary dilatory capacity and ultrastructural changes of the myocardium in patients with angina pectoris but normal coronary angiograms. *Circulation* 1981;**63**:817-825
- Opie LH : Effects of regional ischemia on metabolism of glucose and fatty acids. *Circ Res* 1976;**38**(suppl I):I52-I74
- Opie LH : Hypothesis : Glycolytic flux control cell viability in ischemia. *J Appl Cardiol* 1988;**3**:407-414
- Opie LH : Carbohydrates and Lipids. In: *The Heart, Physiology and Metabolism*. Raven Press, New York, 1991, pp 208-246

- Parodi O : Positron emission tomography, the best available standard for viable myocardium: A "wealthy" tool for what? *J Nucl Biol Med* 1992;**36**:267-272
- Patlak CS, Blasberg RG, Fenstermacher JD : Graphical evaluation of blood-to-brain transfer constants from multiple-time uptake data. *J Cereb Blood Flow Metab* 1983;**3**:1-7
- Patterson DL, Treasure T : The culprit coronary artery lesion. *Lancet* 1991;**338**:1379-1380
- Perroni-Filardi P, Bacharach SL, Dilsizian V, Maurea S, Marin-Neto JA, Arrighi JA, Frank JA, Bonow RO : Metabolic evidence of viable myocardium in regions with reduced wall thickness and absent wall thickening in patients with chronic ischemic left ventricular dysfunction. *J Am Coll Cardiol* 1992a;**20**:161-168
- Perroni-Filardi P, Bacharach SL, Dilsizian V, Maurea S, Frank JA, Bonow RO : Regional left ventricular thickening. Relation to regional uptake of ¹⁸Fluorodeoxyglucose and ²⁰¹Tl in patients with chronic coronary artery disease and left ventricular dysfunction. *Circulation* 1992b;**86**:1125-1137
- Perroni-Filardi P, Bacharach SL, Dilsizian V, Marin-Neto JA, Maurea S, Arrighi JA, Bonow RO : Clinical significance of reduced regional myocardial glucose uptake in regions with normal blood flow in patients with chronic coronary artery disease. *J Am Coll Cardiol* 1994;**23**:608-616
- Peshock RM : Assessing myocardial viability with magnetic resonance imaging. *Am J Cardiac Imag* 1992;**6**:237-243
- Phelps ME, Mazziota JC, Schelbert HR (eds): *Positron Emission Tomography and autoradiography. Principles and Applications for the Brain and the Heart.* New York: Raven Press, 1986

- Pierard LA, De Landsheere CM, Berthe C, Rigo P, Kulbertus HE : Identification of viable myocardium by echocardiography during dobutamine infusion in patients with myocardial infarction after thrombolytic therapy: Comparison with positron emission tomography. *J Am Coll Cardiol* 1990;**15**:1021-1031
- Pigott JD, Kouchoukos NT, Oberman A, Cutter GR : Late results of surgical and medical therapy for patients with coronary artery disease and depressed left ventricular function. *J Am Coll Cardiol* 1985;**5**:1036-1045
- Poppio KA, Gorlin R, Bechtel D, Levine JA : Postextrasystolic potentiation as a predictor of potential myocardial viability: Preoperative analyses compared with studies after coronary bypass surgery. *Am J Cardiol* 1977;**39**:944-953
- Prvulovich EM, Syed GMS, Underwood SR, Jewit DE : Improved assessment of inferior left ventricular wall motion using biplane equilibrium radionuclide ventriculography. *Eur J Nucl Med* 1994;**21**:423-426
- Pupita G, Maseri A, Kaski JC, Galassi AR, Crea F, Gevrialeides S, Davies G : Myocardial ischemia caused by distal coronary constriction in stable angina pectoris. *N Engl J Med* 1990;**323**:514-520
- Ragosta M, Beller GA, Watson DD, Kaul S, Gimple LW : Quantitative planar rest-redistribution ²⁰¹Tl imaging in detection of myocardial viability and prediction of improvement in left ventricular function after coronary bypass surgery in patients with severely depressed left ventricular function. *Circulation* 1993;**87**:1630-1641
- Rahimtoola SH : A perspective on three large multicenter randomized clinical trials of coronary bypass surgery for chronic stable angina. *Circulation* 1985;**72**(Suppl V):V1230V135

- Ratib O, Phelps ME, Huang SC, Henze E, Selin CE, Shelbert HR : Positron tomography with deoxyglucose for estimating local myocardial glucose metabolism. *J Nucl Med* 1982;**23**:577-586
- Reimer KA, Lowe JE, Rasmussen MM, Jennings RB : The wave front phenomenon of ischemic cell death. 1. Myocardial infarct size vs. duration of coronary occlusion in dogs. *Circulation* 1977;**56**:786-794
- Robb RA : A software system for interactive and quantitative analysis of biomedical images. In Höhne, Fuchs KH, Pizer SM ; 3D Imaging in Medicine, NATO ASI, vol F60:333-361
- Rocco TP, Dilsizian V, McKusick KA, Fischman AJ, Boucher CA, Strauss W : Comparison of thallium redistribution with rest "re-injection" imaging for the detection of viable myocardium. *Am J Cardiol* 1990;**66**:158-163
- Ross JJr : Myocardial perfusion-contraction matching. Implications for coronary heart disease and hibernation. *Circulation* 1991;**83**:1076-1083
- Rozanski A, Berman DS, Gray R, Levy R, Raymond M, Maddahi J, Pantaleo N, Waxman AD, Swan HJC, Matloff J: Use of thallium-201 redistribution scintigraphy in the preoperative differentiation of reversible and nonreversible myocardial asynergy. *Circulation* 1981;**64**:936-944
- Rovetto MJ, Whitman JT, Neely JR : Comparison of the effects of anoxia and whole heart ischemia on carbohydrate utilization in isolated working rat hearts. *Circ Res* 1973;**32**:699
- Schelbert HR, Henze E, Schon HR, Najafi A, Hansen H, Huang SC, Barrio JR, Phelps MR : C-11 Palmitic acid for the noninvasive evaluation of regional myocardial fatty acid metabolism with positron computed tomography. IV. In vivo demonstration of impaired fatty acid oxidation in acute myocardial ischaemia. *Am Heart J* 1983;**106**:736-750

- Schelbert HR, Phelps ME, Hoffman EJ, Huang SC, Kuhl DE : Regional myocardial perfusion assessed by N-13 labelled ammonia and positron computerized axial tomography. *Am J Cardiol* 1979;**43**:209-218
- Schwaiger M, Hicks J . *J Nucl Med* 1991;**32**:565-578
- Schwaiger M, Brunken R, Grover-McKay M, Krivokapich J, Child J, Tillisch JH, Phelps ME, Schelbert HR : Regional myocardial metabolism in patients with acute myocardial infarction assessed by positron emission tomography. *J Am Coll Cardiol* 1986;**8**:800-808
- Selwyn AP, Yeung AC, Ryan Jr TJ, Raby K, Barry J, Ganz P : Pathophysiology of ischemia in patients with coronary artery disease. *Prog Cardiovasc Dis* 1992;**35**:27-39
- Spinks TJ, Jones T, Gilardi MC, Heather JD : Physical performance of the latest generation of commercial positron scanner. *IEEE Trans Nucl Sci* 1988;**NS-35**:721-725
- Spinks TJ, Araujo LI, Rhodes CG, Hutton BF : Physical aspects of cardiac scanning with a block detector positron tomography. *J Comp Ass Tomogr* 1991;**15**:893-904
- Strauss HW, Harrison K, Langan JK, Lebowitz E, Pitt B : Thallium-201 for myocardial imaging. Relation of thallium-201 to regional myocardial perfusion. *Circulation* 1975;**51**:641-645
- Takeishi Y, Tono-oka I, Kubota I, Ikeda K, Masakane I, Chiba J, Abe S, Tsuiki K, Komatani A, Yamaguchi I, Washio M : Functional recovery of hibernating myocardium after coronary bypass surgery : Does it coincide with improvement in perfusion? *Am Heart J* 1991;**122**:665-670
- Takemoto KA, Kiat H, Friedmann J, Silber H, Biasio Y, Palmas W, Berman DS. *Circulation (suppl II)*1991;**84**:II-8 [Abstract]

- Tamaki N : Current status of viability assessment with positron tomography. J Nucl Cardiol 1993;**2**:S40-S47
- Tamaki N, Ohtani H, Yamashita K, Magata Y, Yonekura Y, Nohara R, Kambara H, Kawai C, Hirata K, Ban T, Konishi J : Metabolic activity in the areas of new fill-in after thallium-201 reinjection: Comparison with positron emission tomography using fluorine-18- deoxyglucose. J Nucl Med 1991b;**32**:673-678
- Tamaki N, Ohtani H, Yonekura Y, Nohara R, Kambara H, Kawai C, Hirata K, Ban T, Konishi J : Significance of fill-in after thallium-201 reinjection following delayed imaging: Comparison with regional wall motion and angiographic findings. J Nucl Med 1990;**31**:1617-1623
- Tamaki N, Yonekura Y, Yamashita K, Sagi H, Magata Y, Senda M, et al : Positron emission tomography using fluorine-18-deoxyglucose in evaluation of coronary artery bypass grafting. Am J Cardiol 1989;**64**:860-865
- Tamaki N, Yonekura Y, Yamashita K, Senda M, Saji H, Hashimoto T, Fudo T, Kambara H, Kawai C, Ban T, Konishi J : Relation of left ventricular perfusion and wall motion with metabolic activity in persistent defects on thallium-201 tomography in healed myocardial infarction. Am J Cardiol 1988;**62**:202-208
- Tamaki N, Yoshiharu Y, Kawamoto M, Magata Y, Sasayama S, Takahashi N, Nohara R, Kambara H, Kawai C, Konishi J : Simple quantification of regional uptake of fluorine-18 deoxyglucose in the fasting condition. J Nucl Med 1991a;**32**:2152-2157
- Ter-Pogossian MM : The origins of positron emission tomography. Sem Nucl Med 1992;**22**:140-149

- Tillisch J, Brunken R, Marshall R, Schwaiger M, Mandelkern M, Phelps et al :
Reversibility of cardiac wall-motion abnormalities predicted by positron
tomography. *N Engl J Med* 1986;**314**:884-888
- Tillmanns H, Ikeda S, Hansen H, Sarma JSM, Fauvel J, Bing RJ :
Microcirculation in the ventricle of the dog and turtle. *Circ Res*
1974;**34**:561-569
- Tillmanns H, Steinhausen M, Leinberg H, Thederan H, Kubler W : Pressure
measurements in the terminal vascular bed of the epimyocardium of rats
and cats. *Cir. Res* 1981;**49**:1202-1211
- Tousoulis D, Davies G, McFadden E, Clarke J, Kaski JC, Maseri A : Coronary
vasomotor effects of serotonin in patients with angina. Relation to coronary
stenosis morphology. *Circulation* 1993;**88**(Part I):1518-1526
- Uren NG, Melin JA, De Bruyne B, Wijns W, Baudhuin T, Camici PG : Relation
between myocardial blood flow and the severity of coronary artery
stenosis. *N Engl J Med* 1994;**330**:1782-1788
- Van der Wall EE, Van Eck-Smit B, Kuijper AFM, Pauwels EKJ, Brusckhe AVG :
Immediate thallium-201 reinjection: a novel time-saving approach in the
detection of myocardial viability. *J Amer Coll Cardiol* 1993;**21**:250A
[Abstract]
- Vanoverschelde J-L, Melin JA, Bol A, Vanbutsele R, Cogneau M, Labar D,
Robert A, Michel C, Wijns W : Regional oxidative metabolism in patients
after recovery from reperfused anterior myocardial infarction. Relation to
regional blood flow and glucose uptake. *Circulation* 1992;**85**:9-21
- Vatner SF : Correlation between acute reductions in myocardial blood flow and
function in conscious dogs. *Circ Res* 1980;**47**:201-207

- Vita JA, Treasure CB, Yeung AC, Vekshtein VI, Fantasia GM, Fish RD, Ganz P, Selwyn AP : Patients with evidence of coronary endothelial dysfunction as assessed by acetylcholine infusion demonstrate marked increase in sensitivity to constrictor effects of catecholamines. *Circulation* 1992;**85**:1390-1397
- Vom Dahl J, Herman WH, Hicks RJ, Ortiz-Alonso FJ, Lee KC, Allman KC, Wolfe ER, Kalff V, Schwaiger M : Myocardial glucose uptake in patients with insulin-dependent diabetes mellitus assessed quantitatively by dynamic positron emission tomography. *Circulation* 1993;**88**:395-404
- Walsh MN, Geltman EM, Brown MA, Henes CG, Weinheimer CJ, Sobel BE, Bergmann SR : Noninvasive estimation of regional myocardial oxygen consumption by positron emission tomography with carbon-11 acetate in patients with myocardial infarction. *J Nucl Med* 1989;**30**:1798-1808
- Weinberg IN, Huang SV, Hoffman EJ, Araujo LI, Nienaber C, Grover-McKay M, Dahlbom M, Schelbert HR : Validation of PET-acquired input function for cardiac studies. *J Nucl Med* 1988;**29**:241-247
- Weiss JN, Lamp ST : Glycolysis preferentially inhibits ATP-sensitive K⁺ channels in isolated guinea pigs myocytes. *Science* 1987;**238**:67-69
- White CW, Wilson RF, Marcus MI : Methods of measuring myocardial blood flow in humans. *Prog Cardiovasc Dis* 1988;**2**:79-94
- Yang LD, Berman DS, Kiat H, Resser KJ, Friedman JD, Rozanski A, Maddahi J : The frequency of late reversibility in SPECT thallium-201 stress-redistribution studies. *J Am Coll Cardiol* 1990;**15**:334-340
- Zaret BL, Wackers FJ : Nuclear Cardiology (Second of two parts). *N Engl J Med* 1993;**329**:855-863

Zeiber Am, Drexler H, Wollschlaeger H, Just H : Endothelial dysfunction of the coronary microvasculature is associated with impaired coronary blood flow regulation in patients with early atherosclerosis. *Circulation* 1991;**84**:1984-1992

Zeiber Am, Drexler H, Wollschlaeger H, Saubier B, Just H : Coronary vasomotion in response to sympathetic stimulation in humans: The importance of the functional integrity of the endothelium. *J Am Coll Cardiol* 1989;**14**:1181-1190

Lillioja S, Mott DM, Spraul M, Ferraro R, Foley JE, Ravussin E, Knowler WC, Bennet PH, Bogardus C : Insulin resistance and insulin secretory dysfunction as precursors of non-insulin-dependent diabetes mellitus. *N Eng J Med* 1993;**329**:1988-1992

Nuutila P, Knutti J, Ruotsalainen U, Koivisto VA, Eronen E, Teras M, Bergman J, Haarapanta M, Voipio-Pulkki L-M, Viikari J, Ronnema T, Wegelius U, Yki-Jarvinen H : Insulin resistance is localized to skeletal but not heart muscle in type 2 diabetes. *Am J Physiol* 1993;**264**:E756-E762

Voipio-Pulkki L-M, Nuutila P, Knutti J, Ruotsalainen U, Haarapanta M, Teras M, Wegelius U, Koivisto VA : Heart and skeletal muscle glucose disposal in type 2 diabetic patients as determined by positron emission tomography. *J Nucl Med* 1993;**34**:2064-2067